Mercury in blast furnace sludge

I n a u g u r a l - D i s s e r t a t i o n

zur

Erlangung des Doktorgrades

der Mathematisch-Naturwissenschaftlichen Fakultät

der Universität zu Köln

vorgelegt von

Corinna Földi

aus München

2016

Abstract

Blast furnace sludge (BFS) was analyzed for mercury (Hg) for the first time. The content ranged between 0.006 and 20.8 mg kg^{-1} (median: 1.63 mg kg^{-1}) for 65 analyzed samples from seven former BFS dumpsites in Europe. Sequential extraction procedure on 14 of these samples revealed that Hg was mainly present in immobile fractions (> 90 %). The ecotoxically relevant fractions were not of major significance. Volatilization from BFS (mixed with basic oxygen furnace sludge) was low but significant. Mercury release increased with temperature (15 to 25 °C). However, surprisingly Hg flux at 35 °C was lower than at 25 °C.

Nevertheless, BFS should be regarded as potential hazardous waste and Hg source, respectively, as Hg is bioaccumulative and is considered as one of the most important environmental pollutants.

Kurzzusammenfassung

Gichtgasschlämme wurden erstmalig hinsichtlich einer Quecksilberbelastung (Hg) untersucht. Die Gehalte in 65 Proben von sieben ehemaligen Oberflächenhalden in Europa reichten von 0,006 bis 20,8 mg kg^{-1} (Median: 1,63 mg kg^{-1}). Eine sequentielle Extraktion an 14 dieser Proben ergab, dass Hg im Wesentlichen in immobilen Fraktionen vorlag (> 90 %). Die unmittelbar umweltrelevante Fraktionen waren von untergeordneter Bedeutung. Eine Hg-Entgasung aus Gichtgasschlämmen (vermischt mit Konverterschlämmen) war signifikant aber niedrig. Die Entweichungsrate stieg mit der Temperatur (von 15 auf 25 °C), war jedoch bei 35 °C niedriger als bei 25 °C. Trotzdem sollten GGS als Hg-Quelle betrachtet und als potenziell umweltgefährdend eingestuft werden, insbesondere da Hg bioakkumulierend ist und als Umweltschadstoff von übergeordneter Bedeutung anzusehen ist.

Acknowledgements

This thesis would not have been possible without the support of several people who contributed with ideas, guidance, inspirations, and care. First of all, I would like to thank Prof. Dr. Tim Mansfeldt as advisor of this thesis for support and constructive criticism. I am very pleased to have an advisor who gave me the freedom to explore my own ideas but also the guidance not to veer off course. I further more appreciate his constant professional advice and encouragement for this thesis.

Thanks go also to Dr. Reiner Dohrmann for analytical support and to the members of the Soil Science Group of the University of Cologne for experimental assistance and interest in my studies: Karin Greef, Katrin Matern, Anne Kolvenbach, Kristof Dorau, and Marius Gurk. I really appreciate the helpful suggestions and discussions…and last but not least their distraction.

Cologne, September 2015   Corinna Földi

Contents

Chapter 1 Introduction

Introduction

Steel is a widespread basic material in modern societies. The global demand for this material has increased over the last decades from an annual crude steel production of 716,401· 10^6 megagram (Mg) in 1980 to 1,649,303 · 10^6 Mg in 2013 (World Steel Association, 2014a). In a global perspective, two major commercial processes for steel production are applied: the *basic oxygen steelmaking*, where liquid pig iron and scrap steel are maintained, and the *electric arc furnace steelmaking*, which uses scrap steel or direct reduced iron (Fe). According to the (World Steel Association, 2014d), 69.9 % of the global steel production in 2012 were manufactured using the *basic oxygen furnace process*, whereas 29.3 % were produced using the *electric arc furnace process*.

The production of steel results in a rise of considerable amounts of solid byproducts such as slags, ashes, dusts, scales, and sludge. Data of the actual production of by-products per Mg crude steel are rare, as the exact amount varies from production routes, composition of charge material, and process applications. For the steelmaking route via *electric arc furnace* the amount is stated at 181.4 kg per Mg crude steel, whereas crude steel produced in *basic oxygen process* results in 424 kg of by-products per Mg crude steel (World Steel Association, 2014b). These wastes had been frequently deposited in uncontrolled landfills until the commencement of strict environmental laws in the 1960s and 1970s in Europe and elsewhere.

Nowadays, the integrated steel making industry has put a lot of effort into finding ways of utilizing these undesirable materials, due to both from an economical as well as an ecological point of view. Over the last decades, the depositing cost for industrial wastes has increased due to increasing environmental restrictions. The World Steel Association (2014c) designated a material efficiency of 96 %. However, the traditional routes of internal recycling of some wastes, especially several slags and

sludge, are limited due to relatively low intrinsic monetary value as well as chemical (e.g. zinc (Zn), lead (Pb), and alkali metals (Das et al., 2007) and/or physical complex compositions (e.g. too fine-grained material (Makkonen et al., 2002)). In addition, the reuse in other branches of industry is frequently eliminated due to undesirable elements or physical properties of the material itself. Consequently, significant amounts are nowadays still sent for actual disposal or deposition.

Blast furnace sludge

Blast furnace sludge (BFS) is one of the typical steel making related wastes. It is generated during the wet dust separation of blast furnace gas. Blast furnace gas in turn occurs at the melting reduction process to transfer Fe from ores into its elemental form. Therefore, the Fe ores (e.g. wüstite (FeO), hematite (Fe_2O_3), and magnetite (Fe_3O_4)) in form of pellets or sinter are continuously charged into the blast furnace combined with high carbon (C) fuels (mainly coke) and flux additives (e.g. limestone). In a complex process, C is transferred to carbon monoxide (CO) and carbon dioxide (CO_2) which further reduce Fe from the different Fe-bearing materials stepwise to its elemental form. The molten Fe is accumulated as pig iron at the bottom of the blast furnace, tapped frequently, and further processed for steel making.

All reactions in the furnace are enhanced by the countercurrent exchange of the reducing gas streaming up through the furnace and the fresh charge material traveling down into the reaction zone. The process gas composition strongly varies as a function of process applications and the composition of introduced charge material. However, major constituents are CO, CO_2, and nitrogen (N_2), whereas hydrogen (H_2), water vapor, and methane occur in minor amounts. Furthermore, the gas contains significant amounts of low melting point elements such as Zn, lead Pb, potassium (K), and sodium (Na). Besides the gaseous phases, blast furnace gas contains sus-

pended, solid phases such as coke, Fe ores, additives, and their reaction products, which it drags along. The particles content varies from 5.5 to 40 kg per Mg pig iron produced (Remus et al., 2013) depending on process conditions. The gas is discharged at the top of the furnace and subsequent progressively cleaned. After e.g. axial cyclones or dust catchers separate off coarse particles, the gas is disburdened of fine dust (< 0.1 mm) using electrostatic precipitator and annular gap scrubbers. This produces 3.5 to 18 kg of dry dust per Mg pig iron and 2 to 22 kg of sludge per Mg pig iron (Remus et al., 2013). Depending on charge material composition and water availability, the overflow of the circuit normally varies between 100 and 3,500 L process water per Mg pig iron (Remus et al., 2013). The resulting muddy waste is referred to as BFS after the separation of solid material from the bulk of process water.

In general, BFS are neutral to alkaline with a pH ranging from 7.1 to 10.7 (Kretzschmar et al., 2012; Mansfeldt and Dohrmann, 2004; Veres et al., 2012). As pointed out by Mansfeldt and Dohrmann (2004), slightly alkaline conditions (< pH 8.5) of the BFS can be explained by the presence of carbonates ($CaCO_3$). However, during the metallurgical process $CaCO_3$ is converted to burnt lime (CaO) which further hydrolyzes to slaked lime ($Ca(OH)_2$) during storage. Both compounds present in BFS can raise pH of BFS to alkaline conditions. As a result of the progressively gas purification, BFS is a material of rather fine grain-sizes. Blast furnace sludge samples from the U.S. Steel Košice s.r.o. (Slovakia) were analyzed for their granulometric distribution (Veres et al., 2011; Veres et al., 2010; Veres et al., 2012). In one study, the analysis yielded a heterogeneous distribution of particle sizes with a fine grained portion (1 – 10 μm) and a coarser fraction (10 – 100 μm), where 90 % of the particles were smaller than 50 μm. In the other study, 70 to 75 % of the particles had a grain size between 0.9 and 30 μm. The fine-grained particle sizes of BFS result in relatively

large surface areas (Brunauer–Emmet–Teller (BET) method). Surface areas ranging from 15 to 89 (Mansfeldt and Dohrmann, 2004), 17 and 27 (Lopez-Delgado et al., 1996), and 31.5 $m^2 \, g^{-1}$ (Malina and Radenovic, 2014) have been published. Both Mansfeldt and Dohrmann (2004) and Lopez-Delgado et al. (1996) proved a decreasing BET with increasing C content. Malina and Radenovic (2014) further determined total pore volume (1.7 – 300 nm) and average pore diameter yielding values of $157 \cdot 10^{-3} \, cm^3 \, g^{-1}$ and 17.9 mm, respectively. According to IUPAC classification of porous solids into three groups (micropores: $d < 2$ nm; mesopores: $2 < d < 50$ nm; macropores: 50 nm $< d$), BFS was considered as mesoporous material.

The elemental composition of BFS strongly varies as a function of applied charge material and their impurities, respectively. It is dominated by C (median: 149 $g \, kg^{-1}$; min: 69.0 $g \, kg^{-1}$; max: 405 $g \, kg^{-1}$) and Fe (median: 159 $g \, kg^{-1}$; min: 57.9 $g \, kg^{-1}$; max: 275 $g \, kg^{-1}$) which are present in form of particles of coke, carbonates, and Fe ore (Mansfeldt and Dohrmann, 2004). Further major elements are calcium (Ca), silicium (Si), aluminium (Al), Zn, and magnesium (Mg) in descending order ranging from 100 to 10 $g \, kg^{-1}$ (median), which originate from impurities of the charge materials. The median concentrations of Pb, manganese (Mn), K, sulfur (S), N, phosphorous (P), titan (Ti), barium (Ba), and Na range from 9.83 to 0.590 $g \, kg^{-1}$. The clearly elevated contents of Zn (up to 100 $g \, kg^{-1}$) and Pb (up to 12.0 $g \, kg^{-1}$) in BFS are widely described in the literature (Borisov et al., 2014; Kretzschmar et al., 2012; Mansfeldt and Dohrmann, 2004; Remus et al., 2013; Roederer and Gourtsoyannis, 1996; Veres et al., 2011). The enrichment cannot be exclusively explained by mechanical transport with the gas stream. In fact, these elements are enriched in BFS due to their relatively low melting points (Zn: 419.5 °C; Pb: 327.5 °C) which leads to a transition to the gas phase during the combustion process. Fractions of the evaporated elements leave the blast furnace directly, whereas other fractions condense on dust particles

due to the decreasing temperature in the upper shaft of the furnace. Particle-associated Zn and Pb have grain sizes of less than 25 µm and are hence removed from blast furnace gas during the wet purification and thus concentrated in BFS (Remus et al., 2013).

From a mineralogical point of view, BFS clearly reflects the blast furnace process. Kretzschmar et al. (2012) analyzed 32 samples collected from a former dump site by powder X-ray diffraction and Rietveld refinement: the dominated phases were quartz ($18 - 214$ g kg^{-1}), calcite ($48 - 208$ g kg^{-1}), hematite ($9 - 108$ g kg^{-1}), kaolinite ($0 - 78$ g kg^{-1}), magnetite ($10 - 57$ g kg^{-1}), graphite ($0 - 57$ g kg^{-1}), and wüstite ($3 - 49$ g kg^{-1}). Besides these crystalline phases, a very large fraction ($432 - 798$ g kg^{-1}) of BFS was X-ray amorphous. Veres et al. (2012) showed similar, but only qualitative, results also finding hematite, magnetite, calcite, quartz, and amorphous compounds. They explained the indistinct signal by the presence of coke and less crystalline oxides bearing Al, Zn, Pb, and other metals.

Workable data concerning the fate of BFS are hard to obtain as several steel producers publish reports only partial or not at all. Roederer and Gourtsoyannis (1996) most comprehensively documented data for the EU without distinguishing between BFS and blast furnace dust. According to this roughly two thirds of the waste is re-cycled on-site (64 %), one third is landfilled, and minor amounts are either sold, stored, or used externally (each with 1 %). Utilizing BFS in the blast furnace process is preferable under several considerations as the waste contains large amounts of "unused" charge material. Increasing the extraction efficiency of the required elements, mainly C and Fe, would be more sustainable and cost saving (less initial and disposal costs). However, internal recycling of BFS (via e.g. sintering) is currently more difficult for BFS than dust because of the elevated Zn contents, which can cause operational difficulties in the blast furnace. Although much effort is put on Zn recovery from

steel making related sludge (Cantarino et al., 2012; Langova and Matysek, 2010; Trung et al., 2011; Zeydabadi et al., 1997), major amounts of accruing BFS are still deposited due to the chemical composition.

Mercury

Mercury (Hg) is a transition metal of special concern as the element and many of its compounds are highly toxic, persistent, and readily released into the environment due to their high mobility and volatility. It is considered as one of the most important environmental pollutants (WHO, 2005). Overall, Hg occurs naturally in all environmental compartments but rarely as a native metal. The average crustal occurrence is stated in the literature as 56 to 80 µg kg^{-1} (Alekseenko and Alekseenko, 2014; Wedepohl, 1995) with significant local variations. Its major abundances in the lithosphere are the minerals cinnabar (HgS), corderoite ($Hg_3S_2Cl_2$), and livingstonite ($HgSb_4S_8$) with HgS being the most common Hg containing ore. Highest contents of Hg and Hg containing ores, respectively, are found in volcanically and/or hydrothermically active zones. From the predominant occurrence of Hg in volcanically and hydrothermically active zones, the major natural sources of Hg to the atmosphere can be deduced: volcanism, geothermal activity, and weathering of geologic deposits. Major anthropogenic sources of Hg are the combustion of fossil fuels (basically combustion of coal), artisanal and small-scale gold production, cement production, and metal production (> 75 % of anthropogenic Hg emissions). Total emissions to the atmosphere were estimated to be approx. 1960 Mg for 2010 (UNEP, 2013). However, 60 % of the annual emissions to the atmosphere result from "re-emissions" from surface soils and oceans where the original sources cannot be distinguished with certainty. As the anthropogenic sources account for 30 % whereas natural geological

sources only account for 10 %, it is obvious that anthropogenically released Hg is clearly overweighing since the on-set of the industrial era.

Owing to environmental concerns regarding Hg emissions, the United Nations Environmental Programme (UNEP) supports both national and international legislative bodies to reduce Hg emissions (UNEP, 2002). Among others these are the Convention on Long-range Transboundary Air Pollution Protocol on Heavy Metals of the United Nations Economic Commission for Europe (UNECE), the North American Regional Action Plan (NARAP) on Mercury under the auspices of the U.S., Canada, and Mexico, and recent adoption of the international Minamata Convention on Mercury. All these actions have led to a decrease of atmospheric Hg in rural areas from about 1.35 ng m^{-3} around 1996 to about 0.9 ng m^{-3} around 2008 in the southern hemisphere (Cape point, South Africa) and from about 1.75 ng m^{-3} in 1996 to 1999 to about 1.4 ng m^{-3} in 2009 in the northern hemisphere (Mace Head, Ireland) (Slemr et al., 2011). Mercury in the atmosphere exists predominantly as elemental (Hg^0), oxidized (Hg^{2+}), and particulate (Hg$_p$) Hg. Elemental Hg is relatively inert and slightly soluble which results in a rather long atmospheric lifetime ranging from several months to two years (Schroeder and Munthe, 1998; Weiss-Penzias et al., 2003) until it is removed via wet or dry deposition. As it is the predominant species (> 95 %) of Hg in the atmosphere and it persists in air quite long (Valente et al., 2007; Xu et al., 2014), Hg^0 can be dispersed and transported globally, emphasizing the need for international action. Conversely, Hg$_p$ and Hg^{2+} are (highly) reactive and soluble resulting in a rapid removal within one day to one week and thus both species are rather regionally or locally deposited (Valente et al., 2007). Consequently, chemical transformation between these species directly affects the lifetime of atmospheric Hg and deposition rate, respectively, via oxidation to less volatile and more soluble compounds and vice versa. Natural atmospheric deposition rate for preindustrial era in

remote regions typically ranged between 2 and 5 µg of Hg m^{-2} y^{-1} based on lake sediments, sea sediments, and peat cores analyzes (Leipe et al., 2013; Swain et al., 1992). However, Bindler (2003) determined even lower natural background deposition rates (0.5 to 1 µg of Hg m^{-2} y^{-1}) in the period between 4000 and 500 BP analysing long peat cores in southcentral Sweden.

Recent deposition rates strongly vary as a function of exposition, season, and location. Ettler et al. (2008) showed high deposition rates near a lead smelter in the Příbram area, Czech Republic, ranging from 4.7 to 34.4 µg m^{-2} y^{-1} in 1999. Grant et al. (2014) calculated elevated Hg deposition rates for the Great Lakes, United States and Canada, using a comprehensive model evaluation: deposition fluxes ranged from 23.1 ± 0.74 µg m^{-2} y^{-1} (Lake Superior) to 32.6 ± 0.83 µg m^{-2} y^{-1} (Lake Erie) for 2005. Sediment cores from an urban site at South Reservoir near Boston, United States, resulted in a deposition rate of 88 µg m^{-2} y^{-1} (Chalmers et al., 2014). An atmospheric deposition rate of 16 µg m^{-2} y^{-1} was determined by Van Metre (2012) in rural Maine, United States, corresponding well with deposition rate of 20 µg m^{-2} y^{-1} for New England, United States (Driscoll et al., 2007). Van Metre (2012) further analyzed sediment cores from lakes near to (< 50 km) and remote from (> 150 km) several major urban areas in the United States finding clearly elevated deposition rates for near-urban lakes (68 ± 6.9 µg m^{-2} y^{-1}) compared to remote lakes (14 ± 9.3 µg m^{-2} y^{-1}). In this study, also flux ratios (modern to background) were calculated yielding increased deposition rate ratios of 9.8 ± 4.8 for lakes in urban agglomerations and 3.5 ± 1.0 for remote lakes.

Globally, the open ocean receives 90% of it Hg burden via wet or dry atmospheric deposition (Mason et al., 2012). The total Hg burden was stated to be 35,000 Mg (including 15 % human impact) for ocean deep water and 7,000 Mg (including roughly 60 % human impact) for ocean surface water (Selin, 2009).

Coverage of concentration measurement of Hg in ocean waters is limited although it has been increasing recently. However, Hg concentration in the marine system underlies several spatial (horizontally and vertically) and seasonal variations. Mason et al. (2012) summarized numerous data sets, mainly from the Atlantic and Pacific Ocean, stating a total Hg concentration between 0.3 and 3 pM (picomolar, 1 pM = 10^{-12} mol L^{-1}) for open ocean surface (Hammerschmidt and Bowman, 2012; Laurier et al., 2004; Mason et al., 1998). Measurements for deep ocean waters showed values ranging from 0.7 to 2 pM (Gustin et al., 2006; Zhang et al., 2014). Increasing input of Hg to the aquatic environments, mainly from the atmosphere, has led to an anthropogenic enhancement in Hg concentration with a factor of 5 to 6 (Zhang et al., 2014). In the aquatic system, Hg is typically present in three forms: dissolved and particulate Hg^{2+}, dissolved gaseous Hg including Hg^0 and dimethyl Hg ($(CH_3)_2Hg$), and dissolved and particulate monomethyl Hg (CH_3Hg^+) (Ci et al., 2011; Fitzgerald et al., 2007). The former is the predominant form of Hg in most marine environments, whereas dissolved gaseous Hg^0 accounts for less than 30% of total Hg while the latter is basically present in traces (UNEP, 2013). Among the species, Hg^{2+} plays the key role as it drives numerous complex biogeochemical transformation processes in the aquatic system: (i) particulate scavenging of Hg^{2+} via adsorption and the subsequent sinking from surface water to water/sediment interface, (ii) photochemical and microbial reduction of Hg^{2+} to Hg^0, and (iii) biotic methylation to the toxic bioaccumulative CH_3Hg^+ and $(CH_3)_2Hg$. All processes result in Hg lost from marine environments, either via sedimentation on the seafloor or volatilization to the atmosphere. Sedimentary burial to the deep-ocean occurs very slowly and accounts for 200 to 600 Mg of Hg y^{-1} therefore being the major sink (Mason and Sheu, 2002; Selin et al., 2008). On a global basis, 89 % of Hg deposited in aquatic systems is re-emitted to atmosphere, predominantly in the form of Hg^0 (Strode et al., 2007) but also in traces

as $(CH_3)_2Hg$. However, Hg can be re-suspended and re-mineralized from water/sediment interface or re-deposited from the atmosphere completing the oceanic Hg cycle.

Despite the fact that roughly 30 % of Earth' surface is covered by land surface, 60 % of atmospheric Hg is deposited on terrestrial ecosystems (Mason and Sheu, 2002; Selin et al., 2008). This basically results from the emissions' point sources on land and the subsequent wet deposition of Hg_p and Hg^{2+} on a rather regional scale. Furthermore, atmospheric oxidation of Hg^0 to Hg^{2+}, both in clouds and aerosols, might strengthen the disproportionately high terrestrial deposition.

Estimations based on reported Hg concentrations in aboveground plant compartments reveal the removal of over 1000 Mg of atmospheric Hg per year by the global biomass production (Obrist, 2007) being 20 % of total atmospheric Hg burden (Mason et al., 1994; Selin et al., 2008) and 40 % of Hg residing in the lower 5 km of the troposphere (Banic et al., 2003). Naturally, Hg becomes incorporated into soils via litterfall and plant senescence. On a global basis, natural background contents of Hg in most soils are suggested to range between 0.15 and 0.2 mg kg^{-1} (Hooda, 2010). During the post-industrial era combustion of fossil fuels combined with long-range atmospheric transport has increased the Hg in soils and sediments by a factor of 3 to 10 times (UNEP, 2013). Hence, human enhancement of Hg emissions have altered the natural Hg contents throughout global soil profiles to the extent that establishing ambient or background level for Hg in uncontaminated soils is extremely problematic if not unrealistic. Mercury in soils is strongly associated with S groups of organic matter resulting in elevated Hg contents in the upper 15 cm of soils. Selin et al. (2008) calculated the total global soil Hg burden to be in the range of $1 \cdot 10^6$ Mg assuming a global average soil content of 43 µg kg^{-1}. Mason and Sheu (2002) further estimated an additional input of $0.15 \cdot 10^6$ Mg of Hg by anthropogenic influences.

However, Hg is re-emitted to the atmosphere both from Hg-enriched and low Hg-containing substrates. Various authors (Coolbaugh et al., 2002; Engle and Gustin, 2002; Engle et al., 2001; Gustin et al., 2003; Gustin et al., 2006; Zhang et al., 2003) have stated the emissions from soils to contribute substantially to the global Hg load of the atmosphere being in the range of 700 to 1000 Mg y^{-1}.

Depending on its association, Hg in soils can be divided into three pools: i) mineral Hg which is contained in the soil mineral fraction, ii) Hg associated with organic matter (OM), and iii) Hg adsorbed to the surface of soil particles. Although the total Hg content in any given rock type is no more than 0.05 mg kg^{-1} on average (Hooda, 2010) and Hg is only released by weathering over long time scales, the large area covered by mineral soils make this the greatest Hg pool of the environmental compartments (Gustin et al., 2006; Schlüter, 2000). Mercury in the second pool is mainly derived from atmospheric deposition to soils and vegetation. Divalent Hg exhibits a strong affinity towards reduced S groups of OM and is hence protected against reduction until OM is decomposed or emitted by fire. Besides these strong complexes, Hg^{2+} can also be weakly bounded to negatively charged soil particles. Mercury in this third pool can easily be displaced by processes such as cation exchange or water addition (Farella et al., 2006).

Although Hg^{2+} is the predominant form of Hg in soils, it is widely accepted that Hg volatilizing from soils is predominantly in the form of Hg^0 and/or $(CH_3)_2Hg$, probably with minor amounts of CH_3Hg^+ and soluble Hg(II)-salts (Schlüter, 2000). The former are the only Hg species described as volatile species as they are water soluble with at least 500 times higher air/water-distribution constant than the non-volatile species (Iverfeldt, 1984). Environmental parameters affecting Hg emissions at the soil-atmosphere interface are controlled by the fundamental soil properties (soil Hg content, pH, electrical conductivity, organic C, and soil texture), biological processes, and

meteorological parameters (incident light, temperature, precipitation, elevated soil moisture, interaction with atmospheric ozone, and atmospheric turbulences) and their interactions (Coolbaugh et al., 2002; Engle et al., 2005; Engle et al., 2001; Feng et al., 2005; Gustin, 2003; Gustin and Stamenkovic, 2005; Gustin et al., 1997; Lindberg et al., 1979; Lindberg et al., 1999; Nacht and Gustin, 2004; Poissant et al., 1999; Song and Van Heyst, 2005; Zehner and Gustin, 2002).

Formation and turnover of Hg^{2+} to Hg^0 in soils is controlled by both biotic and abiotic reduction (Schlüter, 2000). While abiotic reduction is basically mediated by humic acids, fulvic acids, and other reductants, such as Fe^{2+}, biotic reduction is capable through Hg resistant soil microorganisms. Ravichandran (2004) reviewed the interactions between Hg and humic and fulvic acids suggesting that dissolved organic matter (DOM) inhibit a dual role in determining Hg pathway in the geochemistry cycle: Both by complexation and reduction. Spectroscopic techniques as well as indirect evidence (e.g., inhibition of precipitation and enhanced dissolution of HgS by DOM) have confirmed extremely strong ionic bonding between Hg and reduced S sites of DOM in soils and aquatic organic matter (Skyllberg et al., 2006; Xia et al., 1999). Jiang et al. (2014) used three humic acids (HA) to illustrate abiotic reduction of Hg^{2+} by HA. They showed that increasing HA concentration led to an increase Hg^{2+} reduction and Hg^0 production, respectively, up to a certain concentration (approximately 100 mg C L^{-1}) followed by a decline of Hg^{2+} reduction with excessively large HA concentration. Hence, at this point complexation of Hg^{2+} by HA seemed to be dominant and overshadowed the reduction phenomenon. Similar results were reported by Gu et al. (2011) and Rocha et al. (2003). Jiang et al. (2014) moreover pointed out the effect of visible light on Hg^{2+} reduction: Compared with samples obtained under dark conditions, the reduction process was enhanced by radiation. From their results, the authors further suggested Hg^0 production by HA and catalyzed by light was similar to

the mechanism underlying Fe^{3+} and Cr^{6+} photoreduction by humic substances. This mechanism mainly consists of two steps: i) organic free radicals, hydroxyl radicals, and directive electrons caused by light radiation, and ii) ligand-to-metal charge transfer due to Hg-HA complex formation, in which light radiation could retrieve direct electrons via the charge transfer of Hg-HA complexes to reduce Hg^{2+} to Hg^0. Various author (Choi and Holsen, 2009; Gillis and Miller, 2000; Gustin et al., 2006; Sigler and Lee, 2006) reported strong relations between temperature and Hg emissions from soils: Highest emissions rates were measured in afternoon and summertime, while emissions significantly decreased during nights and winter. As radiation and soil temperature are strongly linked and biological activity is significantly affected by the temperature, differentiation of these influence factors are hard to separate. However, many researches have hypothesized a radiation-induced mechanism separate from soil temperature. Photoreduction of Hg^{2+} is stated as one of the primary mechanisms for Hg^0 production in nature (Costa and Liss, 1999; Fitzgerald et al., 2007; Rocha et al., 2003; Zheng and Hintelmann, 2009).

By transformation of organic or inorganic Hg^{2+} to volatile Hg species which subsequently evaporate, soil microorganisms detoxify their immediate environment via biotic reduction. Soil bacteria are either able to metabolize organic Hg^{2+} for their energy and C cycle or they enzymatically modify the species (organic and inorganic Hg^{2+}) without using it as nutritional source (Schlüter, 2000). Responsible for this ability is the bacterial enzyme mercuric reductase (merA) by catalyzing the conversion of the thiol-affine Hg^{2+} to Hg^0 with lacks of significant affinity for any functional groups. As thiols of proteins in the cytoplasm of the cells also tend to form strong bindings with Hg^{2+}, it is essential that merA is an effective competitor with these cellular thiols to ensure survival of the cell/organism (Barkay et al., 2003). The metabolism of organic Hg^{2+} rather reflects an indirect reduction insofar that biotic decomposition "remove"

OM as a strong binding agent for Hg^{2+} by converting their substrate to compounds such as HA and fulvic acids, which are capable of Hg^{2+} reduction (Fritsche et al., 2008; Obrist et al., 2010).

Another parameter affecting Hg emissions from soils significantly is the water content. Both Gillis and Miller (2000) and Song and Van Heyst (2005) have demonstrated that rising water content can promote reduction of Hg^{2+} and Hg^0 with subsequent volatilization of Hg. Also the addition of small amounts of water simulating the effect of precipitation resulted in increased Hg flux (Gustin and Stamenkovic, 2005). Lindberg et al. (1999) suggested three mechanisms being responsible for enhanced emissions of Hg from a dry desert soil observed with a rain event: i) physical displacement of Hg^0 enriched interstitial soil air by infiltrating water, (ii) replacement of Hg^0 adsorbed to the soil by water molecules, and (iii) desorption of Hg^{2+} bound to the soil and subsequent reduction to Hg^0 through abiotic or biotic factor. A direct relation between enhanced emissions as a response to precipitation events and biological activity was ruled out by Song and Van Heyst (2005) as the main process, as biological reactions require more time to establish, reproduce, and influence emissions.

Scope of this thesis

As outlined above, Hg is preferentially associated with S groups of OM and hence is enriched in coal, being a product of carbonization of peat. As Hg is classified geochemically as a chalcophile element, pyrite (FeS_2), mercuric chloride ($HgCl_2$) and cinnabar (HgS) are the dominant mineral host phases for Hg in coal. Great variations of Hg content in coal are reported in the literature as the Hg content largely depends on the geology of coal fields and the type of coal. However, Hg contents mostly vary between 0.05 and 1.95 mg kg^{-1} (Davidson and Claerke, 1996; Wang et al., 2000). Coal is transferred to coke in a pyrolytic process where Hg loss is reported (Ma et al.,

2010) but coke still contains significant amounts of Hg. Further, it is known that Fe ores contain Hg as trace impurities. The content varies as a function of the geology of Fe ore formation and type of Fe ore. Mercury contents in iron ores from Minnesota ranged between 0.017 and 1.31 mg kg^{-1} (Morey and Lively, 1999) whereas (Fukuda et al., 2011) analyzed samples (n = 54) from different countries (Australia, India, Peru, and South Africa), finding a mean Hg value of 0.031 mg kg^{-1} and a maximum Hg value of 0.108 mg kg^{-1}.

Besides Fe ores in the form of lumps, pellets, or sinter, coal and coke are the main charge material for the production of pig iron in blast furnaces. Altogether they account for a proportion of up to 95 % (Nogami et al., 2006) of the charge material depending on the individual composition of each material, production conditions, and plant devices. Hence, Hg is introduced into the blast furnace in significant amounts, however, the fate of Hg in the blast furnace and its by-products has been unknown. Great attention should be paid to the study of Hg behavior and fate in the environment as Hg is one of 189 toxic air pollutants designated by Title III of the Clean Air Act Amendments of 1990 (1990) and is classified as one of the most important environmental pollutant. It is of major concern as Hg and many of its compounds are accumulative in living tissues and hence can seriously affect human beings through the food chain. Depending on the dose, Hg and its derivatives can cause chronic or acute damages to the neurological system.

The scope of this thesis was hence to study the fate of Hg in BFS as this waste might potentially attribute to the global Hg cycle. Therefore, the following preliminary hypotheses were formed and addressed in the course of this thesis:

Hypothesis 1

Mercury is enriched in BFS due to its low boiling point and high process temperatures in the blast furnace.

Hypothesis 2

Similar to "natural" conditions, Hg in BFS is preferentially associated with car-bon-based sorbents, such as coke particles or graphite.

Hypothesis 3

An Hg-specific sequential extraction procedure developed for soils and sedi-ments can be adopted to BFS to assess the risk potential of Hg in BFS.

Hypothesis 4

Mercury in BFS mainly resides in the fraction of "elemental" Hg, mercuric sul-fides, and Hg in crystalline metal ores and silicates and hence being rather immobile under natural conditions.

Hypothesis 5

Blast furnace sludge inhibits a significant potential for Hg volatilization mean-ing that Hg-fluxes from drying samples is detectable under laboratory condi-tions.

Hypothesis 6

Volatilization rate of Hg from BFS is largely driven by temperature.

Study sites and applied methods

To verify or falsify the formed hypotheses, 65 samples from seven different locations were studied. The BFS sedimentation ponds were located in Herne and Dinslaken (operating) in the Ruhr area (Germany), Eisenhüttenstadt (Germany), Lübeck (Ger-many), Nowa Huta (Krakow, Poland), Esch-Belval (Luxembourg), and Nancy (France).

Elemental composition was analyzed by wavelength dispersive X-ray fluorescence (XRF; Axios, PANalytical) and a CNS-analyzer (Vario EL Cube CNS, Elementar).

Further, Hg was detected by means of a direct mercury analyzer (DMA-80, MLS GmbH). Soluble Hg was determined according to a modified DIN ISO 19730:2009-07 (2009) for samples with a total Hg content > 1.8 mg kg^{-1}. Sequential extraction procedure was conducted on 14 samples according Bloom et al. (2003) and modified by Hall et al. (2005).

For volatilization experiments, a fresh sample of BFS mixed with basic oxygen furnace sludge (a residue of gas purification from steel making, processed simultaneously in the cleaning devices of BFS and hence mixed with BFS) was obtained from the Ruhr area (Germany) and used for sealed column experiments. The experiments were conducted for four weeks in the dark at 15, 25, and 35 °C. Mercury was trapped on gold coated sand and subsequently quantified with the DMA. Chemical and mineralogical composition of this sample was performed with XRF and CNS-analyzer, respectively, and X-ray powder diffraction (XRD).

Chapter 2   Mercury in dumped blast furnace sludge

Co-author: Reiner Dohrmann & Tim Mansfeldt

Highlights

- Blast furnace sludge (BFS) has been analyzed for Hg for the first time

- The Hg content of BFS varied between 0.006 and 20.8 mg kg^{-1} (median 1.64 mg kg^{-1})

- In comparison to the charge material, Hg was enriched in BFS

- Hg correlated with non-calcareous carbon content (coke and graphite)

Abstract

Blast furnace sludge (BFS) is a waste generated in the production of pig iron and was dumped in sedimentation ponds. Sixty-five samples from seven BFS locations in Europe were investigated regarding the toxic element mercury (Hg) for the first time. The charge material of the blast furnace operations revealed Hg contents from 0.015 to 0.097 mg kg^{-1}. In comparison, the Hg content of BFS varied between 0.006 and 20.8 mg kg^{-1} with a median of 1.63 mg kg^{-1}, which indicates enrichment with Hg. For one site with a larger sample set (n = 31), Hg showed a stronger correlation with the total non-calcareous carbon (C) including coke and graphite (r = 0.695; n = 31; p < 0.001). It can be assumed that these C-rich compounds are hosting phases for Hg. The solubility of Hg was rather low and did not exceed 0.43% of total Hg. The correlation between the total Hg concentration and total amount of NH_4NO_3-soluble Hg was relatively poor (r = 0.496; n = 27; p = 0.008) indicating varying hazard potentials of the different BFS. Finally, BFS is a mercury-containing waste and dumped BFS should be regarded as potentially mercury-contaminated sites.

Introduction

Blast furnace sludge (BFS) is a waste generated in the production of pig iron and was dumped in large surface landfills in industrial areas until the commencement of strict environmental laws in the 1960s and 1970s in Europe. During the late 1990s, 6 kg of BFS were generated per ton of pig iron produced (Lopez-Delgado et al., 1998), resulting in 6,300,000 Mg of BFS produced in the European Union alone during the 1990s (World Steel Association, 2013). As these wastes often contain harmful substances, significant hazards to environmental surroundings may arise from former BFS sedimentation ponds.

Pig iron is commonly produced in blast furnaces by smelting several iron (Fe) ores with a high carbon (C) fuel such as coke and flux additives (limestone etc.). Extraction of Fe from its ores and its conversion to alloys is the most important metallurgical process (Coudurier et al., 1985). During the operation, a gaseous phase (top gas) leaves the top of the blast furnace. Besides the gaseous phases, it contains dragged solid phases such as coke, Fe ores, additives, and their reaction products. For the downstream use, the effluent gas was purified from the dust (30 kg of dust per ton of pig iron produced (Mansfeldt and Dohrmann, 2004) long before any environmental laws were enacted. As a result of wet purification, a muddy waste referred to as BFS was generated. Besides Fe and C, other elements are also introduced into the blast furnace. Mansfeldt and Dohrmann (2004) investigated 32 samples from an abandoned BFS landfill in the Ruhr area of Germany, specifically examining their elemental composition and identifying four main categories: (i) Fe and C with a median content of > 100 g kg^{-1}; (ii) elements such as lead (Pb), magnesium (Mg), zinc (Zn), aluminum (Al), silicon (Si), and calcium (Ca), with contents ranging from 10 to 100 g kg^{-1} in ascending order; (iii) potassium (K), sulfur (S), manganese (Mn), nitrogen (N), phosphorous (P), and sodium (Na), with contents ranging from 1 to

10 g kg^{-1}; and (iv) minor elements with mean contents < 1 g kg^{-1}, such as arsenic (As), cadmium (Cd), and many more. All elements were introduced into the process by either Fe ores or coke, and to a lesser extent by flux, in which these elements occur partly as impurities. Due to the presence of significant amounts of As, Cd, Pb, Zn, and cyanides, which are formed during the blast furnace operation, BFS can be regarded as a harmful waste (Trömel and Zischkale, 1971; Van Herck et al., 2000; Mansfeldt and Dohrmann, 2001, 2004; Trung et al., 2011).

Mercury (Hg) is considered as one of the most important environmental pollutants as the element and many of its compounds are highly toxic, persistent, and readily released into the environment due to its high mobility and volatility (WHO, 2005). Considering the enrichment with elements such as Zn, Pb, Na, and K, it is postulated that BFS is enriched with the highly volatile transition metal Hg as well. AMAP/UNEP (2008) estimated a global inventory of Hg to atmosphere to be 1921 Mg. In their Global Mercury Assessment report, the UNEP (2013) stated that the primary production of ferrous metals contributes 45.5 Mg of Hg to the atmosphere being 2% of the global anthropogenic emissions. To the best of our knowledge, no data on Hg in BFS have been published yet, so emissions from BFS are most likely missing in the global inventory.

This study aimed at the determination of i) the total Hg content and ii) the easily mobilized fraction of Hg in BFS samples from different locations in Europe. Furthermore, iii) the Hg content of some charge materials was investigated in order to estimate a possible enrichment with Hg. Overall, the aim of the study is to provide first insights about Hg in BFS and in addition to that to provide primary information about potential Hg emissions for a future global inventory of Hg including these emissions. Overall, this study provides first insights about Hg in BFS and contributes primary information to the global inventory of Hg.

Material and methods

Sampling sites, sampling, and sample preparation

Samples were obtained from six former BFS sedimentation ponds and one operating BFS deposit in Europe: Herne and Dinslaken (operating) in the Ruhr area (Germany), Eisenhüttenstadt (Germany), Lübeck (Germany), Nowa Huta (Krakow, Poland), Esch-Belval (Luxembourg), and Nancy (France) (Figs. 1 and 2). Sampling was performed in three ways: first, near-surface samples (0 to 10 cm) were taken (Lübeck, Eisenhüttenstadt, Nowa Huta, Esch-Belval), and second, samples were taken at different depths from fresh pits up to 1.0 m depth (Herne, Nancy).

Fig. 1 Locations of the sampling sites.

Additionally, core samples from 3.9 to 12 m depth were obtained (Herne). In total, 65 samples (42 from Herne, 1 from Dinslaken, 4 from Eisenhüttenstadt, 4 from Lübeck, 3 from Nowa Huta, 6 from Esch-Belval, 6 from Nancy) were collected. The field-moist samples were dried at room temperature, sieved to a size fraction < 2 mm, and man-

ually homogenized. No material > 2 mm was present. For the analysis of element contents, subsamples were ground to analytical grain size in an agate ball mill (PM 400, Retsch). Furthermore, an exemplarily loading of a blast furnace was investigated for its Hg content: 3 coke samples from Poland (n = 1) and Germany (n = 2), 1 Fe ore sample from South Africa, 1 Fe ore pellet sample from Canada, 1 sinter product sample, and 4 additive samples (olivine, bauxite, gravel, ilmenite). The samples were dried at room temperature and pre-ground by a jaw crusher (BB1, Retsch) before grinding to analytical grain size in an agate ball mill (PM 400, Retsch).

Fig. 2   View of former blast furnace sludge sedimentation ponds in Esch-Belval (Luxembourg).

Chemical analysis

pH value

The pH value of the BFS samples was determined in demineralized water and 0.01 M $CaCl_2$. Approximately 5 g of sample were weighed into a flask and spiked with 25 mL of solution. The sample were shaken for 1 h in a horizontal shaker (3006, GFL) at 200 rpm. The suspension was allowed to settle for 1 h and the pH value of the suspension was measured potentiometrically using a calibrated glass electrode (Sen TIX 81, WTW).

Elemental composition

Total C, N, and S were quantified by dry combustion with an elemental analyzer (Vario EL Cube CNS, Elementar). The evolved gases CO_2, sulfur dioxide (SO_2), and N_2 were measured by thermal conductivity. Samples with a pH value ≥ 6.5 were also indirectly analyzed for carbonate-carbon with the same equipment by initially adding 10% HCl to the sample. Carbonate-carbon was calculated from the difference between total C and total residual C (TRC). Residual C contains C in the form of coke, graphite, and black C.

Other elements were analyzed by wavelength dispersive X-ray fluorescence (XRF; Axios, PANalytical). Powdered samples were mixed with a flux material and melted into glass beads. To determine loss on ignition (LOI), 1000 mg of sample material were heated to 1030 °C for 10 min. After mixing the residue with 5.0 g of lithium metaborate and 25 mg of lithium bromide, it was fused at 1200 °C for 20 min. The calibrations were validated regularly by analysis of reference materials and 130 certified reference materials were used for the correction procedures. In the case of the elements Pb, Zn, and As, 50 mg of the samples were mixed with 800 mg of Na_2O_2 in a zircon crucible and heated over an open flame. After fusion, water was added and

the crucible was set into a water bath until the melting was dissolved. Hence, concentrated HNO_3 was added and the solution was transferred into a 100-mL flask, which was filled with water. The elemental contents were determined by inductive-coupled plasma emission spectrometry (Spectro Ciros CCD, Spectro Analytical Instruments).The samples were digested at low temperature to avoid gaseous loss of these elements.

Mercury was detected by means of a direct mercury analyzer (DMA-80, MLS GmbH). The samples were thermally decomposed at 750 °C in a continuous flow of analytical grade oxygen (O_2) and, hence, combustion products were carried off through a catalyst furnace where chemical interferences were removed. The Hg vapor was trapped on a gold amalgamator and subsequently desorbed for the spectrophotometric determination at 254 nm. A certified reference material for soil/sediments (CRM008-050, Resource Technology Corp., reference value: 0.072 µg kg^{-1}, confidence interval: 0.65 to 0.77 µg kg^{-1}, prediction interval: 0.79 to 0.85 µg kg^{-1}) was used for quality control (0.775 ± 0.05 µg kg^{-1}).

In order to check the solubility of Hg occurring in BFS, extracts with a neutral salt were obtained according to a modified DIN ISO 19730:2009-07 (2009) for samples with a total Hg content > 1.8 mg kg^{-1}. Therefore, 10 mL of 0.5 mol L^{-1} ammonium nitrate (NH_4NO_3) solution was added to 1.0 g of dry sample and shaken end-over-end (3040, GFL) for 24 h at 10 rpm. Subsequently, the extracts were centrifuged for 15 min at 1,700 g and decanted. Then, the extracts were stabilized by adding 100 µl of 0.2 mol L^{-1} BrCl according to US EPA (1999), and Hg was determined with the mercury analyzer mentioned above. We used a 0.5 mol L^{-1} NH_4NO_3 solution instead of 1.0 mol L^{-1} solution to reduce the salt amount introduced into the Hg analyzer.

Statistical evaluation

Statistical data evaluation was performed by the software IBM SPSS Statistics (Version 21). Basically, the non-parametric Spearman rank correlation coefficient was determined as a measure of the statistical dependence between variables.

Results and discussion

Elemental composition

The pH value of the BFS varied between 5.2 and 11.5 with a mean of 8.2 in $CaCl_2$-solution and between 5.3 and 11.7 with a mean of 8.4 in demineralized water (Table 1). The median of 8.2 and 8.4, respectively, indicated that weakly alkaline conditions dominated in dumped BFS. This is caused by carbonates added during the production process. Samples with a slightly acidic pH value presumably resulted from a modified composition of charge materials. During the production processes of these samples, the addition of calcareous charge materials was at least partially replaced by siliceous charge material. Strongly alkaline conditions of BFS are presumably caused by the presence of caustic lime (CaO).

The elemental composition of BFS was largely dominated by C (median 133 g kg^{-1}), Fe (median 149 g kg^{-1}), and O (median 240 g kg^{-1}) (Table 1), which resulted from the application of the charge material coke and Fe oxides. The air, which was blown through the blast furnace, dragged along coke and Fe ore particles, and thereby BFS reflects the process of pig iron production. However, C was also introduced by the addition of calcareous fluxes (e.g. limestone). The carbonate-carbon varied between 0.001 and 43.5 g kg^{-1} with a median of 17.7 g kg^{-1}, and the mean of carbonate-carbon with respect to total C was 16.2%.

 Further elements were detected in BFS with contents ranging from 100 to 10 g kg^{-1} (median): in descending order, Si, Ca, Zn, Al, Mn, Pb, and Mg (Table 1). These ele-

ments originated from impurities of the charge material which were mainly transported by the preheated air in the form of particles. However, the contents of Zn and Pb were clearly enriched in BFS (median 26.2 and 8.21 g kg^{-1}, respectively) as a result of their partial reduction in the vapor phase (Mansfeldt and Dohrmann, 2004). Due to the high temperatures at the bottom of the blast-furnace and their relatively low melting point, parts of the evaporated elements leave the blast furnace directly and hence are enriched in BFS. The median concentrations of K, N, Na, P, Ti, and S ranged from 6.29 to 0.640 g kg^{-1} (Table 1). Similarly to Zn and Pb, K, and Na were enriched in BFS due to their low melting points (63.4 and 97.7 °C, respectively).

Table 1 Chemical composition of blast-furnace sludge samples (n = 65)

Element	Unit	Mean	Median	Min	Max
pH$_{CaCl2}$			8.2	5.2	11.5
pH$_{H2O}$			8.4	5.3	11.7
LOI[a]	g kg^{-1}	275	277	5.80	563
O		248	240	45.1	518
C		157	133	1.08	480
TCC[b]		18.3	17.7	< 0.01	43.5
TRC[c]		139	111	1.44	473
Fe		154	149	5.32	623
Si		91.3	79.9	6.87	434
Ca		73.8	79.8	1.15	144
Zn		45.6	26.2	0.018	424
Al		33.2	33.9	0.320	63.6
Mn		12.8	4.47	0.070	217
Pb		10.7	8.21	0.015	66.9
Mg		10.6	10.7	0.640	23.2
K		8.45	6.29	0.230	37.3
S		6.45	3.39	0.390	33.2
N		3.60	2.50	0.100	26.5
Na		1.97	1.23	< 0.01	6.16

Table 1
Continuation

Element	Unit	Mean	Median	Min	Max
P	g kg^{-1}	1.68	1.60	0.180	5.86
Ti		0.773	0.640	0.010	2.86
Ba	mg kg^{-1}	887	647	< 59.0	7951
Sn		485	197	16.0	4912
Sr		188	169	10.0	651
Rb		175	117	6.00	816
Cr		164	79.0	8.00	4421
As		158	112	7.00	1454
Cu		155	58.0	< 7.00	1941
V		102	73.0	10.0	418
Bi		98.3	44.0	< 3.00	999
Cs		90.0	70.0	27.0	448
Ce		62.9	61.0	18.0	136
Zr		50.2	31.5	< 6.00	229
Sb		46.2	31.0	< 5.00	203
Ni		43.4	24.0	3.00	364
Th		38.6	35.0	< 4.00	91.0
W		38.5	14.0	< 5.00	159
La		38.4	35.5	14.0	78.0
Cd		36.2	33.5	5.60	95.3
Sm		33.8	33.0	< 18.0	53.0
Nd		30.0	30.0	< 13.0	33.0
Mo		28.9	22.0	< 3.00	293
Y		28.9	27.5	16.0	57.0
Ga		27.0	22.0	< 3.00	71.0
Hf		14.0	14.0	< 5.00	14.0
Co		13.1	11.0	3.00	33.0
Nb		9.90	8.50	< 2.00	49.0
Ta		9.00	9.00	< 5.00	< 21.0
Sc		8.50	6.00	3.00	25.0
U		8.10	8.00	< 4.00	13.0

[a] Loss on ignition   [b] Total carbonate-carbon   [c] Total residual carbon

Mercury in charge material

Mercury is a highly volatile element, which is readily transferred to the gaseous phase at low temperature (melting point: –38.8 °C). Consequently, Hg contained in any charge material may be enriched in the BFS.

Coke, as one of the major charge materials in blast furnaces, is processed by heating of coal in the absence of O_2 in coke ovens. It is well known that coal contains Hg in significant contents. The average Hg content of most coals varies between 0.05 and 0.1 mg kg^{-1} (Davidson and Claerke, 1996), but great variations are reported in the literature. Related to the geology of coal fields and the type of coal, Meij (1991) and Wang et al. (2000) reported values up to 1.95 mg kg^{-1} for coal from China (province of Shanxi), up to 1.78 mg kg^{-1} for coal from Poland, up to 0.95 mg kg^{-1} for Australian coal, up to 0.51 mg kg^{-1} for coal from the eastern U.S., and 0.16 mg kg^{-1} for German coal. However, it should be taken into account that during the coke oven operation there is a significant loss of Hg. Ma et al. (2010) reported that 25 to 28% of Hg was retained in coke after the coking process, 9 to 17% was present in byproducts such as tar and ammonia, and 55 to 66% was released into the atmosphere. This depletion is reflected in the current study, since the Hg content of the analyzed coke samples from Germany and Poland varied between 0.015 and 0.093 mg kg^{-1} (Table 2), which is well below the amount found in coal.

Additionally, it is known that Fe ores, another major charge material in the blast furnace operation, contain Hg as trace impurities. Similar to coke, the Hg contents vary as a function of the geology of Fe ore formation and type of Fe ore. Morey and Lively (1999) reported the Hg content of iron ores from Minnesota. The Hg contents of the samples (n = 191) ranged from 0.017 to 1.31 mg kg^{-1}, having a mean value of 0.0792 mg kg^{-1}. Fukuda et al. (2011) analyzed samples (n = 54) from different countries (Australia, India, Peru, and South Africa), finding a mean Hg value of 0.031 mg kg^{-1}

and a maximum Hg value of 0.108 mg kg^{-1}. Samples analyzed in this study had Hg contents of 0.047 and 0.02 mg kg^{-1} for the Fe ores and 0.02 mg kg^{-1} for the sinter, which are within the natural range of variation reported in the literature (Table 2). Mercury contents of the additives varied in a similar range to those of the Fe oxides. Olivine (($Mg,Fe)SiO_4$) had the lowest Hg content, with 0.015 mg kg^{-1}, followed by ilmenite ($FeTiO_3$), with 0.023 mg kg^{-1}, and gravel (SiO_2), with 0.049 mg kg^{-1}. Bauxite ($Al(OH)_3$, $AlO(OH)$, Fe_2O_3, $FeO(OH)$)) yielded the maximum value, with 0.068 mg kg^{-1}.

Table 2 Mercury contents in different materials [mg kg^{-1}]

	Number of samples	Mean	Median	Min.	Max.	Enrichment factor
Coke	3	0.059	0.062	0.014	0.097	1.05
Fe ores	2	0.035	0.044	0.019	0.048	0.625
Sinter	1	0.019 ± 0.0015[a]				0.339
Additives						
Olivine	1	0.015 ± 0.0017				0.268
Bauxite	1	0.068 ± 0.0018				1.21
Gravel	1	0.049 ± 0.0029				0.875
Ilmenite	1	0.023 ± 0.002				0.411
Blast furnace sludge	65	3.08	1.64	0.006	20.8	50
NH_4NO_3-soluble Hg in blast furnace sludge	28	0.006	0.002	0.0001	0.053	–
		0.747[b]	0.239	0.0197	6.322	–

[a] Standard deviation   [b] In µg L^{-1}

Mercury in blast furnace sludge

The total Hg content in BFS varied between 0.006 and 20.8 mg kg^{-1} with a median of 1.63 mg kg^{-1} (Table 2). The sample from the operating deposit site had a relatively high value of 10.3 mg kg^{-1}. Overall, Hg contents showed a quite large variability. To

the best of our knowledge no data on Hg in BFS have been published yet, so any comparison is hard to undertake. In comparison to the charge material, BFS was rather enriched with Hg, which was presumably a result of the accumulation of Hg in the vapor phase. This can be inferred from the enrichment factor (EF) which was calculated for Hg in BFS and charge materials compared to the abundance in the Earth's crust stated by Wedepohl (1995) (0.056 mg kg^{-1}). The EF for the charge materials ranged between 0.625 for Fe ores and 0.339 for the sinter product, 0.696 for the additives, and 1.05 for coke, while EF for the BFS samples was 50 (min.: 0.11; max.: 390). The lower EF for the sinter product in comparison to the Fe ores resulted from the production process: While the Fe ores were directly introduced to the blast furnace, the sinter educts were preheated between 800 and 1,400 °C depending on the ore composition. The correlation of Hg versus C (Fig. 3, illustrated in dark grey) for one site with a larger set of samples (Herne, Germany) showed a strong significance (r = 0.673, p ≤ 0.001, n = 31), indicating the function of coke as a major adsorbent. Mercury and TRC (Fig. 3, illustrated in light grey) showed a stronger correlation of r = 0.695 (p ≤ 0.001, n = 31), while the correlation of Hg versus TIC was negative (r = −0.542, p ≤ 0.001, n = 31). It can be assumed that compounds with a high fraction of residual C (e.g. coke, graphite) were hosting phases for Hg. Mansfeldt and Dohrmann (2004) found graphite contents in BFS up to 60 g kg^{-1} with a median of 27 g kg^{-1} by using Rietveld refinement of XRD analysis. A correlation of the Hg content versus the graphite content yielded a correlation coefficient of r = 0.614 (p = 0.02, n = 14). It is well described in the literature that Hg preferentially resides with organic matter in soils and sediments (Louchouarn et al., 1993; Dmytriw et al., 1995). Carbon-based sorbents are found to be most effective for the removal of Hg from flue gas. In comparison to metal sorbents, silica-alumina- or calcium-containing sorbents, and alkaline sorbents (De et al., 2013), carbon-based sorbents result in a removal of

more than 90% of total Hg (Lee and Park, 2003; Yan et al., 2003; McLarnon et al., 2005), which is mainly Hg^0 in gaseous phases.
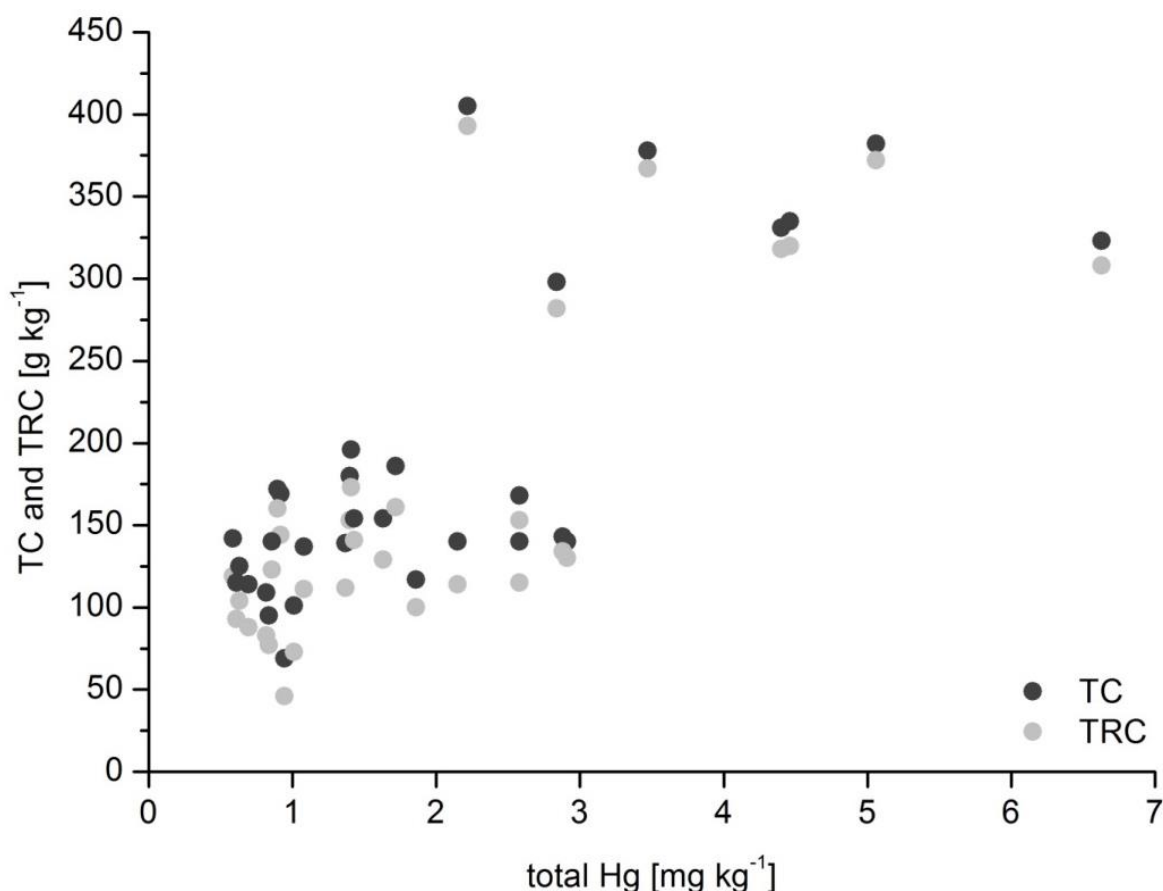

Fig. 3   Relationship between total mercury (Hg) and total carbon (TC, illustrated in dark grey) and total residual carbon (TRC, illustrated in light grey), respectively, (Herne, Germany). The Spearman correlation coefficient for Hg vs. TC is 0.69 (n = 32, p < 0.001) and that for Hg vs. TRC is 0.71 (n = 32, p < 0.001).

Activated carbon possesses an extended surface area and high surface reactivity (Diamantopoulou et al., 2010), but the Hg adsorption is not fully understood. As X-ray absorption fine structure (XAFS) spectroscopy showed, the adsorption of Hg on the sorbents' surface is dominated by anionic species, such as sulfides, chlorides, oxides, and iodides, which were present within the matrix or bound to the surface of the sorbent (Huggins et al., 2003). It was further suggested that chemisorption may be the primary adsorption mechanism. The XAFS results indicated that little or no Hg^0

was present after sorption, indicating oxidation processes by Hg bonding to anionic species of iodine, chlorine, sulfur, or oxygen on the carbon surface. Indeed, a significant correlation of Hg vs. S ($r = 0.501$; $p = 0.003$; $n = 31$) might underline this. Sasmaz et al. (2012) studied the bulk and chemical composition of brominated carbon surface reacted with Hg^0 by using extended XAFS and X-ray photoelectron spectroscopy (XPS). They found the oxidation state to be Hg^{2+} and that Hg^{2+} was bonded to two bromine atoms inside the C matrix with no detectable bonding to O. All this emphasizes the preference of Hg for C.

However, correlations of Hg versus C, TRC, and TIC of samples from all locations were relatively poor (Hg vs. C: $r = 0.222$, $p = 0.075$, $n = 65$; Hg vs. TRC: $r = 0.193$, $p = 0.123$, $n = 65$; Hg vs. TIC: $r = 0.039$, $p = 0.151$, $n = 65$). This leads to the assumption that although the same product was produced at all locations, a variety of charge materials, pre- and post-treatment processes, and production conditions were applied. Additionally, conditions of deposition and storage, such as climatic effects, may have affected the distribution of Hg in BFS during the last decades due to constant leaching and potential volatilization.

Soluble mercury in blast furnace sludge

The soluble Hg was determined in samples with total Hg contents > 1.8 mg kg^{-1} ($n = 27$) due to the fact that the soluble Hg of samples with lower contents ($n = 38$) was below the detection limit of the analytical equipment. Ammonium nitrate is the extracting agent of the standard national protocol in Germany for the determination of the mobile fraction of trace elements in soils (BBodSchV, 1999). This fraction should include the water-soluble and exchangeable Hg. Soluble Hg varied between 0.0197 and 6.321 µg L^{-1} with a median of 0.232 µg l^{-1}, corresponding to 0.0001 and 0.053 mg kg^{-1} with a median of 0.0017 mg kg^{-1} (Table 2). The correlation between

soluble Hg and total Hg (Fig. 4) yielded a rather low but statistically significant rela-
tion (r = 0.496; n = 27; p = 0.008).
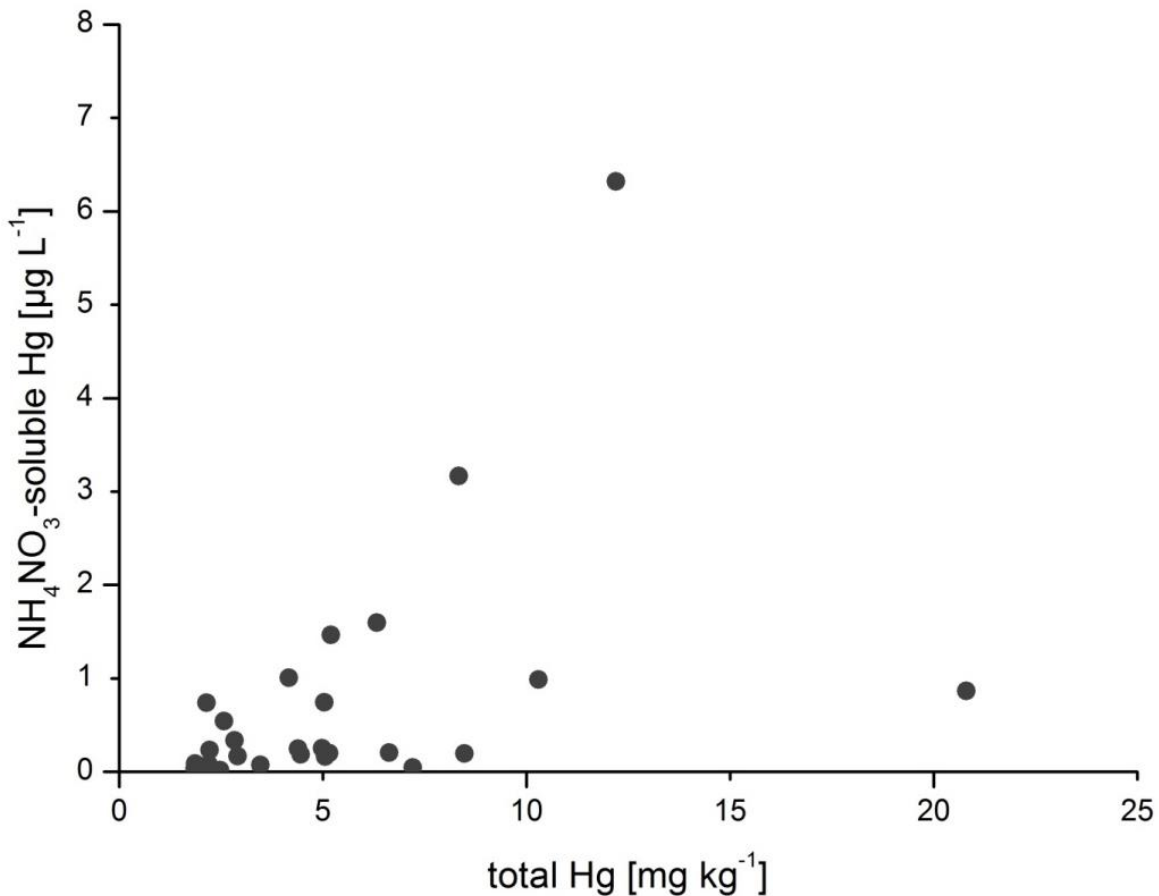
Fig. 4   Relationship between total mercury and NH_4NO_3-soluble mercury (Herne,
Germany). The Spearman correlation coefficient is 0.525 (n = 28, p =
0.004).

It is known from coal fly ashes that leaching of Hg typically occurs only in small
amounts (Graydon et al., 2009). Similar, the solubility of Hg in BFS was rather low
and did not exceed 0.43% of total Hg. Nevertheless, BFS poses special concern
even after decades with regard to the potentially mobilized Hg. According to the
WHO (2005), the guideline value for Hg in drinking water is 0.006 mg L^{-1}. Indeed,
only one sample out of 27 exceeded this value, but due to constant leaching into the
groundwater in the vicinity of the disposal sites, the groundwater may be contaminat-
ed with Hg, especially from a long-term perspective.

Conclusions

Blast furnace sludge can be regarded as hazardous waste since besides other elements Hg is significantly enriched in this waste, as proven in this study. Consequently, BFS poses a certain environmental threat, especially considering potential volatilization and leaching of toxic Hg species. Mercury in BFS deposit sites mainly resides with compounds with a high fraction of TRC. The adsorption processes of Hg on these compounds are still unknown and further studies should be undertaken.

References

AMAP/UNEP. Technical background report to the global atmospheric mercury assessment. Geneva, Switzerland: Arctic Monitoring and Assessment Programme / UNEP chemical Branch, 2008.

BBodSchV. Verordnung zur Durchführung des Bundes-Bodenschutzgesetzes (Bundes-Bodenschutz- und Altlastenverordnung - BBodSchV vom 16.07.1999. BGB1. I., 1554-1582, 1999.

Coudurier I, Hopkins DW, Wilkomirsky I. Fundamentals of metallurgical processes. Oxford: Pergamon Press, 1985.

Davidson R, Claerke L. Trace Elements in Coal. IEA Coal Research, London, 1996.

De M, Azargohar R, Dalai AK, Shewchuk SR. Mercury removal by bio-char based modified activated carbons. Fuel 2013; 103: 570-578.

Diamantopoulou I, Skodras G, Sakellaropoulos GP. Sorption of mercury by activated carbon in the presence of flue gas components. Fuel Processing Technology 2010; 91: 158-163.

DIN ISO 19730:2009-07. Gewinnung, Extraktion/Elution mobiler oder mobilisierbarer Fraktionen. Weinheim: Wiley-VCH, 2009.

Dmytriw R, Mucci A, Lucotte M, Pichet P. The partioning of mercury in the solid components of dry and flooded forest soils and sediments from a hydroelectric reservoir, Quebec (Canada). Water, Air, & Soil Pollution 1995; 80: 1099-1103.

Fukuda N, Takaoka M, Doumoto S, Oshita K, Morisawa S, Mizuno T. Mercury emission and behavior in primary ferrous metal production. Atmospheric Environment 2011; 45: 3685-3691.

Graydon JW, Zhang X, Kirk DW, Jia CQ. Sorption and stability of mercury on activated carbon for emission control. Journal of Hazardous Materials 2009; 168: 978-982.

Huggins FE, Yap N, Huffman GP, Senior CL. XAFS characterization of mercury captured from combustion gases on sorbents at low temperatures. Fuel Processing Technology 2003; 82: 167-196.

Lee SH, Park YO. Gas-phase mercury removal by carbon-based sorbents. Fuel Processing Technology 2003; 84: 197-206.

Lopez-Delgado A, Perez C, Lopez FA. Sorption of heavy metals on blast furnace sludge. Water Research 1998; 32: 989-996.

Louchouarn P, Lucotte M, Mucci A, Pichet P. Geochemistry of mercury in 2 hydroelectric reservoirs in Quebec, Canada Canadian Journal of Fisheries and Aquatic Sciences 1993; 50: 269-281.

Ma JJ, Yao H, Luo GQ, Xu MH, Han J, He XM. Distribution of Hg, As, Pb, and Cr in a Coke Oven Plant. Energery & Fuel 2010; 24: 5289-5290.

Mansfeldt T, Dohrmann R. Identification of a crystalline cyanide-containing compound in blast furnace sludge deposits. Journal of Environmental Quality 2001; 30: 1927-1932.

Mansfeldt T, Dohrmann R. Chemical and mineralogical characterization of blast-furnace sludge from an abandoned landfill. Environmental Science & Technology 2004; 38: 5977-5984.

McLarnon CR, Granite EJ, Pennline HW. The PCO process for photochemical removal of mercury from flue gas. Fuel Processing Technology 2005; 87: 85-89.

Meij R. The fate of mercury in coal-fired power-plants and the influence of wet flue-gas desulfurization. Water, Air, & Soil Pollution 1991; 56: 21-33.

Morey GB, Lively RS. Background levels of mercury and arsenic in Paleoproterozic rocks of the Mesabi iron range, northern Minnesota. Minnesota Geological Survey Information Circular 1999; 43.

Sasmaz E, Kirchofer A, Jew AD, Saha A, Abram D, Jaramillo TF, et al. Mercury chemistry on brominated activated carbon. Fuel 2012; 99: 188-196.

Trömel G, Zischkale W. Gmelin-Durrer: Metallurgie des Eisens. Vol 3. Weinheim, Germany: Verlag Chemie, 1971.

Trung ZH, Kukurugya F, Takacova Z, Orac D, Laubertova M, Miskufova A, et al. Acidic leaching both of zinc and iron from basic oxygen furnace sludge. Journal of Hazardous Materials 2011; 192: 1100-1107.

UNEP. Global Mercury Assessment 2013: Sources, Emissions, Releases and Environmental Transport. Geneva, Switzerland: UNEP Chemicals Branch, 2013.

US EPA. Method 1631, Mercury in water by oxidation, purge and trap, and cold vapor atomic flourescence spectrometry. US EPA 821-R-95-027, 1999.

Van Herck P, Vandecasteele C, Swennen R, Mortier R. Zinc and lead removal from blast furnace sludge with a hydrometallurgical process. Environmental Science & Technology 2000; 34: 3802-3808.

Wang Q, Shen WG, Ma ZW. Estimation of mercury emission from coal combustion in China. Environmental Science & Technology 2000; 34: 2711-2713.

Wedepohl KH. The composition of the continental crust. Geochimica et Cosmochimica Acta 1995; 59: 1217-1232.

WHO. Mercury in drinking-water. Background document for develoment of WHO Guidelines for drinking-water quality. Geneva: World Health Organisation (WHO/SDE/WSH/05.08/10), 2005.

World Steel Association. Annual direct reduced iron production, 2013. http://www.worldsteel.org/statistics/statitistic-archive/annual-iron-archive.html, 2013-10-09

Yan R, Ng YL, Liang DT, Lim CS, Tay JH. Bench-scale experimental study on the effect of flue gas composition on mercury removal by activated carbon adsorption. Energery & Fuel 2003; 17: 1528-1535.

Chapter 3   Sequential extraction of inorganic mercury in dumped blast furnace sludge

Co-author: Corlin-Anna Andrée & Tim Mansfeldt

Abstract

Blast furnace sludge (BFS) is an industrial waste with elevated mercury (Hg) contents due to the enrichment during the production process of pig iron. To investigate the potential pollution status of dumped BFS, 14 samples with total Hg contents ranging from 3.91 to 20.8 mg kg^{-1} from five different locations in Europe were sequentially extracted. Extracts used included demineralized water (Fraction 1, F1), 0.1 mol L^{-1} CH_3COOH + 0.01 mol L^{-1} HCl (F2), 1 mol L^{-1} KOH (F3), 7.9 mol L^{-1} HNO_3 (F4), and aqua regia (F5). The total recovery ranged from 72.3 to 114%, indicating that the procedure was reliable when adapted to this industrial waste. Mercury mainly resided in the fraction of "elemental" Hg (48.5–98.8%) rather being present as slightly soluble Hg species associated with sludge particles. Minor amounts were found as mercuric sulfide (F5; 0.725–37.3%) and Hg in crystalline metals ores and silicates (F6; 2.21–15.1%). The ecotoxically relevant fractions (F1 and F2) were not of significance (F1: < limit of quality; F2: 0.509–9.61%, n = 5). Thus, BFS dumped for many years has a rather low environmental risk potential regarding Hg.

Introduction

Blast furnace sludge (BFS) is a waste generated in the production of pig iron. During the metallurgical process, charge material, such as iron (Fe) ores, high carbon (C) fuels (e.g. coke), and flux additives, are smelted in the blast furnace at temperatures up to 2200 °C. By combusting the coke, both the required melting temperature and the formation of reaction gases are accomplished. The reaction gases, mainly emerging carbon monoxide (CO) and molecular hydrogen (H_2), reduce the Fe from the ore and change it into its metallic form. During combustion, the reaction gases drag along solid phases of the charge material and their reaction products and leave the top of the blast furnace. These are composed of roughly 49% molecular nitrogen (N_2), 22% carbon dioxide (CO_2), 23% CO, 3% H_2, and 3% water (H_2O) (Peacey and Davenport, 1979). Furthermore, the gases contain significant amounts of lead (Pb), potassium (K), sodium (Na), and zinc (Zn) (Trömel and Zischkale, 1971; Van Herck et al., 2000; Mansfeldt and Biernath, 2001; Mansfeldt and Dohrmann, 2004; Trung et al., 2011), which cannot be exclusively explained by a mechanism based on mechanical transport by reaction gases (Mansfeldt and Dohrmann, 2004) but rather results from internal enrichment. These elements are partially reduced during the metallurgical process due to the high temperatures and their relatively low melting point. As a consequence, the effluent gases are enriched in volatile elements.

As the effluent gas has a calorific value of 3300 to 4000 kJ m³ (Mansfeldt and Dohrmann, 2004), it is reused for generating electricity. Therefore, and because 30 kg of dust per Mg of pig iron are generated, the gases must be purified from the dust. As a result of wet purification, a muddy waste is generated which is referred to as BFS. Lopez-Delgado et al. (1998) stated that 6 kg of BFS per Mg of pig iron were produced during the late 1990s. Based on that and on an annual worldwide production of 1,168 · 10⁶ Mg pig iron (World Steel Association, 2014), approximately

$7 \cdot 10^6$ Mg of BFS are sent for actual disposal or deposition. Nevertheless, this waste was dumped in large surface landfills in industrial areas until the commencement of strict environmental laws in the 1960s and 1970s in Europe. However, this might be an ongoing procedure in countries with less strict environmental laws. As these wastes often contain harmful substances as outlined above, significant hazards to environmental surroundings may arise from former BFS sedimentation ponds.

Mercury (Hg) is considered as one of the most important environmental pollutants, as the element and many of its compounds are highly toxic, persistent, and readily released into the environment due to their high mobility and volatility (WHO, 2005). Besides artisanal and small-scale gold production, coal combustion is the largest point source of anthropogenic Hg, as coal always contains some Hg (the average content of most coal varies between 0.05 and 0.1 mg kg^{-1} (Davidson and Claerke, 1996) and due to the major role of coal combustion (40% of the total primary energy consumption (International Energy Agency, Coal Information 2014) for the global energy production.

Considering the enrichment with elements such as K, Na, Pb, and Zn it was postulated that BFS is enriched with the highly volatile transition metal Hg as well.

In our previous work (Foeldi et al., 2014), we analyzed 65 BFS samples from seven different locations in Europe, proving the enrichment of Hg in most samples. The content ranged from 0.006 up to 20.8 mg kg^{-1} (median: 1.63 mg kg^{-1}; mean: 3.08 mg kg^{-1}) while the calculated enrichment factor was 50 (min: 0.11; max: 390). This factor was calculated by comparing the Hg content of each BFS sample with the Earth´s crust abundance of Hg (0.056 mg kg^{-1}) as stated by Wedepohl (1995). However, this data does not provide any information about potential mobilization of Hg and, hence, the potential environmental risk.

Sequential extraction procedures (SEP) are frequently used to determine the association of potentially toxic elements with specific phases such as mineral and organic matter. Although SEPs have several disadvantages (lack of selectivity of reagents, re-adsorption and redistribution of elements previously solubilized, incomplete dissolution, non-homogeneity of samples) as summarized by Bacon and Davidson (2008), the merits of SEP dominate: They facilitate the evaluation of the potential mobility of the elements and their environmental accessibility, as well as their plant available fraction. However, most of the SEPs for metals and semimetals are not suitable for Hg. Therefore, Bloom et al. (2003) developed an Hg-specific procedure for soils and sediments by cross-checking already published SEPs. Based on extraction kinetics and the effects of solid-to-liquid ratios, they developed and validated a five-step Hg-specific SEP. This procedure makes it possible to distinguish inorganic Hg into operationally defined behavioral classes. Despite the fact that this procedure was developed for soils and sediments, it was also conducted on other solid matrices and wastes. For instance, coal (Yuan et al., 2010), coal fly ash, and slag (Wei et al., 2011) were analyzed for Hg fractionation, yielding reliable and repeatable data. The objective of this study is the differentiation of inorganic Hg compounds into various biochemical fractions (behavioral classes) to assess the risk potential of Hg in BFS.

Materials and methods

Sampling sites, sampling, and sample preparation

Sampling sites and sampling were illustrated in detail previously (Foeldi et al., 2014). Briefly, 14 samples out of 65 samples from six former BFS sedimentation ponds and one operating BFS deposit in Europe were studied: Herne and Dinslaken (operating) in the Ruhr area (Germany), Eisenhüttenstadt (Germany), Lübeck (Germany), Nowa Huta (Krakow, Poland), and Nancy (France). The field-moist samples were dried at

room temperature, sieved to a size fraction < 2 mm, and manually homogenized. No material > 2 mm was present. For the analysis of element contents, subsamples were ground to analytical grain size in an agate ball mill (PM 400, Retsch).

Chemical analysis

pH value

The pH value of the BFS samples was determined in 0.01 M $CaCl_2$. Approximately 5 g of sample were weighed into a flask and 25 mL of solution was added. The samples were shaken for 1 h in a horizontal shaker (3006, GFL) at 200 rpm. The suspension was allowed to settle for 1 h and the pH value of the suspension was measured potentiometrically using a calibrated glass electrode (Sen TIX 81, WTW).

Elemental composition

Total C, nitrogen (N), and sulfur (S) were quantified by dry combustion with an elemental analyzer (Vario EL Cube CNS, Elementar). The evolved gases CO_2, sulfur dioxide (SO_2), and N_2 were measured by thermal conductivity. Samples with a pH value ≥ 6.5 were also indirectly analyzed for total carbonate-carbon with the same equipment by initially adding 10% hydrochloric acid (HCl) to the sample. Carbonate-carbon was calculated from the difference between total C and total residual C (TRC). Residual C contains C in the form of coke, graphite, and black C.

Other elements were analyzed by wavelength dispersive X-ray fluorescence (XRF; Axios, PANalytical). Powdered samples were mixed with a flux material and melted into glass beads. To determine loss on ignition (LOI), 1000 mg of sample material were heated to 1030 °C for 10 min. After mixing the residue with 5.0 g of lithium metaborate ($Li_2B_4O_7$) and 25 mg of lithium bromide (LiBr), it was fused at 1200 °C for

20 min. The calibrations were validated regularly by analysis of reference materials and 130 certified reference materials were used for the correction procedures.

Sequential extraction procedure

The SEP for soils and sediments developed by Bloom et al. (2003) and modified by Hall et al. (2005) was adapted to BFS samples. Samples with rather high total Hg contents were chosen for the SEP to ensure quantifiable Hg contents values in the fractions. This procedure allows inorganic Hg to be assigned into operationally de-fined behavioral classes (Table 1): water soluble Hg, "human stomach acid" soluble Hg, organo-chelated Hg, "elemental" Hg, and mercuric sulfides. An additional sixth fraction was received by composting (see below) the residual representing Hg in crystalline metal ores and silicates. For F1 to F5 the following solutions were pre-pared (Table 1) using chemicals of analytical grade: F1, demineralized water; F2, 0.1 mol L^{-1} CH_3COOH + 0.01 mol L^{-1} HCl; F3, 1 mol L^{-1} KOH; F4, 7.9 mol L^{-1} HNO_3; and F5, aqua regia (conc. HCl : conc. HNO_3, 10:3). The original protocol was slightly modified by Hall et al. (2005) for F4 by reducing the concentration from 12 to 7.9 mol L^{-1} HNO_3. Demineralized water used for dilution was generated by reverse osmosis (min. 18.2 MΩ), and stored in PET bins for at least one week. In the follow-ing, this is referred to as Hg-free water. All the vials, bottles, and storage bins used for the procedure were prepared using special cleaning protocols: After cleaning by a laboratory washing machine, all vessels were binned in an acid bath (Hg-free water and HNO_3, pH≤1) for at least 24 hours, flushed out with Hg-free water, and stored with stabilized water (0.1 µl BrCl L^{-1}). Bromine monochloride (BrCl) was prepared for stabilization of Hg according to the US EPA (1999). Briefly, 2.7 g of potassium bro-mide (KBr) were dissolved in 250 ml of conc. HCl, and stirred for 1 h under a fume hood. Then, 3.8 g of potassium bromate ($KBrO_3$) were slowly but continuously added

to the acid mixture. The solution should change from yellow to red to orange. The bottle was loosely capped, and stirred for another hour before tightening the lid.

Table 1   Sequential extraction scheme including behavioral classes of mercury according to Bloom et al. (2003) and modified by Hall et al. (2005)

	Extracting agent		Behavioral classes
F1	Hg-free water		water soluble Hg
F2	"human stomach acid"	0.1 mol L^{-1} CH_3COOH $+ 0.01$ mol L^{-1} HCl	"human stomach acid" soluble Hg
F3	potassium hydroxide	1 mol L^{-1} KOH	organo-chelated Hg & calomel
F4	nitric acid	7.9 mol L^{-1} HNO_3	"elemental" Hg
F5	aqua regia	conc. HCl : conc. HNO_3 (10:3)	mercuric sulfide
F6	residual		Hg in crystalline metal ores & silicates

Extractions were carried out by weighing 0.4 ± 0.04 g of sample in 50 ml vials. An aliquot of 40 ml of the respective extractant was added to the sample, shaken in an end-to-end shaker (3040, GFL) for 18 ± 4 h, centrifuged at 1,600 g (Rotina 46, Hettich) for 20 min, and the supernatant liquid was decanted for vacuum filtration through a 0.4 µm cellulose nitrate filter. The extractions were placed into 125 ml trace metal clean borosilicate bottles with PTFE-lined caps and immediately stabilized using 1.25 ml of 0.2 mol L^{-1} BrCl. Deviating from that, F3 was oxidized by the addition of 10.0 ml BrCl due to the high acid neutralizing capacity of the specific extractant. Then, the BFS residues were refilled with the same extractant, shaken vigorously to resuspend, re-centrifuged, and filtered as before. This rinse step was then added to the extract from the same sample, diluted to 125 ± 1 ml with Hg-free water, and stored at 4 °C in a refrigerator until analysis. Afterwards, the next extractant was added to the sample residue and the described procedure was repeated. For F5, 10 ml of conc. HCl and 3 ml of conc. HNO_3 were added to the remaining BFS pellet

from F4. The vials were loosely capped and allowed to digest overnight under a fume hood. Then, the pellets and extractants were diluted to 40 ml with Hg-free water. As a significant residue remained after digestion, the extractant was filtered through qualitative filter paper (medium filtration rate, particle retention: 5 to 13 μm, Sartorius). While the liquid phase represented F5, the residual fraction remained in the filter, was dried, carefully scraped from the filter paper, and Hg in this fraction (F6) was determined in the solid phase.

Mercury in all fractions and total Hg were analyzed by means of a direct Hg analyzer (DMA-80, MLS GmbH). The samples were thermally decomposed at 750 °C in a continuous flow of analytical grade oxygen (O_2) and, hence, combustion products were carried off through a catalyst furnace where chemical interferences were removed. The Hg vapor was trapped on a gold amalgamator and subsequently desorbed for the spectrophotometric determination at 254 nm. The SEP was conducted in three replications per sample, and the determination of Hg was carried out in four replications per sample. Limit of quality (LOQ) was calculated by the mean value of ten blanks added to the nine-fold standard deviation. Repeatability was determined for sample #2116 with F4 (mean 3.43 mg kg^{-1} Hg), F5 (0.32 mg kg^{-1} Hg), and F6 (0.22 mg kg^{-1} Hg) (the other fractions were below LOQ) at four subsequent days and standard deviations were found to be 0.22 (relative standard deviation 6.7%), 0.05 (16.1%), and 0.02 (9.2%) mg kg^{-1} Hg. A certified reference material for soil/sediments (REF; CRM008-050, Resource Technology Corp., reference value: 0.72 mg kg^{-1}, confidence interval: 0.65 to 0.77 mg kg^{-1}, prediction interval: 0.79 to 0.85 mg kg^{-1}) was used for quality control both in the SEP (F4: 0.655 ± 0.063 mg kg^{-1}; F6:0.020 ± 0.001 mg kg^{-1}; other fractions below LOQ) and for analysis of total Hg (0.775 ± 0.05 mg kg^{-1}).

Statistical evaluation

Statistical data evaluation was performed by the software IBM SPSS Statistics (Version 21). Basically, the non-parametric Spearman rank correlation coefficient was determined as a measure of the statistical dependence between variables.

Results and discussion

Elemental composition

The pH value of the BFS analyzed in this study varied between 6.1 and 10.2 with a mean of 8.3 (Table 2). The median of 8.1 indicated that weakly alkaline conditions dominated in the dumped BFS. This is caused by carbonates added during the production process. Samples with a slightly acidic pH value presumably resulted from a modified composition of charge materials. During the production processes of these samples, the addition of calcareous charge materials was at least partially replaced by siliceous charge material. Strongly alkaline conditions of BFS are presumably caused by the presence of caustic lime (CaO).

The elemental composition of BFS was largely dominated by C (median 114 g kg^{-1}) and Fe (median 83 g kg^{-1}) (Table 2), resulting from the charge material coke and Fe oxides. The air that was blown through the blast furnace dragged along coke and Fe ore particles, and thereby BFS reflects the process of pig iron production. However, C was also introduced by the addition of calcareous fluxes (e.g. limestone). Carbonate-carbon varied between 4.21 and 37.1 g kg^{-1} with a median of 15.1 g kg^{-1}, and the mean of carbonate carbon with respect to total C was 31.8%.

 Further elements were detected in BFS with contents ranging from 100 to 5 g kg^{-1} (median): in descending order, silicon (Si), calcium (Ca), aluminum (Al), Zn, Pb, magnesium (Mg), K, and manganese (Mn) (Table 2). These elements originated from

Table 2 Selected chemical characteristics of blast furnace sludge

Sample	pH$_{CaCl_2}$	C [g kg^{-1}]	TIC [g kg^{-1}]	TOC [g kg^{-1}]	S [g kg^{-1}]	Fe [g kg^{-1}]	Si [g kg^{-1}]	Al [g kg^{-1}]	K [g kg^{-1}]	Na [g kg^{-1}]	P [g kg^{-1}]	Pb [g kg^{-1}]	Zn [g kg^{-1}]
#2076	6.2	130	37.1	92.3	4.91	-	-	-	-	-	-	-	-
#2153	7.9	465	4.21	461	12.9	220	26.3	13.8	11.4	1.48	6.75	3.64	21.9
#2116	8.0	335	15.0	320	10.6	82.8	80.5	38.7	6.75	0.220	8.38	10.4	37.9
#2119	8.1	331	13.0	318	14.6	79.3	85.3	33.7	8.38	<0.01	3.99	18.3	64.7
#2120	7.8	268	10.2	258	4.50	152	96.1	34.0	3.99	0.300	8.33	19.5	43.0
#2121	8.0	382	9.90	372	9.60	112	87.8	38.8	8.33	0.590	11.4	6.73	27.2
#2188	10.2	97.8	34.9	62.9	2.00	143	84.1	44.5	17.4	3.12	17.4	8.16	26.6
#2225	6.1	480	6.78	473	33.2	188	24.5	12.7	6.20	0.070	6.20	1.27	31.9
#2230	8.3	6.46	4.31	2.15	0.70	617	6.87	0.320	0.460	<0.01	0.46	3.04	32.9
#2241	7.8	37.6	15.2	22.4	1.50	35.2	93.1	47.2	2.52	<0.01	2.52	36.7	41.6
#2242	7.9	59.8	31.9	28.0	2.80	75.5	90.5	51.7	7.36	0.740	7,36	30.6	24.5
#2243	8.3	30.6	19.2	11.4	1.80	26.5	80.0	55.3	6.38	<0.01	6.38	5.95	22.3
#2244	8.2	25.0	28.1	20.0	2.40	60.5	94.6	63.6	7.68	<0.01	7.68	13.9	26.3
#2245	8.2	48.0	16.8	8.21	3.10	10.7	79.3	40.5	9.74	<0.01	9.74	10.2	7.12

impurities of the charge material which were transported by the preheated air in the form of particles as already mentioned above. However, the contents of Zn and Pb were clearly enriched in the BFS (median 27.2 and 10.2 g kg^{-1}, respectively) as a result of their partial reduction in the vapor phase as outlined above. The median concentrations of S, N, phosphorus (P), Na, and titanium (Ti) ranged from 3.79 to 0.500 g kg^{-1} (Table 2). Similarly to Pb and Zn, K, and Na were enriched in the BFS due to their low melting points (63.4 and 97.7 °C, respectively).

Sequential extraction procedure

The total Hg content of the BFS samples ranged from 3.91 to 20.8 mg kg^{-1} with a median of 5.15 mg kg^{-1} (Table 3). The recovery of Hg obtained as the sum of Hg in each fraction was between 72.3 and 114%. As this method was originally designed for soils and sediments, this range indicates that the method can be successfully used to assess the fraction of inorganic Hg in BFS. Lower recoveries may result from hydrophobic characteristics of several samples. After the addition of Hg-free water, several samples partially separated into a fraction of material floating in the vial and a fraction that settled at the bottom or remained in suspension, respectively. During filtration after each step, the floating fraction was captured in the filter membranes and, hence, the Hg potentially contained could not be determined in the subsequent extraction steps. Unfortunately, the captured floating fraction contained too little ma-terial for further analyzes. Most likely, this fraction was dominated by hydrophobic C rich compounds (e.g. char or graphite). Graphite was previously determined in BFS by (Mansfeldt and Dohrmann, 2004). As C rich compounds are known as effective Hg sorbent, Hg sorbed onto the floating fraction was eliminated from the potential Hg pool. As Al-Abed et al. (2008) showed in the floating fraction of flue gas desulphuriza-tion (FGD) residue, the lighter fraction was less than 0.01 wt. % but was

Table 3 Total Hg and different Hg fractions in blast furnace sludge

sample	total Hg [mg kg^{-1}]	F1 [mg kg^{-1}]	F2 [mg kg^{-1}]	F3 [mg kg^{-1}]	F4 [mg kg^{-1}]	F5 [mg kg^{-1}]	F6 [mg kg^{-1}]	recovery [%]
#2076	5.14 ± 0.213*	< LOQ**	< LOQ	< LOQ	2.56 ± 0.321	1.92 ± 0.141	0.794 ± 0.048	103
#2153	9.68 ± 0.102	< LOQ	< LOQ	< LOQ	10.0 ± 0.123	0.380 ± 0.027	0.236 ± 0.012	110
#2116	4.41 ± 0.259	< LOQ	< LOQ	< LOQ	3.46 ± 0.175	0.291 ± 0.027	0.217 ± 0.010	89.9
#2119	3.91 ± 0.200	< LOQ	< LOQ	< LOQ	3.72 ± 0.100	0.997 ± 0.013	0.134 ± 0.007	101
#2120	20.8 ± 0.172	< LOQ	< LOQ	< LOQ	18.2 ± 0.573	2.83 ± 0.402	0.911 ± 0.023	106
#2121	4.82 ± 0.091	< LOQ	< LOQ	< LOQ	4.05 ± 0.088	0.214 ± 0.014	0.149 ± 0.012	91.5
#2188	5.16 ± 0.085	< LOQ	0.032 ± 0.009	< LOQ	3.74 ± 0.390	< LOQ	0.171 ± 0.012	76.4
#2225	11.4 ± 0.314	< LOQ	< LOQ	< LOQ	8.29 ± 0.303	< LOQ	0.547 ± 0.003	77.6
#2230	4.00 ± 0.119	< LOQ	< LOQ	< LOQ	2.77 ± 0.296	0.848 ± 0.281	0.169 ± 0.050	94.7
#2241	4.90 ± 0.098	< LOQ	0.207 ± 0.006	< LOQ	3.26 ± 0.285	< LOQ	0.078 ± 0.010	72.3
#2242	19.5 ± 0.818	< LOQ	< LOQ	< LOQ	12.0 ± 0.295	7.41 ± 0.078	0.466 ± 0.041	102
#2243	4.75 ± 0.129	< LOQ	0.453 ± 0.031	< LOQ	4.26 ± 0.400	< LOQ	< LOQ	99.2
#2244	6.21 ± 0.073	< LOQ	0.035 ± 0.005	< LOQ	6.97 ± 0.421	0.051 ± 0.005	< LOQ	114
#2245	8.01 ± 0.258	< LOQ	0.061 ± 0.005	< LOQ	7.93 ± 0.295	< LOQ	0.952 ± 0.061	112
REF	0.72 ± 0.023	< LOQ	< LOQ	< LOQ	0.655 ± 0.063	< LOQ	0.020 ± 0.001	93.7

* Standard deviation calculated from three replications

** Limit of quality (µg kg^{-1}; F1: 0.134; F2: 0.135; F3: 3.89; F4: 1.95; F5: 1.47)

enriched with Hg almost 100 times (115 mg kg^{-1}). As the flue gas temperature decreases along the combustion process, the fine particles act as condensation nuclei for Hg, thereby enriching their Hg content. Also their high surface area provides high potential for physical and chemical adsorption of Hg. Similar processes are conceivable and reasonable during the metallurgical process yielding BFS. However, not all samples with low recovery showed a hydrophobic characteristic and vice versa.

Although the obtained data provided only limited information about the binding forms of Hg in BFS, it yielded some useful details about the mobility and bioavailability (Fig. 1). Mercury in BFS primarily resided in F4, which accounted for a median of 91.1% (4.16 mg kg^{-1}, n = 15), ranging from 48.5 up to 98.8% (2.56 to 18.2 mg kg^{-1}; Tab. 3). It is known from coal post-combustion flue gas that Hg exists in three principal forms: particulate Hg, elemental Hg (Hg^0) in gas phase, and gas phase oxidized Hg (Hg^{2+}) (Galbreath and Zygarlicke, 2000). During the combustion of coal, all forms of Hg are vaporized through thermal decomposition and hence converted to Hg^0. As the coal flue gas cools, Hg^0 can be oxidized under appropriate conditions and is potentially absorbed into fly ash (Galbreath and Zygarlicke, 2000). Similar processes can be expected in blast furnace gas and it's cooling, respectively, as it is well known that carbon based sorbents are most effective for Hg adsorption (McLarnon et al., 2005). During the wet purification the particles are washed out and captured in BFS, resulting in elevated Hg contents in BFS. However, it is rather unlikely that Hg extracted in F4 is actually Hg^0 as BFS remained in the sedimentation ponds for decades and it is known to easily vaporize at room temperatures. Consequently, Hg^0 would have already degased during the deposition period. Most likely, Hg extracted in F4 was present as inorganic Hg^{2+} compounds and adsorbed Hg^{1+} und Hg^{2+} species (Liu et al., 2006).
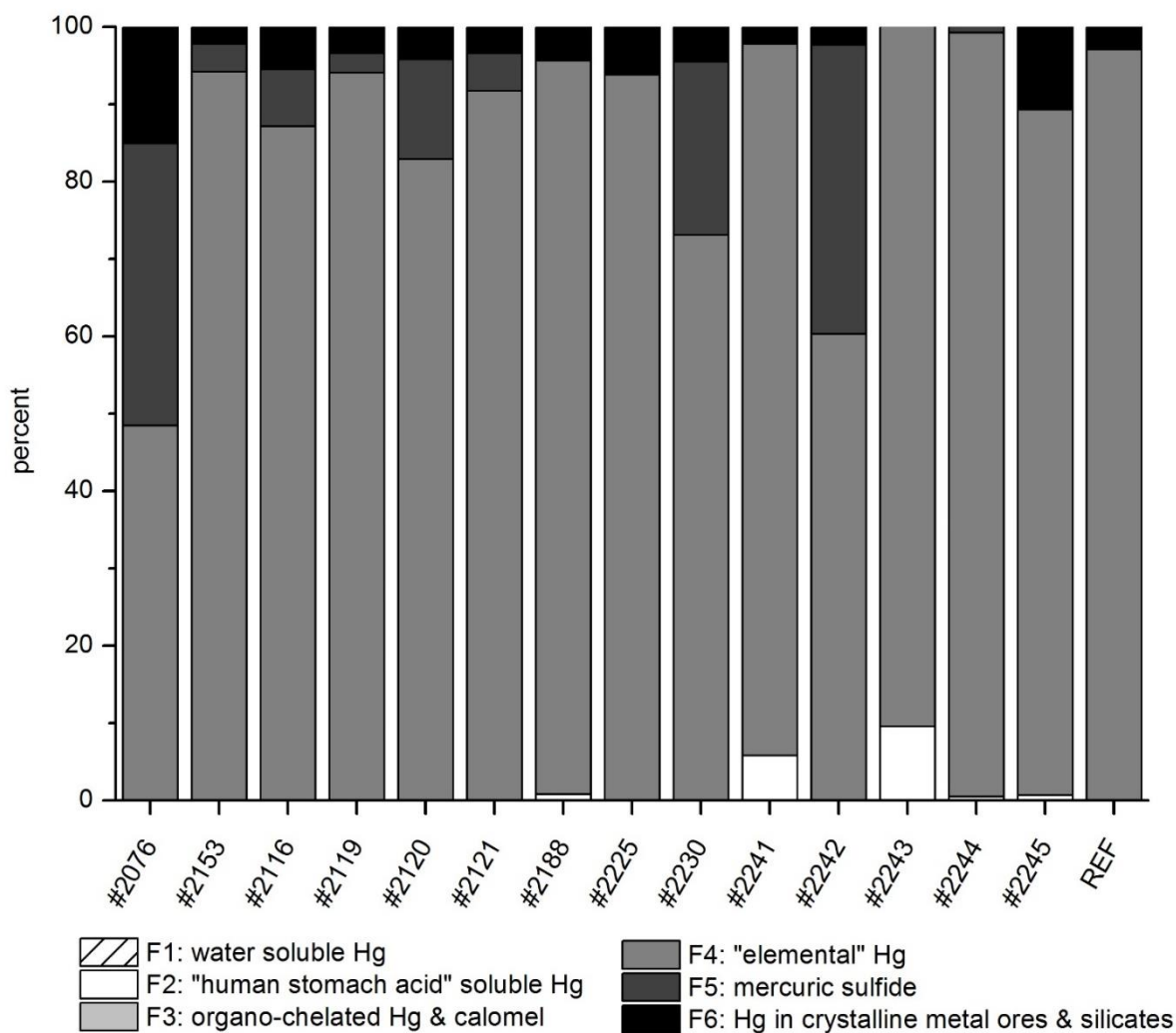
Fig. 1   Extraction fingerprint in blast furnace sludge from different locations in Europe (Lübeck: #2076; Dinslaken: #2153, Herne: #2116 to #2188; Eisenhüttenstadt: #2225; Nowa Huta: #2230; Nancy: #2241 to #2245)

Sulfide-Hg (F5) accounted for from 0.725 to 37.3% (0.051 to 7.41 mg kg^{-1}) with a median of 7.34 % (0.848 mg kg^{-1}; n = 10), whereas the residual fraction (F6) accounted for up to 15.1% (0.951 mg kg^{-1}) with a median of 4.25% (0.227 mg kg^{-1}; n = 13). Mercury in these three fractions is not hazardous to the environment because of its low mobility and bioavailability under natural water regime conditions.

The first fractions (F1 – F3) contributed nothing or little to the total Hg in BFS: Whereas F1 and F3 were below the LOQ (0.134 and 3.89 µg kg^{-1}, respectively) in all samples, F2 ranged between 0.509 and 9.61% (0.032 to 0.452 mg kg^{-1}; median:

0.802% and 0.061 mg kg^{-1}, respectively; n = 5). Both fractions represent ecotoxically relevant amounts of Hg in BFS as these correspond theoretically to diluted acid and water extractable Hg, such as Hg(II) chloride ($HgCl_2$), Hg(II) sulfate ($HgSO_4$), Hg(II) nitrate ($Hg(NO_3)_2$), and Hg(II) oxide (HgO). Both scenarios, the input of weak acids and salts via precipitation or wet deposition, are prevalent under natural conditions. Low proportions of these fractions either indicate a rather low environmentally haz-ardous potential of BFS or that these fractions were already leached out during dep-osition and storage at the dumpsites. Also, the volatilization of Hg from the dumped BFS is reasonable. This SEP was also used by Yuan et al. (2010) to fractionate Hg in ten coal samples from China, yielding a similar distribution pattern (dominance of F4 and F5) and total recoveries (86 to 116%). However, they found notable amounts of organic matter-bounded Hg (5.5 to 30%) in the coal. During the subsequent coking pyrolysis or at latest during combustion of coke in the blast furnace, organic matter-bounded Hg was most likely translated to Hg^0 or particulate Hg, resulting in minimum values of F3. As the input of chlorine (Cl) to the pig iron production process was lim-ited, and more than 95% of Cl present in coal was liberated as HCl gas during the coking process (Shao et al., 1994), it is reasonable that there was no presence of F3 in BFS.

Mercury in coal fly ash and slag amongst others was sequentially extracted by Wei et al. (2011) using the same procedure as in this study. For the coal fly ash, Hg^0 was the dominating fraction (85.3–90.6%), followed by from 6.0 to 13.2% of Hg in F5, and less than 2.6% for organo-chelated Hg and 0.9% for human stomach acid soluble Hg, respectively. Fractionation patterns in slag were different: Hg existed primarily in the sulfidic fraction (59%), whereas 23.1% was found in F4 and 15.4% in F3. Although these wastes differ significantly in their chemical composition from BFS (Li et al., 2014; Shaheen et al., 2014), they have in common the highest abundance of Hg ei-

ther in F4 or F5. In addition, the minor relevance of the ecotoxically fractions F1 and F2 in all materials is obvious.

While we could show a strong significance between total Hg and C and total residual C, respectively, in our previous work (Foeldi et al., 2014), such correlations were not found to be significant with this set of samples. We expected high correlations between fractional Hg with elements such as Fe, S, or C indicating a certain binding form, but no such correlation was given. As we concluded in our previous work, this may be attributed to the variation of charge material, pre- and post-treatment processes, and/or production and deposition conditions. However, we found a significant (significance level: 0.05) correlation between F6 (%) vs. Si ($r = 0.645$, $p = 0.032$, $n = 11$). Blast furnace sludge mainly consists of calcite ($CaCO_3$), hematite (α-Fe_2O_3), magnetite (Fe_3O_4), wüstite (FeO), and quartz (SiO_2). In minor amounts, the mineral composition includes graphite, α-Fe, dolomite ($CaMgCO_3$), siderite ($FeCaO_3$), and maghemite (γ-Fe_2O_3) (Van Herck et al., 2000; Mansfeldt and Dohrmann, 2004; Das et al., 2007; Trung et al., 2011). It is known that crystalline metal ores such as bauxite ($Al(OH)_3$, AlO(OH), γ-Fe_2O_3, FeO(OH)), and α-Fe_2O_3 remained after aqua regia digestion (Bloom et al., 2001). The same also applies for silicates like SiO_2. Consequently, Hg contained in these mineral phases was released in F6.

Conclusions

Blast furnace sludge contains a significant amount of Hg and consequently has an environmental risk potential, as revealed in an earlier study. The results of this study showed that Hg in BFS mainly resided in F4 and in minor amounts as mercuric sulfides and residual Hg, respectively. As these fractions are rather immobile under natural conditions, the long-term risk is rather low, particularly taking into account the low amount of Hg measured in the ecotoxically relevant fractions (water and human

stomach acid soluble fractions). However, it must be considered that the analyzed BFS samples had been dumped partly for up to 80 years before sampling. Hence, Hg in mobile fractions might already have been leached out or volatilized. Our results show that BFS dumped for up to several decades does not pose a significant environmental risk. It remains questionable if this waste never in fact possessed ecotoxically relevant Hg or if it is lacking due to leaching or volatilization. In order to make a precise and explicit statement for a detailed environmental risk assessment, fresh BFS should be studied by sequential extraction procedures before deposition.

References

Al-Abed SR, Jegadeesan G, Scheckel KG, Tolaymat T. Speciation, characterization, and mobility of As, Se, and Hg in flue gas desulphurization residues. Environmental Science & Technology 2008; 42: 1693-1698.

Bacon JR, Davidson CM. Is there a future for sequential chemical extraction? Analyst 2008; 133: 25-46.

Bloom NS, Prestbo EM, Dobbs CL. Proceedings of the POST-CSI XXXII Conference on Environmental and Health Aspects of Mining, Refining and Related Industries, Kruger National Park, South Africa, 2001.

Bloom NS, Preus E, Katon J, Hiltner M. Selective extractions to assess the biogeochemically relevant fractionation of inorganic mercury in sediments and soils. Analytica Chimica Acta 2003; 479: 233-248.

Das B, Prakash S, Reddy PSR, Misra VN. An overview of utilization of slag and sludge from steel industries. Resources, Conservation and Recycling 2007; 50: 40-57.

Davidson R, Claerke L. Trace Elements in Coal. IEA Coal Research, London, 1996.

Foeldi C, Dohrmann R, Mansfeldt T. Mercury in dumped blast furnace sludge. Chemosphere 2014; 99: 248-253.

Galbreath KC, Zygarlicke CJ. Mercury transformations in coal combustion flue gas. Fuel Processing Technology 2000; 65: 289-310.

Hall GEM, Pelchat P, Percival JB. The design and application of sequential extractions for mercury, Part 1. Optimization of HNO3 extraction for all non-sulphide forms of Hg. Geochemistry: Exploration Environment Analysis 2005; 5: 107-113.

International Energy Agency. Coal Information 2014, published online 2014, retrieved May 29, 2015 http://www.iea.org/bookshop/646-Coal_Information_2014.

Li P, Yu Q, Qin Q, Du W. The effects of slag compositions on the coal gasification reaction in molten blast furnace slag. Energy Sources, Part A: Recovery, Utilization, and Environmental Effects 2014; 36: 73-79.

Liu G, Cabrera J, Allen M, Cai Y. Mercury characterization in a soil sample collected nearby the DOE Oak Ridge Reservation utilizing sequential extraction and thermal desorption method. Science of the Total Environment 2006; 369: 384-392.

Lopez-Delgado A, Perez C, Lopez FA. Sorption of heavy metals on blast furnace sludge. Water Research 1998; 32: 989-996.

Mansfeldt T, Biernath H. Method comparison for the determination of total cyanide in deposited blast furnace sludge. Analytica Chimica Acta 2001; 435: 377-384.

Mansfeldt T, Dohrmann R. Chemical and mineralogical characterization of blast-furnace sludge from an abandoned landfill. Environmental Science & Technology 2004; 38: 5977-5984.

McLarnon CR, Granite EJ, Pennline HW. The PCO process for photochemical removal of mercury from flue gas. Fuel Processing Technology 2005; 87: 85-89.

Peacey JG, Davenport WG. The iron blast furnace. Oxford: Pergamon Press, 1979.

Shaheen SM, Hooda PS, Tsadilas CD. Opportunities and challenges in the use of coal fly ash for soil improvements - A review. Journal of Environmental Management 2014; 145: 249-267.

Shao DK, Hutchinson EJ, Cao HB, Pan WP, Chou CL. Behavior of chlorine during coal pyrolysis. Energy & Fuels 1994; 8: 399-401.

Trömel G, Zischkale W. Gmelin-Durrer: Metallurgie des Eisens. Vol 3. Weinheim, Germany: Verlag Chemie, 1971.

Trung ZH, Kukurugya F, Takacova Z, Orac D, Laubertova M, Miskufova A, et al. Acidic leaching both of zinc and iron from basic oxygen furnace sludge. Journal of Hazardous Materials 2011; 192: 1100-1107.

US EPA. Method 1631, Mercury in water by oxidation, purge and trap, and cold vapor atomic flourescence spectrometry. US EPA 821-R-95-027, 1999.

Van Herck P, Vandecasteele C, Swennen R, Mortier R. Zinc and lead removal from blast furnace sludge with a hydrometallurgical process. Environmental Science & Technology 2000; 34: 3802-3808.

Wedepohl KH. The composition of the continental crust. Geochimica et Cosmochimica Acta 1995; 59: 1217-1232.

Wei Z, Wu G, Su R, Li C, Liang P. Mobility and contamination assessment of mercury in coal fly ash, atmospheric deposition, and soil collected fron Tianjin, China. Environmental Toxicology and Chemistry 2011; 30: 1997-2003.

WHO. Mercury in drinking-water. Background document for develoment of WHO Guidelines for drinking-water quality. Geneva: World Health Organisation (WHO/SDE/WSH/05.08/10), 2005.

World Steel Association. Blast furnace iron production, 1980-2013, published online November 2014, retrieved on June 12, 2015 from http://www.worldsteel.org/statistics/statistics-archive/annual-steel-archive.html, 2014.

Yuan CG, Li QP, Feng YN, Chang AL. Fractions and leaching characteristics of mercury in coal. Environmental Monitoring and Assessment 2010; 167: 581-586.

Chapter 4   Volatilization of elemental mercury from fresh blast furnace sludge mixed with basic oxygen furnace sludge under different temperatures

Co-author: Reiner Dohrmann & Tim Mansfeldt

Environmental impact

Mercury (Hg) is considered as one of the most important environmental pollutants, as the element and many of its compounds are highly toxic and bioaccumulative. Blast furnace sludge (BFS) is an industrial waste with elevated Hg contents due to enrichment during the production process of pig iron. This study is the first to analyze Hg volatilization from BFS and the effect of temperature on Hg fluxes. The results are of significant implications as this waste has long been dumped in large surface landfills in Europe, which might be an ongoing procedure in countries with less strict environmental laws. Hence, volatilization potential of Hg from this waste is of special environmental concern.

Abstract

Blast furnace sludge (BFS) is a waste with elevated mercury (Hg) content due to en-
richment during the production process of pig iron. To investigate the volatilization
potential of Hg, fresh samples of BFS mixed with basic oxygen furnace sludge
(BOFS; a residue of gas purification from steel making, processed simultaneously in
the cleaning devices of BFS and hence mixed with BFS) were studied in sealed col-
umn experiments at different temperatures (15, 25, and 35 °C) for four weeks (total
Hg: 0.178 mg kg^{-1}). The systems were regularly flushed with ambient air (every 24 h
for the first 100 h, followed by every 72 h) for 20 min at a flow rate of 0.25 ±
0.03 L min^{-1} and elemental Hg vapor was trapped on gold coated sand. Volatilization
was 0.276 ± 0.065 ng ($\overline{x}_m$: 0.284 ng) at 15 °C, 5.55 ± 2.83 ng ($\overline{x}_m$: 5.09 ng) at 25 °C,
and 2.37 ± 0.514 ng ($\overline{x}_m$: 2.34 ng) at 35 °C. Surprisingly, Hg fluxes were lower at 35
than 25 °C. For all temperature variants, an elevated Hg flux was observed within the
first 100 h followed by a decrease of volatilization thereafter. However, the back-
ground level of ambient air was not achieved at the end of the experiments indicating
that BFS mixed with BOFS still possessed Hg volatilization potential.

Introduction

Blast furnace sludge (BFS) and basic oxygen furnace sludge (BOFS) are typical steelmaking-related wastes. Both are generated during the wet purification process of effluent gases. While BFS occurs in the cleaning of blast furnace top gas, BOFS is a residue of gas purification from steel making in so-called basic oxygen furnaces, more popularly known as Linz-Donauwitz (LD) converters. The latter converts molten pig iron into low carbon steel via lancing pure oxygen (O_2) in a mixture of pig iron, iron (Fe) scrap, ferroalloys, lime, and Fe ores. During the blowing process, large amounts of fumes and gases are generated containing fine particles of the charge materials. Pig iron is produced in blast furnaces by transferring Fe from ores into its elemental form. Thereby, charge material, such as Fe ores, high carbon (C) fuels (e.g. coke), and flux additives, are smelted in the blast furnace at temperatures up to 2200 °C. During the combustion process, the blast furnace gas drags along solid phases of the charge material and their reaction products. Both effluent gases are progressively cleaned in, for example, axial cyclones or dust-catchers to separate out coarse particles, while fine particles are removed using electrostatic precipitators or annular gap scrubbers. After the separation of solid material from the bulk of the process water, the resulting muddy waste is referred to as BFS and BOFS, respectively.

To reduce financial expense for virgin raw material and depositing costs, the integrated steel-making industry has put in a lot of effort to find ways of utilizing its byproducts, especially as many of the byproducts still contain high amounts of the demanded C and Fe compounds. However, due to the high temperatures in both processes, low melting point elements, such as lead (Pb), potassium (K), sodium (Na), and zinc (Zn) are partially vaporized. In the effluent gas, they are either present in their gaseous phase or associated with fine particles. Hence, these elements are ac-

cumulated and enriched in BFS and BOFS, respectively (Das et al., 2007; Gargul
and Boryczko, 2015; Makkonen et al., 2002; Mansfeldt and Dohrmann, 2004; Trung
et al., 2011; Van Herck et al., 2000). These elements among others (sulfur (S), cad-
mium (Cd), and cyanides) inhibit the utilization of BFS and BOFS in the integrated
steel industry as they can cause operational difficulties in the blast furnace (Das et
al., 2007). Also, the rather fine grain size character of this waste hinders the internal
recycling as feed for the sintering process (Hyoung-Ky et al., 1995).

The accurate amount of sludge per Mg of pig iron varies from plant to plant. Howev-
er, based on an annual worldwide production of $1.168 \cdot 10^6$ Mg of pig iron (World Steel
Association, 2014a) and the stated 6 kg of BFS per Mg of pig iron (Lopez-Delgado et
al., 1998) approximately $7 \cdot 10^6$ Mg of BFS are generated each year. As 70 % of the
annual crude steel production of $1.600 \cdot 10^6$ Mg (World Steel Association, 2014b) are
produced via the basic oxygen furnace process with an estimated 17.0 to 22.8 kg of
BOFS per Mg of crude steel (Cantarino, 2011), roughly $31 \cdot 10^6$ Mg of BOFS are gen-
erated globally per year.

Consequently, large amounts of this industrial waste need to be deposited. Despite
their toxic properties, BFS and BOFS have long been deposited in large surface land-
fills in industrial areas in Europe, which still might be an ongoing procedure in coun-
tries with less strict environmental laws.

In our previous study (Földi et al., 2014), we proved the enrichment of the volatile
element Hg in BFS with contents ranging from 0.006 up to 20.8 mg kg^{-1} (median
($\overline{x}_m$): 1.64 mg kg^{-1}; mean ($\overline{x}_a$): 3.08 mg kg^{-1}). Mercury is considered to be one of the
most important environmental pollutants, as the element and many of its compounds
are highly toxic, persistent, and readily released into the environment due to their
high mobility and volatility (WHO, 2005). Anthropogenic activities have led to a signif-

icant increase in Hg concentration in all environmental compartments (UNEP, 2013).

Besides anthropogenic release, re-emission of "natural and anthropogenic" Hg from

the Earth's surface contributes significantly to the global Hg cycle (approximately

60 %) (UNEP, 2013). Whereas re-emissions from oceans have undergone recent

scientific interest, little is known about the amounts, species, and the factors causing

Hg volatilization from the land's surface.

Although oxidized Hg (Hg^{2+}) is the predominant form of Hg in soils, it is widely ac-

cepted that Hg volatilizing from soils is predominantly in the form of elemental Hg

(Hg^0) and/or dimethyl Hg, probably with minor amounts of monomethyl Hg and solu-

ble Hg(II)-salts (Schluter, 2000). The former are the only Hg species described as

volatile species as they are water soluble with at least 500 times higher air/water-

distribution constant than the non-volatile species (Iverfeldt, 1984). Formation and

turnover of Hg^{2+} to Hg^0 in soils is controlled by both biotic and abiotic reduction

(Schluter, 2000). While abiotic reduction is basically mediated by humic acids, fulvic

acids, and other reductants, such as Fe^{2+}, biotic reduction is capable through Hg re-

sistant soil microorganisms.

Several key factors besides total Hg content and speciation were identified as influ-

encing Hg degassing from soils. Besides solar radiation, temperature, and elevated

soil moisture, interactions with atmospheric ozone and turbulences significantly affect

Hg fluxes. Previous work showed that Hg emissions from soils correlate positively

with ambient air temperature, soil surface temperature, and solar radiation, while they

are negatively correlated with relative humidity and soil wetness (Choi and Holsen,

2009). As soil surface temperature is basically a result of ambient air temperature

and solar radiation, both these factors are the main key factors driving Hg emissions

at a given Hg content.

Even less is known about Hg emissions from industrial wastes and their disposal sites, respectively. Few publications deal with Hg fluxes from municipal solid waste landfill sources, emphasizing the importance for the global Hg cycles (Li et al., 2010; Lindberg et al., 2005; Southworth et al., 2005). Mercury in the atmosphere exists predominantly as elemental (Hg^0), oxidized (Hg^{2+}), and particulate (Hg_p) Hg with Hg^0 typically making up more than 98 % of total gaseous Hg (Gustin and Jaffe, 2010). We henceforth use Hg to refer to elemental Hg vapor.

However, to our knowledge, no data has been published about the degassing of Hg from metallurgical wastes such as BFS or BOFS. In this study, our objectives were (i) to study if any Hg is degassed from the described wastes, (ii) to quantify the amount of volatizing Hg, and (iii) to determine the effect of temperature on the Hg flux by excluding other known parameters affecting Hg degassing.

Material and methods

Sampling site, sampling, and sample preparation

One sample of BFS mixed with BOFS, henceforth referred to as BFS/BOFS, was taken from after the settling tank as the integrated steel plant in Germany, to be most cost effective, uses a joint cleaning process for both effluent gases. Unfortunately, pure BFS was not available. The sample was transferred into 10-litre buckets made of high-density polyethylene (HDPE) and homogenized. The buckets were completely filled, sealed with Teflon tape, directly transported to the laboratory, and stored in the refrigerator (4 °C) until used. The buckets, as all other equipment used in the column experiments, were previously washed with detergent, soaked several days with 10 % nitric acid (HNO3), and rinsed with milli-Q Millipore water. A subsample was

dried at room temperature and ground to analytical grain size in a mixer mill (MM400,

Retsch) with zirconium oxide grinding tools.

Material characterization

Elemental composition

Total C, nitrogen (N), and sulfur (S) were quantified by dry combustion with an ele-

mental analyzer (Vario EL Cube CNS, Elementar). The evolved gases carbon dioxide

(CO_2), sulfur dioxide (SO_2), and nitrogen (N_2) were measured by thermal conductivity.

Total carbonate-carbon (TCC) was determined by the suspension method using a

DIMATOC® 100 liquid analyzer (Dimatec Corp.) Total residual C (TRC) was calcu-

lated from the difference between total C and TCC. Residual C contains C in the form

of coke, graphite, and black C.

Other elements were analyzed by wavelength dispersive X-ray fluorescence (XRF;

Axios, PANalytical). Powdered samples were mixed with a flux material and melted

into glass beads. To determine loss on ignition (LOI), 1.0 g of sample material was

heated to 1030 °C for 10 min. After mixing the residue with 5.0 g of lithium metabo-

rate ($Li_2B_4O_7$) and 25 mg of lithium bromide (LiBr), it was fused at 1200 °C for 20 min.

The calibrations were validated regularly by analysis of the reference materials and

130 certified reference materials were used for the correction procedures.

Total Hg was analyzed by means of a direct Hg analyzer (DMA-80, MLS GmbH). The

sample was thermally decomposed at 750 °C in a continuous flow of analytical grade

O_2 and, hence, combustion products were carried off through a catalyst furnace

where chemical interferences were removed. The Hg vapor was trapped on a gold

amalgamator and subsequently desorbed for spectrophotometric determination at

254 nm. The instrument was calibrated with 7 levels of concentrations for each "ab-

sorbance cell" of the detector (low concentration "absorbance cell" ranged up to 2 ng, higher concentration "absorbance cell" ranged from 2 to 22 ng). Mercury solutions for calibration were prepared by serial dilution from 1000 ± 2 mg L−1 Hg standard solution (CertiPur Merck, traceable to SRM from NIST) in 2 mM BrCl. The coefficient of determination was 0.9989 for the low concentration "absorbance cell" and 0.9999 for higher concentration "absorbance cell". The instrument did not have to be recalibrated every day as no significant instrumental parameter had to be replaced. In every-day operation, analytical quality was assured by measuring the same liquid standards as used for the calibration prior, during and after sample analyses. The amount of detected Hg in the standards was chosen for the range of experimental values (0.1 ng (σrel = 9.1 %), n = 108; 1 ng (σrel = 3.75 %), n = 54; and 10 ng (σrel = 4.16 %), n = 36).

Mineralogical composition

X-ray powder diffraction (XRD) patterns were recorded using X-ray diffraction (X'Pert PRO MPD theta–theta, PANalytical) with Co-Kα radiation generated at 40 kV and 40 mA. The device was equipped with a variable divergence slit (20 mm irradiated length), primary and secondary sollers, diffracted beam monochromator, a point detector, and a sample changer (sample diameter 28 mm). The samples were investigated from 1° to 80° 2Θ with a step size of 0.03° 2Θ and a measuring time of 10 s per step.

For specimen preparation, the back-loading technique was used. Phase identification was made by reference to patterns in the International Center for Diffraction Data (ICDD) PDF-2 database, released in 2009.

Column experiments

To study the gaseous release of elemental Hg under different temperatures, column experiments were conducted. The column installation consisted of a borosilicate glass flux chamber with one outlet and four inlets according to Rinklebe et al. (2009), a PVC cylinder with a height of 6 cm and a diameter of 11.5 cm, a column frame to seal the column base, and a gas sampler (GS 212, Desaga) (Fig. 1). Aliquots of BFS/BOFS (500 to 800 g fresh material) were transferred into the columns in four replicates; the flux chambers were fixed on the cylinders, and sealed tightly using Teflon tape. Re-homogenization was not carried out before sampling for each temperature variant to avoid further contact with O_2. The column installations were placed in an incubator (KB 400, Binder) at 15, 25, and 35 °C for 28 days. Inlets and outlets, respectively, of the flux chamber were sealed with blind plugs made of borosilicate glass. Experiments were conducted in the dark to exclude solar radiation and hence possible photocatalytic reduction of soluble Hg^{2+} to volatile Hg^0 at the surface. The lowest temperature variant was chosen to be 15 °C as it is the annually-averaged temperature across global land and ocean surfaces for 2014 (14.59 °C) (NOAA National Climatic Data Center, 2015). However, as the BFS/BOFS was black, it exhibits a rather lower albedo (< 15 %) and hence the surface can easily be warmed at temperatures higher than the ambient air. That is why we chose temperature variants of 25 and 35 °C.
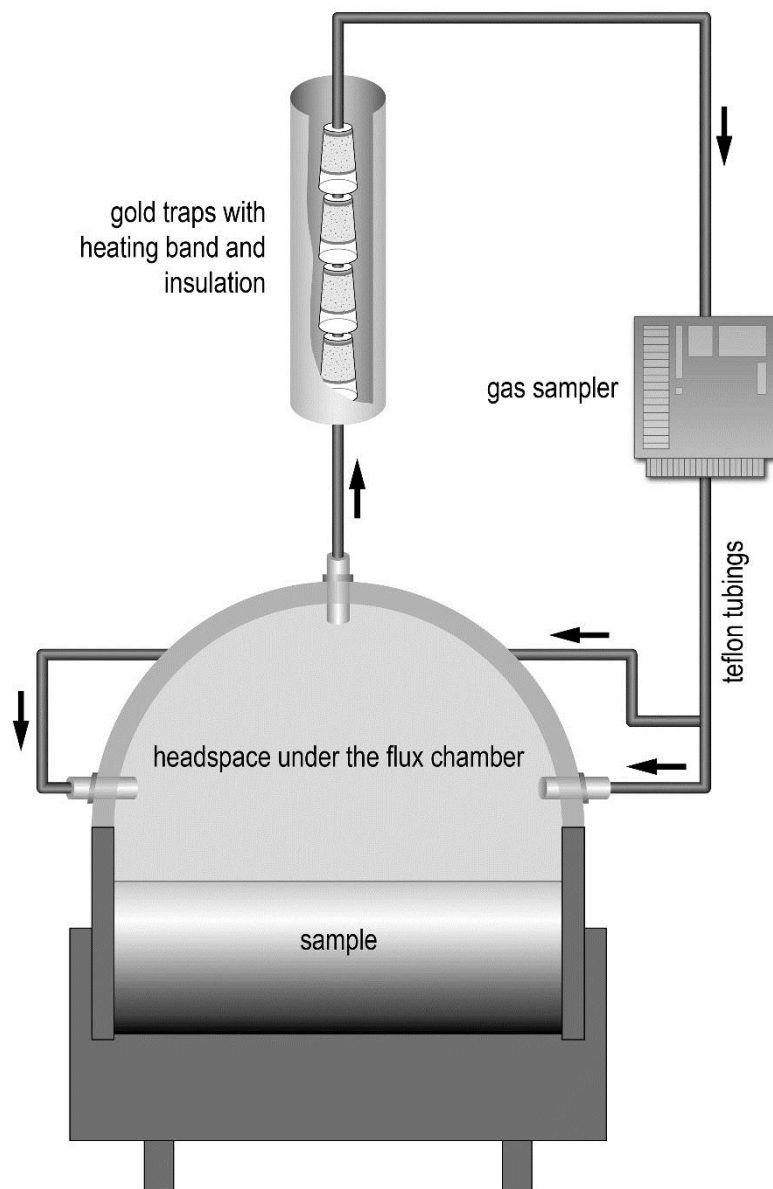
Fig. 1   Scheme of experimental design for sampling elemental Hg

To determine Hg volatilization, four gold traps were connected in line directly to the

flux chamber's outlet. The gold traps were heated at 110 °C using a heating band

(HS, Horst GmbH) and thermostat (HT22, Horst GmbH) to avoid water re-

condensing. To close the circulation, the gold traps were further connected to the gas

sampler and tubing lines were connected between the gas sampler and the four in-

lets of the flux chamber using borosilicate glass, Tygon, and Teflon tubings, respec-

tively. Ambient air was pumped through the closed circulation system using the gas sampler for 20 min at 0.25 ± 0.03 L min^{-1}, as these parameters had been shown to be the most effective in preliminary experiments. Sampling was undertaken after 24, 48, 72, 96, and then every 72 h resulting in 12 sampling events. Blanks of ambient air were taken at the beginning of the experiment by connecting four gold traps to the gas sampler and sucking air through the traps for 20 min with a flow rate of 0.25 L min^{-1}. Sampling blanks were found to be 0.0433 ng on average. This value was subtracted from the quantities of Hg collected on the traps during the experiments.

To reduce the Hg capacity of the gold coated sand (GCSI; Timmerman gold trap, Symalab) to an effective measuring range of the DMA-80, GCSI was mixed with quartz powder (pro analysis, Merck) with a weight-to-weight ratio of 1 to 50, referred to as GCSII hereafter. Gold traps consisted of borosilicate glass tubings filled with 1 g GCSII and fixed with quartz wool. Each gold trap was stored in a separate borosilicate vessel with a Teflon-lined cap and was measured within 3 days using the DMA-80.

Three procedural standards were processed with the column and analyzed with known amounts of 1, 10, and 100 g Hg resulting in recoveries of 80.6, 64.3, and 73.3 %, respectively.

Water content at the beginning and the end of each experiment was calculated by mass using the following formula:

$$water\ content\ [\%] = \frac{mass\ (a) - mass\ (b)}{mass\ (a)} * 100$$

water content$_{start}$: a = mass$_{start}$; b = mass$_{105\ °C}$

water content$_{end}$: a = mass$_{end}$; b = mass$_{105\ °C}$

For mass at 105 °C, the residue of each column was dried for one week at room temperature; a subsample of each column was weighed (15 g) and dried for 24 h at 105 °C. Further, the factor of each subsample at 105 °C to the mass of each column at room temperature (start and end, respectively) was calculated and considered for the water content.

All measured Hg values were calculated on a dry mass basis ($mass_{105\,°C}$) to ensure an accurate comparison.

Results and discussions

Material characterization

Elemental composition

The elemental composition of BFS and BOFS differed significantly due to the applied raw materials and byproducts (Földi et al., 2014; Gargul and Boryczko, 2015; Kretzschmar et al., 2012; Mansfeldt and Dohrmann, 2004; Trung et al., 2011; Veres et al., 2010). The composition of the analyzed sample was clearly dominated by C (60.6 g kg^{-1}) and Fe (564 g kg^{-1}) reflecting the metallurgical production process (Table 1). The higher proportion of Fe was typical for BOFS as it is known that it may contain from about 50 to as much as 75 % Fe (Gargul and Boryczko, 2015). In fact, since two-thirds of the sludge was made up of Fe it might be a potential raw material to be recycled in the sintering process. High Fe content indicated a dominance of BOFS in the studied sample as Fe content in BFS mainly ranged from around 100 to 300 g kg^{-1} (Földi et al., 2014; Kretzschmar et al., 2012; Mansfeldt and Dohrmann, 2004; Veres et al., 2010). In addition, the rather low C content of the sample underlined this, as C in BFS normally ranged between an average of 160 and 190 g kg^{-1}

(Földi et al., 2014; Mansfeldt and Dohrmann, 2004; Veres et al., 2010). However,

TCC in respect to total C was 16.8 %, in the same range as BFS.

Table 1 Chemical composition of blast furnace sludge mixed with basic oxygen
furnace sludge

element	unit	value
C	g kg^{-1}	60.6
TCC[a]		10.2
TRC[b]		50.4
S		2.34
Fe		564
O		280
Ca		45.2
Zn		14.8
Si		10.6
Mn		9.12
Al		2.65
Mg		2.29
Pb		1.06
Cr	mg kg^{-1}	665
P		524
Ti		444
K		340
Cu		286
Ni		207
Hg		0.178
Na		<0.01
LOI[c]	[%]	5.70

[a] Total carbonate-carbon
[b] Total residual carbon
[c] Loss on ignition

The chromium (Cr), titanium (Ti), copper (Cu), and nickel (Ni) contents ranged from

665 to 207 mg kg^{-1} and were considered to be low. However, the Zn content of

14.8 g kg^{-1} was significantly higher being rather in the range stated for BOFS (Trung et al., 2011) than for BFS (Földi et al., 2014; Kretzschmar et al., 2012; Mansfeldt and Dohrmann, 2004; Veres et al., 2011). As stated by Makkonen et al. (2002) the Zn content in BOFS was generally around 2 mass-% but could be increased to 25 mass-% if scrap was recycled in the converter. Consequently, the Zn content of the sample in this study suggested a rather low recycling fraction of scrap. Moreover, the elevated Zn value most likely inhibited direct recycling of this material to the sintering process as was suggested before. The Zn content entering the blast furnaces should not exceed 120 g Zn per Mg of pig iron as its compounds may form solids on the furnace walls, which in turn cause operational difficulties in the blast furnace operation (Veres et al., 2011). The maximum loading would be reached with only 8 kg of the material under study. Common loadings of Fe-making blast furnaces range between 576 and 1320 kg of sinter and 351 and 734 kg of pellets per Mg of pig iron (Nogami et al., 2006). As a consequence, BFS/BOFS needed either to be used as landfill or further processed to reduce the Zn content. The processing of steelmaking dust, such as electric arc furnace dust, by hydrometallurgical or pyrometallurgical methods has attracted recent scientific interest. However, for BFS and BOFS further processing is far more complicated due to the relatively low Zn content compared with electric arc furnace dust (Trung et al., 2011).

The total Hg content of the sample was 178 ± 3.26 µg kg^{-1} (n = 4). In our previous study the Hg content of 65 dumped BFS samples from seven locations varied between 0.006 up to 20.8 mg kg^{-1} with a $\overline{x}_m$ of 1.64 mg kg^{-1} ($\overline{x}_a$: 3.08 mg kg^{-1}). Consequently, the analyzed sample was rather low in Hg content, which most likely resulted from the addition of the BOFS to the BFS during the cleaning process. In fact, soils

with a similar Hg content (between 0.15 and 0.2 mg kg^{-1}) would be regarded as re-flecting the natural background content of Hg (Hooda, 2010).

Mineralogical composition

The phase composition of BFS/BOFS (Fig. 2) revealed the presence of different Fe phases, such as magnetite (Fe_3O_4), wüstite (FeO), hematite (Fe_2O_3), and α-Fe. Fur-thermore, quartz (SiO_2), calcite ($CaCO_3$), and perovskite ($CaTiO_3$) were detected by XRD. Other phases, as indicated by the chemical composition, could not be clearly identified either as a result of their minor amounts and/or their vanishing in the back-ground of the XRD pattern. Despite the elevated Zn content of 14.8 g kg^{-1}, no Zn-bearing phase was detected. Trung et al. (2011) summarized several approaches for the lack of identified Zn phases. According to these authors, Zn might be distributed in various phases such as zincite (ZnO), franklinite ($ZnFe^{III}O_4$), and solid solutions of franklinite and hence their diffraction could vanish into the background of the pattern. Furthermore, they pointed out that amorphous fractions as well as present C in-creased the background signal, intensifying the vanishing of certain peaks. However, Kretzschmar et al. (2012) identified five major types of Zn in BFS using a combination of synchrotron XRD, micro-XRF, and X-ray adsorption spectroscopy at the Zn K-edge for solid phase. These were (i) Zn in the octahedral sheets of phyllosilicates, (ii) Zn sulfide minerals (ZnS, sphalerite, or wurtzite), (iii) Zn in a KZn−ferrocyanide phase ($K_2Zn_3[Fe(CN)_6]_2 \cdot 9H_2O$), (iv) hydrozincite ($Zn_5(OH)_6(CO_3)_2$), and (v) tetrahedrally co-ordinated adsorbed Zn occurring in variable amounts. Zincite was detected only in traces, while $ZnFe^{III}O_4$ was not detected at all. Another approach explained the lack of Zn phases by the isomorphic structures of identified ferrites and the resulting diffi-culties in distinguishing the diffraction peaks, e.g. Fe_3O_4 and $ZnFe^{III}_2O_4$. In addition,

the structural substitution of Fe by Zn in Fe_3O_4 is reasonable. The increasing baseline between 30 and 45 °2Θ in this pattern indicated the significant presence of X-ray amorphous phases underlying this statement. Various authors have shown the presence of significant amounts of XRD amorphous phases in BFS, mainly being coke- and graphite-bound C (Kretzschmar et al., 2012; Mansfeldt and Dohrmann, 2004; Veres et al., 2012).
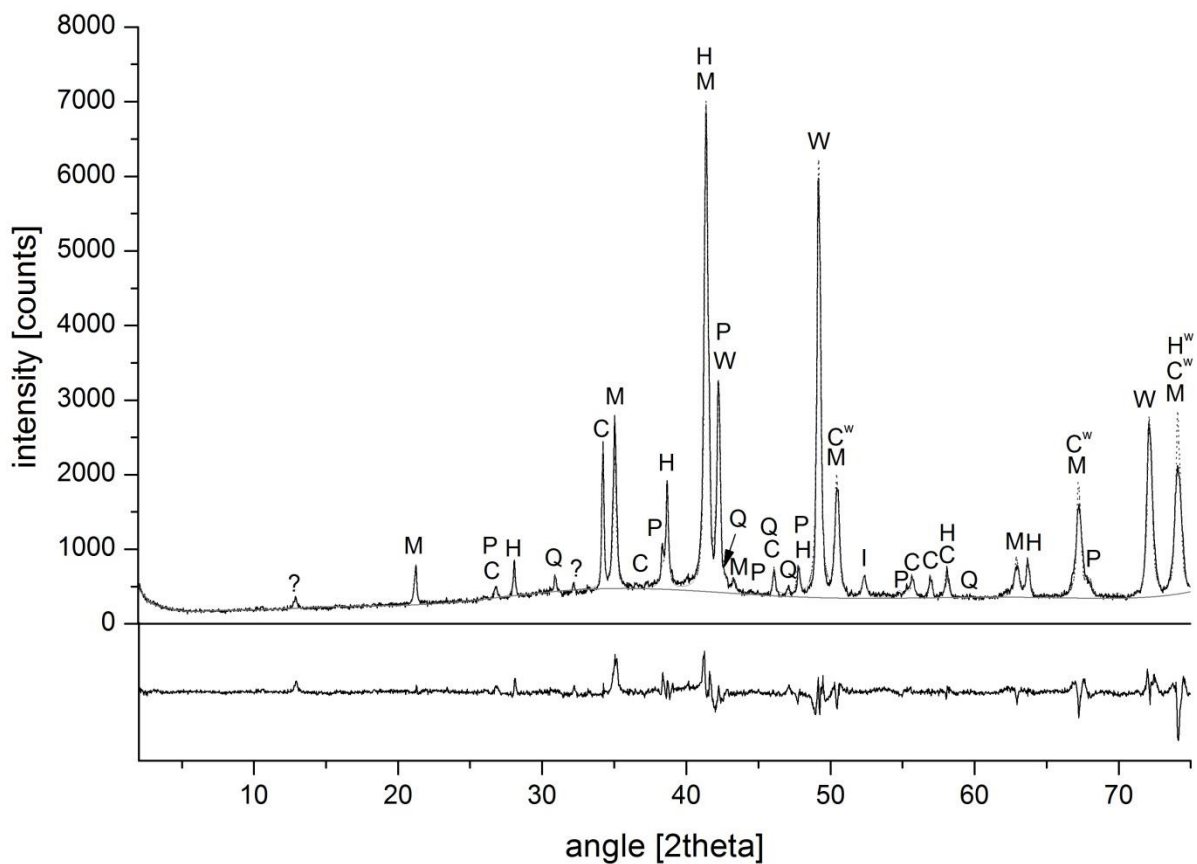

Fig. 2   Powder X-ray diffraction (XRD) pattern of a mixture of blast furnace sludge and basic oxygen furnace sludge. The black line represents the experimental XRD pattern, the dotted black line the calculated Rietveld pattern, and the baseline is given as the approximately horizontal line below (light grey). C: calcite; H: hematite; I: α-Fe; M: magnetite; P: perovskite; Q: quartz; W: wüstite; ^{w}: weak signal

Column experiments

The water content of the columns was 53.1 ± 1.5 % (Table 2; $\overline{x}_m$: 53.7 %; n = 4) for

15 °C, 51.4 ± 1.0 % ($\overline{x}_m$: 51.4 %; n = 4) for 25 °C, and 44.6 ± 3.2 % ($\overline{x}_m$: 43.6 %; n =

4) for 35 °C at the beginning of the experiment as a suspension was formed during

storage.

Table 2 Weight and water content specification of the columns and the tempera-
ture variants

		column I	column II	column III	column IV
15 °C	mass$_{start}$	750	688	799	858
	mass$_{end}$	653	610	717	785
	mass$_{105\ °C}$	347	318	377	425
	water content$_{start}$ [%]	54.2	54.1	53.3	51.0
	water content$_{end}$ [%]	47.2	48.2	47.8	46.3
25 °C	mass$_{start}$	665	553	515	530
	mass$_{end}$	613	519	460	479
	mass$_{105\ °C}$	319	273	251	268
	water content$_{start}$ [%]	52.6	51.1	51.8	50.2
	water content$_{end}$ [%]	48.4	47.9	45.9	44.7
35 °C	mass$_{start}$	582	604	584	611
	mass$_{end}$	519	554	543	550
	mass$_{105\ °C}$	330	344	342	313
	water content$_{start}$ [%]	43.7	43.5	42.0	49.2
	water content$_{end}$ [%]	36.7	38.3	37.6	43.4

For all temperature ranges, the columns were not fully dewatered due to the limited

headspace and resulting water vapor pressure. However, water content of the col-

umns after four weeks was 47.4 ± 0.8 % ($\overline{x}_m$: 47.5 %; n = 4) for 15 °C, 46.7 ± 1.7 %

($\overline{x}_m$: 46.9 %; n = 4) for 25 °C, and 39.0 ± 3.0 % ($\overline{x}_m$: 37.9 %n = 4) for 35 °C. This rep-

resented a decrease of 5.7 ± 1.0 % ($\overline{x}_m$: 5.7 %; n = 4) for 15 °C, 4.7 ± 1.2 % ($\overline{x}_m$: 4.8

%; n = 4) for 25 °C, and 5.6 ± 1.1 % ($\overline{x}_m$: 5.5 %; n = 4) for 35 °C. As the samples were not re-homogenized before each individual experiment variant, higher bulk density and hence lower water content are reasonable for the later experiments.

Figure 3 shows the averaged vapor phase Hg release from the columns at different temperatures. Within the first 100 h, daily Hg flux was 0.297 ± 0.077 ng ($\overline{x}_m$: 0.301 ng) for the 15 °C temperature variant. Afterwards, trapped Hg release was 0.266 ± 0.061 ng ($\overline{x}_m$: 0.284 ng). However, the sampling period after the first 100 h was on 72 h instead of daily bases. Consequently, volatilization was elevated during the first days and decreased slightly thereafter. In total, less than 0.001 % of total Hg of the BFS/BOFS degassed within 4 weeks. The background level of ambient air (0.0433 ± 0.0035 ng per 5.2 L), however, was not achieved at the end of the experiment, indicating that BFS/BOFS still possessed the potential for Hg volatilization after storage at 15 °C. To exclude Hg saturation in the headspace and hence reduced Hg volatilization, saturation concentration of Hg at 15 °C was calculated using data from the Occupational Safety & Health Administration (2010) and was approximately 9 µg L^{-1}. With respect to the headspace volume of 0.65 L, this would result in a max. Hg release of approximately 6,000 ng, being far higher than the actual measured values. Besides, reduced air pressure was avoided by using headspaces with air circulation systems as described by Rinklebe et al. (2009). The continuous gas movement over the sample's surface virtually eliminated reduced air pressure.

The saturation concentration for 25 °C (20 µg L^{-1}, which corresponds to about 15 µg Hg release to the headspace volume of 0.65 L) was also higher than the measured Hg values: Hg fluxes was 8.45 ± 3.01 ng ($\overline{x}_m$: 7.23 ng) per day within the first 100 h and decreased from 6.20 to 2.82 ng per 72 h thereafter (4.10 ± 1.24 ng; $\overline{x}_m$: 3.48 ng), resulting in volatilization of 0.25 % of the total Hg. Hindersmann et al. (2014) ana-

lyzed Hg volatilization from undisturbed floodplain soil samples with a total Hg con-
tent of 9.2 ± 0.2 mg kg^{-1} at 20 °C using similar column installations. Mercury flux
ranged between 0.4 ng and 411 ng per 72 h. Hence, Hg volatilization from
BFS/BOFS can be described as rather low for this temperature range. It is known
that two predominant factors control emissions from Hg-enriched soils, being soil Hg
content and incident radiation (Gustin et al., 2006). Most likely, the significant higher
Hg content of the floodplain soils was the main factor resulting in the vastly elevated
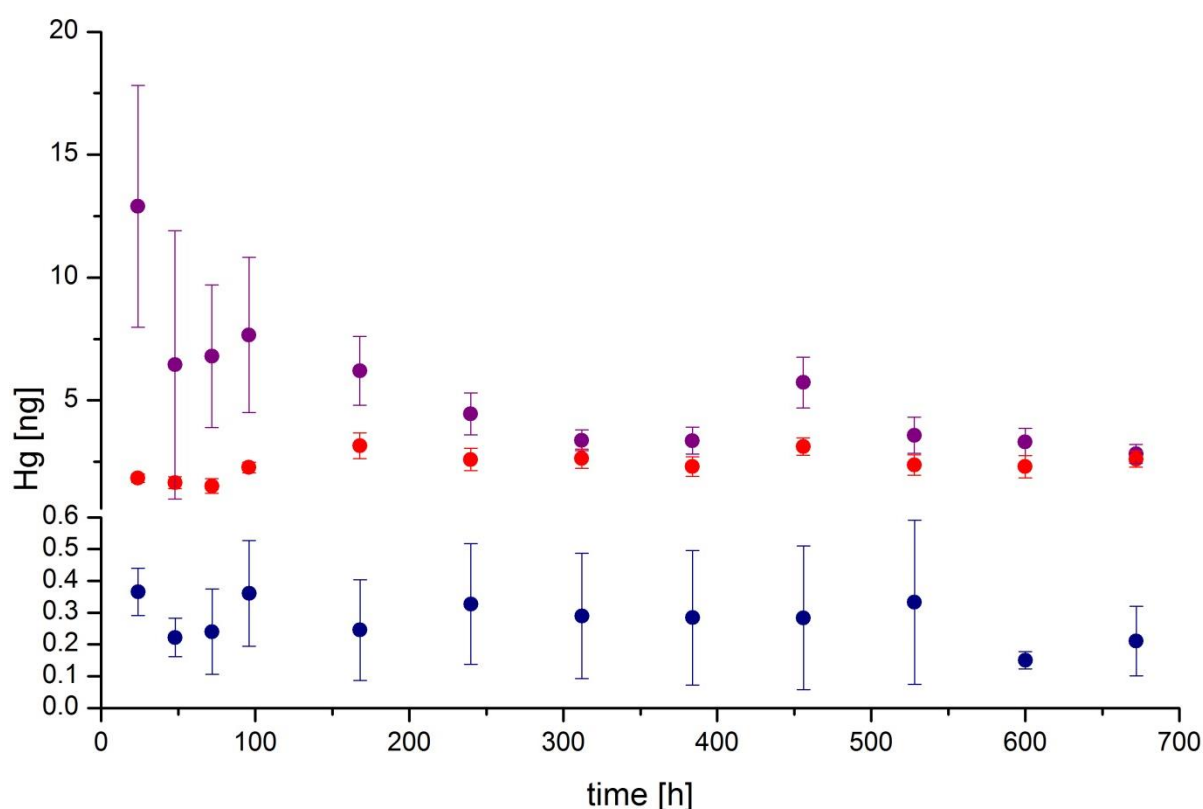Hg flux from soils compared with BFS/BOFS.

Fig. 3   Averaged vapor phase Hg release from the columns at different tempera-
tures (blue, 15 °C; purple, 25 °C; red, 35 °C). Note the different scale at
the y-axis. Error bars were calculated from four replications.

Mercury flux at 35 °C showed similar trends as observed for 15 and 25° C: Hg re-
lease was 1.82 ± 0.330 ng ($\bar{x}_m$: 1.75 ng) per 24 h within 100 h and decreased thereaf-

ter being 2.64 ± 0.337 ng (($\overline{x}_m$: 2.60 ng) per 72 h. Mercury flux was below the saturation concentration of 43 µg L^{-1}. Surprisingly, the Hg fluxes at 35 °C were significantly lower than at 25 °C. Various research groups have confirmed that temperature favored Hg desorption from soils due to the increase in Hg vapor pressure with increasing temperature. Gillis and Miller (2000) showed that Hg emissions in low-Hg, fine sandy loam soils could be largely explained by variations in surface soil temperature and the Hg concentration gradient between the soil and the ambient air. This temperature dependence had also been observed in both diurnal (Gustin et al., 2006) and seasonal studies (Sigler and Lee, 2006). Choi and Holsen (2009) investigated the impact of solar radiation and soil surface temperature on Hg emissions fluxes using, among others, native deciduous soils (DS) and sterilized deciduous soils (SDS). Experiments conducted in the dark gave high correlations with Hg emissions from both DS and SDS. The average Hg emissions increased from 10 ng m^{-2} h^{-1} at 25 °C to 120 ng m^{-2} h^{-1} at 35 °C for DS and from < 5 ng m^{-2} h^{-1} at 23 °C to 15 ng m^{-2} h^{-1} at 30 °C for SDS. They assumed that the differences between emissions from DS and SDS at the same temperature resulted from differences in biological Hg reduction, mediated by soil microbes. However, this is in contrast with our finding of 25 and 35 °C temperature variants. An explanation of the decreasing Hg flux with increasing temperature from 25 to 35 °C in our experiments might be the water content of the BFS/BOFS sample. Pannu et al. (2014) comprehensively summarized the effect of varying water-filled pore space (WFPS) on soil respiration, indicating that a soil water content equivalent to 60 % of a soil's water holding capacity delineated the point of maximum aerobic microbial activity. In their study, they found that the maximum mass of cumulative Hg^0 was formed at 60 % WFPS and the lowest at 15 % WFPS. Further research reported likewise: Gustin and Stamenkovic (2005)

observed increased Hg emissions for low-Hg soils with increased water content. A threefold increase in Hg volatilization rate was also described in a field study from November to March (soil moisture increased from 2.8 to 8.4 %) in Hungry Valley, Nevada (Gustin et al., 2006). Besides bacterial activity, chemical and physical interactions were suggested for enhanced Hg emissions with rising soil moisture: i) physical displacement of Hg^0 enriched interstitial soil air by infiltrating water, (ii) replacement of Hg^0 adsorbed to the soil by water molecules, and (iii) desorption of Hg^{2+} bound to the soil and subsequent reduction to Hg^0 through abiotic or biotic factors (Lindberg et al., 1999). Most likely, BFS/BOFS exhibited vastly limited microbial communities compared to soils, hence biological processes should be inhibited. However, we have no proof for or against biological activity.

Further, it must be stated that column IV at 35 °C had similar water content to all the columns at 25 °C (Table 2) but showed no higher Hg flux; the decreased volatilization rate at 35 °C cannot be solely explained by the water content. At the moment, this phenomenon remains unclear.

As is known for soils and was recently shown by Wang et al. (2014b) for baghouse filter dust (BFD), Hg emissions from surface material were affected by the Hg content in the upper few centimeters and hence by the air exchange surface area. Extrapolating volatilization from the columns' diameter yielded total Hg emissions of roughly 500 ng per m^2 and 4 weeks for 25 °C. Assuming a linear correlation between total Hg and the volatilization rate from BFS/BOFS (0.25 % within 4 weeks at 25 °C), this would have led to Hg flux of 0.410 µg per m^2 and 4 weeks ($\overline{x}_m$ Hg content of BFS: 1.64 mg kg^{-1}) and to Hg flux of 5.2 mg per m² and 4 weeks (max. Hg content of BFS: 20.8 mg kg^{-1}) for the previously studied BFS (Földi et al., 2014).

However, transferring this data to other BFS or BFS/BOFS samples can be done only with caution. As Huggins et al. (1999) have shown by X-ray absorbance spectroscopy, Hg formed a variety of surface species on unburned C. Thus, differences in C levels of the charge material may affect the speciation of Hg and hence the release of these species.

Furthermore, it must be stated that various research groups have shown that a significant proportion of gaseous Hg from industrial locations may comprise oxidized Hg, such as $HgBr_2$ and $HgCl_2$. Wang et al. (2014a) recently studied Hg emissions in flue gases of three cement plants in China, showing that oxidized Hg was the major species of total Hg in flue gas (61 to 91 %). Moreover, Wang et al. (2014b) determined Hg concentration and speciation in BFD from a cement kiln in the State of Florida. They found that the concentration of oxidized Hg ranged between 62 and 73 %. Also, in coal-fired flue gas, oxidized Hg species have a significant presence. The fraction of oxidized Hg in the flue gas of a particular power plant largely depends on the coal type, combustion efficiency, and the pollution control equipment used. However, as oxidized Hg species are water soluble and the BFS/BOFS had already passed a wet cleaning process, most of these species should already be removed. Hence, volatilization of oxidized Hg from BFS/BOFS should be significantly lower or below the detection limit.

Conclusions

Blast furnace sludge mixed with BOFS contained a significant amount of Hg. Volatilization of Hg from BFS/BOFS was proved for the first time. Despite rather low volatilization of Hg from fresh BFS/BOFS for all temperature ranges, emissions of Hg to the atmosphere are of environmental concern due to its long atmospheric lifetime and

the bioaccumulation after deposition. However, in countries with less strict environ-

mental laws, pure BFS or BFS/BOFS with significantly higher Hg content may be

used in landfill and hence vastly contribute to the global Hg cycle via volatilization. As

only elemental Hg vapor was determined in this study, but as oxidized Hg species

may be present as well, experiments quantifying these species (e.g. with potassium

chloride denuders) also should be conducted to quantify the environmental exposure

by volatilization from BFS and/or BOFS. Further, the potential sunlight driven reduc-

tion of oxidized Hg to elemental Hg should be studied, as this may influence Hg

emissions.

References

Cantarino MV. Estudo da remoção de zinco e de álcalis contidos em lamas de aciaria LD. Master of Science Thesis. Universidade Federal de Minas Gerais, Belo Horizonte, Brazil, 2011, pp. 97.

Choi H-D, Holsen TM. Gaseous mercury emissions from unsterilized and sterilized soils: The effect of temperature and UV radiation. Environmental Pollution 2009;157:1673–1678.

Das B, Prakash S, Reddy PSR, Misra VN. An overview of utilization of slag and sludge from steel industries. Resources, Conservation and Recycling 2007;50:40–57.

Földi C, Dohrmann R, Mansfeldt T. Mercury in dumped blast furnace sludge. Chemosphere 2014;99:248–253.

Gargul K, Boryczko B. Removal of zinc from dusts and sludges from basic oxygen furnaces in the process of ammoniacal leaching. Archives of Civil and Mechanical Engineering 2015;15:179–187.

Gillis AA, Miller DR. Some local environmental effects on mercury emission and absorption at a soil surface. Science of the Total Environment 2000;260:191–200.

Gustin MS, Engle M, Ericksen J, Lyman S, Stamenkovic J, Xin M. Mercury exchange between the atmosphere and low mercury containing substrates. Applied Geochemistry 2006;21:1913–1923.

Gustin M, Jaffe D. Reducing the uncertainty in measurement and understanding of mercury in the atmosphere. Environmental Science & Technology 2010;44:2222–2227.

Gustin MS, Stamenkovic J. Effect of watering and soil moisture on mercury emissions from soils. Biogeochemistry 2005;76:215–232.

Hindersmann I, Hippler J, Hirner AV, Mansfeldt T. Mercury volatilization from a floodplain soil during a simulated flooding event. Journal of Soils and Sediments 2014;14:1549–1558.

Hooda PS. Trace Elemnts in Soils. West Sussex: John Wiley & Sons Ltd, 2010.

Huggins FE, Yap N, Huffman GP, Senior CL. Identification of mercury species in unburned carbon from pulverized coal combustion. Air & Waste Management Association, Annual Meeting, Pittsburgh, PA, June 20–24, 1999; pp 2116–2127. 1999.

Hyoung-Ky S, Seok-Min M, Jin-Nam J. Recycling of waste materials for iron ore sintering. Seminar on the Steel Industry and Recycling, 24–27 April 1995. The United Nations Economic Commission for Europe, Düsseldorf, Germany, 1995.

Iverfeldt Å. Structural, thermodynamic and kinetic studies of mercury compounds; applications within the environmentlal mercury cycle. (PhD). University of Göteborg, 1984.

Kretzschmar R, Mansfeldt T, Mandaliev PN, Barmettler K, Marcus MA, Voegelin A. Speciation of Zn in blast furnace sludge from former sedimentation ponds us-

ing synchrotron X-ray diffraction, fluorescence, and absorption spectroscopy. Environmental Science & Technology 2012;46:12381–12390.

Li ZG, Feng X, Li P, Liang L, Tang SL, Wang SF, et al. Emissions of air-borne mercury from five municipal solid waste landfills in Guiyang and Wuhan, China. Atmospheric Chemistry and Physics 2010;10:3353–3364.

Lindberg SE, Southworth GR, Bogle MA, Blasing TJ, Owens J, Roy K, et al. Airborne emissions of mercury from municipal solid waste. I: New measurements from six operating landfills in Florida. Journal of the Air & Waste Management Association 2005;55:859–869.

Lindberg SE, Zhang H, Gustin M, Vette A, Marsik F, Owens J, et al. Increases in mercury emissions from desert soils in response to rainfall and irrigation. Journal of Geophysical Research: Atmospheres 1999;104:21879–21888.

Lopez-Delgado A, Perez C, Lopez FA. Sorption of heavy metals on blast furnace sludge. Water Research 1998;32:989–996.

Makkonen HT, Heino J, Laitila L, Hiltunen A, Poylio E, Harkki J. Optimisation of steel plant recycling in Finland: Dusts, scales and sludge. Resources, Conservation and Recycling 2002;35:77–84.

Mansfeldt T, Dohrmann R. Chemical and mineralogical characterization of blast-furnace sludge from an abandoned landfill. Environmental Science & Technology 2004;38:5977–5984.

NOAA National Climatic Data Center. State of the Climate: Annual Global Analysis for 2014, published online January 2015, retrieved on May 27, 2015 from http://www.ncdc.noaa.gov/sotc/global/201413.

Nogami H, Yagi J-i, Kitamura S-y, Austin PR. Analysis on material and energy balances of ironmaking systems on blast furnace operations with metallic charging, top gas recycling and natural gas injection. Isij International 2006;46:1759–1766.

Occupational Safety & Health Administration USDoL. Mercury vapor in workplace atmospheres, 2010.

Pannu R, Siciliano SD, OʼDriscoll NJ. Quantifying the effects of soil temperature, moisture and sterilization on elemental mercury formation in boreal soils. Environmental Pollution 2014;193:138–146.

Rinklebe J, During A, Overesch M, Wennrich R, Staerk H-J, Mothes S, et al. Optimization of a simple field method to determine mercury volatilization from soils-Examples of 13 sites in floodplain ecosystems at the Elbe River (Germany). Ecological Engineering 2009;35:319–328.

Schluter K. Review: evaporation of mercury from soils. An integration and synthesis of current knowledge. Environmental Geology 2000;39:249-271.

Sigler JM, Lee X. Gaseous mercury in background forest soil in the northeastern United States. Journal of Geophysical Research: Biogeosciences 2006;111.

Southworth GR, Lindberg SE, Bogle MA, Zhang H, Kuiken T, Price J, et al. Airborne emissions of mercury from municipal solid waste. II: Potential losses of airborne mercury before landfill. Journal of the Air & Waste Management Association 2005;55:870–877.

Trung ZH, Kukurugya F, Takacova Z, Orac D, Laubertova M, Miskufova A, et al.
    Acidic leaching both of zinc and iron from basic oxygen furnace sludge. Jour-
    nal of Hazardous Materials 2011;192:1100–1107.

UNEP. Global Mercury Assessment 2013, Sources, emissions, releases and envi-
    ronmental transport, UNEP Chemicals Branch, Geneva, Switzerland, 2013.

Van Herck P, Vandecasteele C, Swennen R, Mortier R. Zinc and lead removal from
    blast furnace sludge with a hydrometallurgical process. Environmental Science
    & Technology 2000;34:3802–3808.

Veres J, Jakabsky S, Lovas M. Zinc recovery from iron and steel making wastes by
    conventional and microwave assisted leaching. Acta Montanistica Slovaca
    2011;16:185–191.

Veres J, Jakabsky S, Sepelak V. Chemical, physical, morphological and structural
    characterization of blast furnace sludge. Diffusion Fundamentals 2010;12:88–
    91.

Veres J, Lovas M, Jakabsky S, Sepelak V, Hredzak S. Characterization of blast fur-
    nace sludge and removal of zinc by microwave assisted extraction. Hydromet-
    allurgy 2012;129:67–73.

Wang F, Wang S, Zhang L, Yang H, Wu Q, Hao J. Mercury enrichment and its ef-
    fects on atmospheric emissions in cement plants of China. Atmospheric Envi-
    ronment 2014a;92:421–428.

Wang J, Hayes J, Wu C-Y, Townsend T, Schert J, Vinson T, et al. Characterization of
    vapor phase mercury released from concrete processing with baghouse filter
    dust added cement. Environmental Science & Technology 2014b;48:2481–
    2487.

WHO. Mercury in drinking-water. Background document for develoment of WHO
    Guidelines for drinking-water quality. Geneva: World Health Organisation
    (WHO/SDE/WSH/05.08/10), 2005.

World Steel Association. Blast furnace iron production, 1980-2013, published online
    November 2014, retrieved on June 12, 2015 from
    http://www.worldsteel.org/statistics/statistics-archive/annual-steel-archive.html,
    2014a.

World Steel Association. World steel in figures 2014, published online May 2014, re-
    trieved on June 12, 2015 from
    http://www.worldsteel.org/dms/internetDocumentList/bookshop/World-Steel-in-
    Figures-
    2014/document/World%20Steel%20in%20Figures%202014%20Final.pdf,
    2014b.

Chapter 5   Comprehensive discussion

General discussion

The aim of this thesis was to give first insights about Hg in BFS as no data has been published before. Therefore, analytical methods were chosen and applied to falsify or verify the hypotheses formed in chapter 1 (scope of the study). These hypotheses will be discussed in the following:

Hypothesis 1

Mercury is enriched in BFS due to its low boiling point and high process temperatures in the blast furnace.

The fundamental hypothesis on which this thesis was based on was the assumption that Hg would be enriched in BFS like elements such as Zn and Pb. As pointed out by Mansfeldt and Dohrmann (2004) high contents of both elements in BFS cannot be exclusively explained by a mechanism based on mechanical transport. They further stated that Zn and Pb are partially reduced to their elemental form in the vapor phase due to high process temperatures and relatively low boiling points of the elements. In the upper shaft of the blast furnace, Zn and Pb partially condense on particles in the effluent gas due to the decreasing temperature. Hence, Zn and Pb are discharged with the effluent gas and "captured" by the wet cleaning process generating BFS.

Mercury is a highly volatile transition metal with a boiling point of roughly 357 °C. Theoretically, at process temperatures of up to 2200 °C any Hg contained in the charge material should be transferred to its elemental form being gaseous. Similar to Pb and Zn, to some extent Hg should condense on solid phases in the upper shaft where temperature decreases and Hg should leave the blast furnace with effluent gas.

The analyzes auf 65 BFS samples from seven different dumping sites in Europe revealed elevated Hg contents verifying Hypothesis 1. The content ranged from 0.006

to 20.8 mg kg^{-1} with a median of 1.63 mg kg^{-1} and mean of 3.08 mg kg^{-1}. For a rough risk assessment, precautionary and trigger values of the German Federal Soil Protection and Contaminated Sites Ordinance (BBodSchV, 1999) from 12 July 1999 were considered. Precautionary values are defined as values which, if exceeded, normally mean there is a reason that concern for a harmful soil change exists, taking geogenic or wide spread, settlement related pollutant content into account. The precautionary values are differentiated by the main soil type and metal: the values for Hg are 0.1 mg kg^{-1} for sand, 0.5 mg kg^{-1} for loam/silt, and 1 mg kg^{-1} for clay. As grain size distribution of BFS was described to be dominated by the silt fraction (Veres et al., 2011; Veres et al., 2010; Veres et al., 2012), precautionary value for loam/silt were chosen for a risk assessment. The vast majority of BFS samples (58 out of 65) exceeded the precautionary value of 0.5 mg kg^{-1}. Hence, environmental concerns arising from BFS are not possible to dismiss. For instance, the abandoned BFS landfill in the Ruhr area (Germany) had long been used as a recreational area – remediation and sealing have started recently. In a worst-case scenario the landfill must be regarded as a playground for playing children. In this case, trigger values of the German Federal Soil Protection Act (BBodSchG, 1998) for the direct exposure pathway solid matrix → human have to be considered. This value is 10 mg kg^{-1} for Hg being exceeded by three samples. Trigger values are defined as values which, if exceeded, shall mean that investigation with respect to the individual case in question is required, taking the relevant soil use into account, to determine whether a harmful soil change or site contamination exists.

For a further risk assessment, the soluble fraction of Hg in blast furnace sludge was determined using a slightly modified version of the German Federal Soil Protection Act. The trigger value for the assessment of the soil → groundwater pathway for Hg is 1 µg L^{-1}. Five out of 27 analyzed samples exceeded this value. However, it must

be taken into consideration that most of the BFS were already dumped for decades and hence might have (partially) leached out already. Hence, the exceedance of the trigger value is even more significant and potentially soluble Hg species are still detectable and might contaminate the dumpsites vicinity even after decades of deposition. It is known from soils that Hg easily forms complexes with chloride ions (Cl^-) resulting in water soluble mercury chlorides ($HgCl_2$, Hg_2Cl_2) or tetrahedral coordination complexes (($HgCl_4)^{2-}$). Also Hg(II) sulfate ($HgSO_4$), Hg(II) nitrate ($Hg(NO_3)_2$), and Hg(II) oxide (HgO) are water soluble Hg species being reasonable as soluble Hg species in BFS. These compounds can contaminate lower layers through vertically infiltration-induced leaching or even leak into groundwater tables.

In fact, BFS and its deposition can undergo pedological processes, however, BFS and its deposition sites shall not be regarded as soils in a legal sense. The German Federal Soil Protection Act and the German Federal Soil Protection and Contaminated Sites Ordinance were only considered to give an impression of potential environmental hazards.

For a further approach of assessing Hg contamination in BFS, enrichment factors (EF) based on Earth's crust abundance of Hg (0.056 mg kg^{-1}) stated by Wedepohl (1995) were calculated. They varied between 0.107 and 371 with a mean of 49.9 and a median of 29.1, respectively, for BFS. As EF for analyzed charged material was in the range of 0.268 (olivine) and 1.21 (bauxite), elevated Hg content in BFS and EF for BFS displayed the internal enrichment during the metallurgical process as already stated for Pb and Zn and previously assumed for Hg.

Hypothesis 2

Similar to "natural" conditions, Hg in BFS is preferentially associated with carbon-based sorbents, such as coke particles or graphite.

Once the enrichment of Hg in BFS was proved, the question arose on which particles Hg condenses during metallurgical process and cooling/cleaning of the effluent gas, respectively. The affinity of Hg towards carbon-based sorbents, such as activated C, is well described in the literature and for instance used for Hg removal from flue gases (De et al., 2013; Diamantopoulou et al., 2010; Galbreath and Zygarlicke, 2000). Spearman correlation between total Hg and total C (TC) was undertaken to show if Hg in BFS is also preferentially associated with C-based sorbents. Correlation of all samples, however, was relatively poor ($r = 0.222$, $p = 0.075$, $n = 65$). Furthermore, correlation of Hg vs. total inorganic C (TIC) and total residual C (TRC) showed low significance (TIC: $r = 0.039$, $p = 0.151$, $n = 65$; TRC: $r = 0.1093$, $p = 0.123$, $n = 65$). In contrast, the correlation of Hg vs. TC for one site with a larger set of BFS samples (Herne, Germany, $n = 31$) revealed a statistical significance with coefficient of 0.673 ($p < 0.001$). Also Hg vs. TRC showed a strong correlation ($r = 0.695$, $p < 0.001$) for the same set of samples. This indicates that, at least for dumped BFS at the Herne site, Hg is associated with sorbents having a high fraction of residual C (e.g. coke, graphite). Rietveld refinement of XRD analysis conducted by Mansfeldt and Dohrmann (2004) for the same sample set found graphite contents in BFS up to $60 \, \text{g kg}^{-1}$ with a median of $27 \, \text{g kg}^{-1}$. A correlation of the Hg content versus the graphite content yielded a correlation coefficient of $r = 0.614$ ($p = 0.02$, $n = 14$).

An explanation for the low correlation of Hg vs. TC and TRC, respectively, for all samples might be variations in the applied charge materials, pre- and post-treatment processes, and production conditions at each individual plant. Additionally, conditions of deposition and storage, such as climatic effects, may have affected the distribution of Hg on carbon-based sorbents during the last decades due to constant leaching and potential volatilization.

However, more reasonable might be the deposition of other steel making related wastes, such as basic oxygen furnace sludge (BOFS), on the same dumps sites or even a process related mixture of BFS with BOFS or other metallurgical wastes. Two samples from Nowa Huta (Krakow, Poland) previously declared as BFS had extraordinarily high Fe contents (617 and 623 g kg^{-1}, respectively) and C content (6.46 and 7.55 g kg^{-1}, respectively) far below the median of BFS (133 g kg^{-1}). The elemental composition of both samples encourages the assumption that they are rather BOFS than BFS. Correlation of Hg vs. TC for all other samples, however, still revealed a low coefficient (r = 0.244, p = 0.054, n = 63). Hence, the preferential association of Hg with carbon-based sorbents in BFS could not be clearly verified or falsified.

Hypothesis 3

An Hg-specific sequential extraction procedure developed for soils and sediments can be adopted to BFS to assess the risk potential of Hg in BFS.

Determining the chemical speciation and fractionation, respectively, of a certain pollutant is essential for an accurate risk assessment. In general, various techniques have been developed and applied to determine speciation of Hg in geochemical samples, ranging from sequential extraction procedure (SEP), sequential thermal decomposition, electron microprobe analysis, to X-ray absorption spectroscopic analysis. Among these, SEP has been widely adopted, in part because of the simplicity, efficiency, and reproducibility of the procedure (Kim et al., 2003). However, inherent disadvantages of this technique exist: besides a potential transformation of Hg species during the extraction steps, the lack of selectivity of reagents, and non-homogeneity of samples are such limitations. Nevertheless, SEP developed by Bloom et al. (2003) for inorganic Hg in soils and sediments was tested on BFS to provide further information about the distribution of Hg in different operationally defined behavioral clas-

ses. It was shown before by various authors that Hg fractionation of other solid materials and wastes was successful using the SEP by Bloom et al. (2003). For instance, coal (Yuan et al., 2010), coal fly ash, and slag (Wei et al., 2011) were analyzed for Hg fractionation, yielding reliable and repeatable data. In their studies they revealed recoveries of the total Hg content between 79.6 and 90.8 % for coal fly ash, 75 % for slag from coal-fired thermal power plants, and 72.6 % and between 86 and 115 %, respectively, for coal.

Sequential extraction was conducted on 14 BFS from five locations in Europe having total Hg contents from 3.91 to 20.8 $mg\,kg^{-1}$. Total recoveries obtained as the sum of Hg in each fraction ranged between 72.3 and 114 %. Standard deviations for the recoveries for each sample (three replicants per sample) were below 5 %. Repeatability was exemplarily determined at four subsequent days for one sample (#2116) with a total content of 4.41 $mg\,kg^{-1}$. Standard deviations were found to be 0.22 $mg\,kg^{-1}$ for F4 (relative standard deviation: 6.7 %), 0.05 $mg\,kg^{-1}$ for F5 (16.1 %), and 0.02 $mg\,kg^{-1}$ for F6 (9.2 %). Other fractions were below the limit of quality. These data indicate a reliable adoption of the soil and sediment specific SEP for BFS.

Hypothesis 4

Mercury in BFS mainly resides in the fraction of "elemental" Hg, mercuric sulfides, and Hg in crystalline metal ores and silicates and hence being rather immobile under natural conditions.

The SEP developed by Bloom et al. (2003) allows a distinction of inorganic Hg into operationally defined behavioral classes. Based on extraction kinetics and the effects of solid-to-liquid ratios, the authors developed and validated this five-step procedure. Extracts used include demineralized water (F1) representing water soluble Hg, 0.1 $mol\,L^{-1}$ CH_3COOH + 0.01 $mol\,L^{-1}$ HCl (F2) as the fraction of "human stomach

acid" soluble Hg, 1 mol L^{-1} KOH (F3) as extractant for organo-chelated Hg and calomel, 12 mol L^{-1} HNO_3 (F4) for "elemental" Hg, and aqua regia (F5) soluble fraction being mercuric sulfide. Extractant for F4 was slightly modified according to Hall et al. (2005). They proved that 7.9 mol L^{-1} HNO_3 was sufficient to dissolve non-sulfide forms of Hg without a partially dissolution of mercuric sulfides which actually supposed to be extracted afterwards.

Further, a sixth fraction was revealed by measuring the solid residue of F5 directly with a total Hg analyzer. Bloom et al. (2003) stated that a significant residue may remain after aqua regia digestion in the case of crystalline metal ores such as bauxite and Fe_2O_3. Such a procedure was not necessary as the DMA-80 is able to detect Hg in solid phases as well. So the solid residue of F5 was dried and measured with the DMA to obtain Hg in crystalline metal ores and silicates.

Distribution of Hg in the particular fractions revealed a clear trend: low amounts of Hg in the first three fractions and more than 90 % of extracted Hg being present in the last three fractions. In detail, F1 and F3 were below LOQ (0.134 and 3.89 µg kg^{-1}, respectively) in all 14 samples whereas only five samples of F2 exceeded the LOQ (0.135 µg kg^{-1}). Mercury in this fraction ranged between 0.509 and 9.61 % (median: 0.802 %). Minor amounts of Hg were determined as mercuric sulfides (F5) with a median of 7.34 % (0.848 mg kg^{-1}, n = 10) ranging from 0.725 to 37.3 % (0.051 to 7.41 mg kg^{-1}) and in F6 (Hg in crystalline metal ores and silicates) with a median of 4.25 % (0.227 mg kg^{-1}) and values up to 15.1 % (0.951 mg kg^{-1}). The majority of Hg in BFS was present in the fraction of "elemental" Hg with a median of 91.1 % (4.16 mg kg^{-1}) and contents between 2.56 and 18.2 mg kg^{-1} (48.5 to 98.8 %).

To support the established behavioral classes, Bloom et al. (2003) conducted "extraction fingerprints" by dispersing pure Hg compounds in powdered kaolin and sequentially extracting these materials. Compounds with relatively high water solubility

such as $HgCl_2$, HgO, and $HgSO_4$ were leached in the first two fractions with proportions higher than 97 %. In most studied BFS samples, none of these compounds were present as measured values were mostly below the LOQ in both fractions. However, this was reasonable as BFS were dumped for years up to decades and hence highly water soluble Hg compounds were already able to migrate into deeper layers or groundwater as a consequence of filtrating precipitation. Samples exceeding LOQ for F2 were none-surface samples, meaning that they were covered by other BFS samples or even other material. Either these compounds have not been leached out due to oversaturation of the interstitial solution, their initial content was extraordinarily high and was not totally leached out, or these compounds were leached out from upper layers and precipitated in these particular layers for unknown reasons. However, #2241 to #2245 represented a set of samples taken at the same spot but in different depths (20 to 145 cm below surface) with #2241 being the uppermost layer and #2245 being the lowest layer. The distribution pattern of high water soluble compounds yielded no clear pattern in terms of decreasing contents with depth for this set of BFS. It varied with 0.207 ± 0.006 mg kg^{-1} for #2241, 0.452 ± 0.031 mg kg^{-1} for #2243, 0.035 ± 0.005 mg kg^{-1} for #2244, and 0.061 ± 0.005 mg kg^{-1} for #2245. Sample 2242 was below LOQ. Hence, initially extraordinarily high contents of water soluble Hg compounds were suggested which had not leached out completely at the time of sampling. Further, variations of the contents were believed to result from process' or charge materials' variations. Most likely, a higher proportion of coal instead of coke was applied to the blast furnace generating these particular BFS samples. As 95 % of Cl in coal is liberated as HCl gas during the coking process (Shao et al., 1994), the Cl input increases in blast furnaces with increasing proportions of coal as a charge material. Gale et al. (2008) summarized the fundamental mechanisms governing the fate of Hg in coal flue gas. They pointed

out that unburned C can effectively catalyze Hg^0 oxidation by reacting with gaseous HCl and forming chlorinated-C sites, which then react with Hg to form HgCl. These oxidized Hg species can further react with either Cl^- or Cl_2 to form $HgCl_2$. Similar reactions are reasonable in blast furnace gas and hence higher proportions of F2 in BFS were interpreted as a result of increased coal proportions of the charge material. However, extraction fingerprints of $HgCl_2$ revealed a primary extraction of this compound in the first instead of the second fraction.

As already mentioned, Hg in BFS mainly resided in F4 as "elemental" Hg with a median of 91.1 %. However, it remained questionable if Hg extracted in this fraction was indeed Hg^0, which is why it was enclosed in quotation marks. Though all Hg is vaporized and converted to Hg^0 through thermal decomposition, it is known from cooling coal flue gas that Hg^0 can be oxidized under appropriate conditions (see above). Oxidation to Hg^{2+} is capable via homogenous (gas-gas) or heterogeneous (gas-solid, surface catalyzed) pathways (Wilcox et al., 2012). It is hence either present in flue gas as Hg^0, Hg^{2+}, or adsorbed on solid phases such as fly ash particles (Galbreath and Zygarlicke, 2000) or activated carbon (Diamantopoulou et al., 2010). The amount of Hg^0 being oxidized largely depends on the coal type, in particular its chemical composition, combustion efficiency, and pollution control devices. Detailed information about potential oxidation and its occurrence is not at hand for cooling of blast furnace gas. Nevertheless, similar processes as for the coal flue gas are reasonable for blast furnace gas. However, Hg^0 is the most difficult species to capture as it is highly volatile and low water soluble. Hence, such a dominance of Hg being present as Hg^0 in BFS is rather unlikely.

Furthermore, studied BFS samples have been dumped for years, partially up to decades. Even if Hg^0 was present in BFS due to the massive use of process water and subsequent dissolution of Hg^0 species, it would have been in minor amounts and

most likely already degassed during deposition. Though Bloom et al. (2003) suggest-ed a quick coating with a gas-impervious layer of microscopic balls of Hg^0 preserving the droplets from further oxidation and/or diffusion, no such balls were found neither on macroscopic nor microscopic scale for samples with highest total Hg contents. Consequently, Hg residing in F4 were rather interpreted as Hg compounds such as Hg(I), Hg associated with amorphous organo-sulfur, Hg–gold amalgams, and Hg as-sociated with crystalline Fe/Mn oxide phases which were shown to be dissolved in F4 as well (Bloom et al., 2003).

Although this data provided only limited information about the exact binding forms of Hg in BFS, however, it yielded some useful details about the mobility and hence the potential risk arising from Hg in dumped BFS. Mercury mainly resided in fractions being immobile under natural conditions, hence the long-term risk arising from Hg is rather low, particularly taking into account the low amount of Hg in ecotoxically rele-vant fractions. However, it must be noted that Hg in mobile fractions might already have been leached out or volatilized during deposition.

Hypothesis 5

> *Blast furnace sludge inhibits a significant potential for Hg volatilization mean-ing that Hg-fluxes from drying samples is detectable under laboratory condi-tions.*

As previously studied BFS were partially dumped for decades and hence Hg might have already been volatilized during that time, the volatilization potential should be studied on fresh samples. However, state-of-the-art integrated steel plants use joint cleaning devices for gas purification of effluent gases from both blast furnaces and so-called basic oxygen furnaces to be most cost effective. In basic oxygen furnaces pig iron, Fe scrap, ferroalloys, lime, and Fe ores are converted into low carbon steel

via lancing pure O_2 into the cast. During the blowing process, large amounts of fumes and gases are generated containing fine particles of the charge materials. Wet purification of the effluent gas results in so-called basic oxygen furnace sludge.

Unfortunately, fresh and pure BFS samples were not available for this reason. Hence, a mixture of fresh BFS with BOFS was taken from after the settling tank. Detailed information about the proportion of both effluent gases generating the studied sample, henceforth referred to as BFS/BOFS, was not given either. However, elemental composition, in particular Fe and C content, indicated a higher proportion of BOFS. Further, the Hg content of 0.178 mg kg^{-1} might suggest a minor proportion of BFS as previous BFS samples had a median Hg content of 1.63 mg kg^{-1}.

To study the volatilization potential of Hg from BFS/BOFS, sealed column experiments were conducted for four weeks in an incubator at controlled temperatures (15, 25, and 35 °C). For all temperature variants an increased volatilization rate was observed within the first 100 h (sampling took place on a daily basis) followed by a slightly decrease of trapped Hg (sampling on a 72 h basis). However, background level of the ambient air was not achieved at the end of experiment. Hence, BFS/BOFS still possessed potential for Hg degassing after four weeks.

Total Hg released within four weeks varied between 3.31 (15 °C) and 66.6 ng per kg (25 °C). However, Hg emissions are mainly influenced by Hg contents in the upper few centimeters of soils (Gillis and Miller, 2000) and Wang et al. (2014) recently showed similar results for Hg emissions from baghouse filter dust. Extrapolating volatilization from the columns' diameter yielded total Hg emissions ranging from 28.5 (15 °C) and 436 ng per m^2 and 4 weeks (25 °C). Comparing this flux with Hg released from soils yielded very low rates. Mean Hg fluxes from 13 floodplain ecosystems at the Elbe River (Germany) ranged between 138 and 711 ng per m^2 and h (Rinklebe et al., 2009; Rinklebe et al., 2013) being 92.7 and 478 µg per m^2 and h.

However, it should be stated that the analyzed soil samples were regarded as contaminated sites with total Hg content ranging from 0.54 and 16.7 mg kg^{-1} (median: 3.89 mg kg^{-1}). Soils are considered to be Hg enriched with contents higher than 0.1 mg kg^{-1}. Hence, Hg fluxes from BFS/BOFS should be rather compared with low Hg soils. The Hg volatilization rate from theses soils reported in the literature ranged from –2 to 12 ng per m^2 and h (Carpi and Lindberg, 1998; Ericksen et al., 2006; Kim et al., 2003; Yao et al., 2006; Zhang and Lindberg, 1999a; Zhang et al., 2001) being up to 8 µg per m^2 and 4 weeks and hence significant higher than rates from BFS/BOFS.

Despite BFS/BOFS possessed a rather low volatilization rate at studied temperature variants, it should be considered as a significant Hg source to the global Hg cycle as steel is still a mandatory material for modern mankind civilization and related by-products or wastes has been and will further be generated in large amounts. Quantifying Hg degassing from dumped BFS, BOFS, and their mixture, respectively, on a global basis is hard to establish as required data are not available. Neither representative studies of Hg content in this metallurgical waste are published nor reliable details about spatial extent of dumpsite, their frequency, and intensity of use are available.

Hypothesis 6

Volatilization rate of Hg from BFS is largely driven by temperature.

Unlike other trace metals, Hg exhibits a relatively high vapor pressure (0.16 Pa at 20 °C). Besides the total Hg content, this predominantly determines the potential volatilization rate. With increasing temperature, kinetic energy increases and more Hg can volatilize hence resulting in increasing vapor pressure.

Various research groups have confirmed a temperature related increase of Hg desorption with subsequent volatilization from soils and sediments. Variations of Hg emissions from low-Hg soils (0.214 ng kg^{-1}) were explained by variations in surface soil temperature and Hg content gradient between soil and ambient air surface (Gillis and Miller, 2000). Further, temperature dependence was demonstrated in both diurnal (Gustin et al., 2006) and seasonal studies (Sigler and Lee, 2006).

As initially expected, Hg flux increased from an averaged 0.300 ng kg^{-1} per 24 h for 15 °C to an averaged 8.45 ng kg^{-1} per 24 h for 25 °C within the first 100 h. Also the lower Hg rate thereafter was higher for the 25 °C variant (4.10 ng kg^{-1} per 72 h) as for 15 °C (0.284 ng kg^{-1} per 72 h). However, Hg emissions at 35 °C were surprisingly lower than for 25 °C both within the first 100 h (1.82 ng kg^{-1} per 24 h) and thereafter (2.60 ng kg^{-1} per 72 h). Factors which have been correlated with Hg^0 from soils, besides total Hg content and temperature, are atmospheric oxidants and ozone, respectively, (Engle et al., 2005), meteorological conditions (Gustin et al., 2006; Gustin et al., 1997; Poissant et al., 1999; Schlüter, 2000; Zhang and Lindberg, 1999b), and soil moisture (Gustin and Stamenkovic, 2005). Variations in atmospheric ozone and meteorological conditions as a reason for lower volatilization from BFS/BOFS at 35 °C were excluded as experiments were conducted under identical laboratory conditions. However, water contents at the start and end of experiments, respectively, at 35 °C were significantly lower than for both other temperature variants: contents decreased during the performance of experiments from 53.7 to 47.1 % (median of 15 and 25 °C) in contrast to a decrease from 44.6 to 39 % for 35 °C. Decreasing water content was determined to result in decreased Hg flux in low-Hg soils (Gustin and Stamenkovic, 2005). A threefold increase in Hg flux was observed in a field study with increasing soil moisture from 2.8 to 8.4 % (Gustin et al., 2006). Also Lindberg et al. (1999) described similar results. They further suggested chemical and physical interactions for

enhanced Hg emissions with rising soil moisture: i) physical displacement of Hg^0 enriched interstitial soil air by infiltrating water, (ii) replacement of Hg^0 adsorbed to the soil by water molecules, and (iii) desorption of Hg^{2+} bound to the soil and subsequent reduction to Hg^0 through abiotic or biotic factors. Similar mechanisms are reasonable for BFS/BOFS. Consequently, decreased water content in BFS/BOFS could have resulted in countervailing interactions and hence in lower Hg fluxes at 35 °C.

However, it must be stated that column IV at 35 °C exhibited similar water contents both at the start of the experiment (49.2 %) and at the end of the experiment (43.4 %) as water contents of the other temperature variants. Nevertheless, Hg flux of this particular column was not significantly higher as the other columns at 35 °C. Hence, a decreased Hg volatilization from BFS/BOFS at 35 °C cannot be solely explained by lower water content.

Future prospects

This thesis should be rather understood as a first approach of describing Hg distribution and mobility of Hg in BFS than a complete and detailed description of Hg in BFS. Hence, further research should be undertaken for a full understanding of Hg in this industrial waste. The following aspects should be taken into consideration:

− Nothing is known about species distribution of Hg in blast furnace gas, which therefore should be studied. Most likely a proportion of Hg is present as Hg^0. Hence, a significant amount of Hg is not captured by gas purification processes generating BFS. The fate of this Hg is unclear.

− Only limited information about the exact binding forms of Hg in BFS was revealed by the SEP. Further research in this filed should be undertaken. For instance near edge X-ray absorption fine structure spectroscopy or wave dis-

persive X-ray microprobe spectroscopy might give further information. However, high limits of analytical detection might prevent this approach.

− In modern integrated steel plants, BFS and/or BOFS are sent to open settling tanks to separate solid material from most of the bulk water. Mercury volatilization potential from these tanks should be determined as it might be an unknown Hg source to the global Hg cycle.

− To quantify Hg fluxes from BFS/BOFS on a global basis, a representative data set of total Hg content in this material and accruing quantities should be collected.

− Effects of varying water contents of BFS on Hg fluxes should be studied as this waste is most likely dumped in open surface landfills in countries with less strict environmental laws. Hence, rainfall might increase Hg volatilization as it is known for soils.

− As background level of ambient air was not achieved after four weeks in sealed column experiments, longtime studies should be conducted till no further Hg is released. Further, sampling with higher temporal resolution would reveal more details about primarily elevated Hg fluxes.

Chapter 6   References

Alekseenko V, Alekseenko A. The abundances of chemical elements in urban soils. Journal of Geochemical Exploration 2014; 147: 245-249.

Banic CM, Beauchamp ST, Tordon RJ, Schroeder WH, Steffen A, Anlauf KA, et al. Vertical distribution of gaseous elemental mercury in Canada. Journal of Geophysical Research: Atmospheres 2003; 108.

Barkay T, Miller SM, Summers AO. Bacterial mercury resistance from atoms to ecosystems. FEMS Microbiology Reviews 2003; 27: 355-384.

BBodSchG. Federal Soil Protection Act (Bundes-Bodenschutzgesetz - BBodSchG) from 17.03.1998. BGBl. I pp. 502-510, 1998.

BBodSchV. Federal Soil Protection and Contaminated Sites Ordinance (Bundes-Bodenschutz- und Altlastenverordnung - BBodSchV) from 12.07.1999. BGBl. I pp. 1554-1582, 1999.

Bindler R. Estimating the natural background atmospheric deposition rate of mercury utilizing ombrotrophic bogs in southern Sweden. Environmental Science & Technology 2003; 37: 40-46.

Bloom NS, Preus E, Katon J, Hiltner M. Selective extractions to assess the biogeochemically relevant fractionation of inorganic mercury in sediments and soils. Analytica Chimica Acta 2003; 479: 233-248.

Borisov VV, Ivanov SY, Fuks AY. Factory Tests of a Technology for Recycling Metallurgical Sludge that Contains Iron and Zinc. Metallurgist 2014; 58: 3-10.

Cantarino MV, de Carvalho Filho C, Mansur MB. Selective removal of zinc from basic oxygen furnace sludges. Hydrometallurgy 2012; 111: 124-128.

Carpi A, Lindberg SE. Application of a Teflon (TM) dynamic flux chamber for quantifying soil mercury flux: Tests and results over background soil. Atmospheric Environment 1998; 32: 873-882.

Chalmers AT, Krabbenhoft DP, Van Metre PC, Nilles MA. Effects of urbanization on mercury deposition and New England. Environmental Pollution 2014; 192: 104-112.

Choi H-D, Holsen TM. Gaseous mercury emissions from unsterilized and sterilized soils: The effect of temperature and UV radiation. Environmental Pollution 2009; 157: 1673-1678.

Ci Z, Zhang X, Wang Z, Niu Z. Phase speciation of mercury (Hg) in coastal water of the Yellow Sea, China. Marine Chemistry 2011; 126: 250-255.

Clean Air Act Amendments of 1990. Pub. L. No. 101-549, sec. 701, § 113, 104 Stat. 2399, 2672-80 (codified at 42 U.S.C. § 7413 (1994)), 1990.

Coolbaugh MF, Gustin MS, Rytuba JJ. Annual emissions of mercury to the atmosphere from natural sources in Nevada and California. Environmental Geology 2002; 42: 338-349.

Costa M, Liss PS. Photoreduction of mercury in sea water and its possible implications for Hg^0 air-sea fluxes. Marine Chemistry 1999; 68: 87-95.

Das B, Prakash S, Reddy PSR, Misra VN. An overview of utilization of slag and sludge from steel industries. Resources, Conservation and Recycling 2007; 50: 40-57.

Davidson R, Claerke L. Trace Elements in Coal. IEA Coal Research, London, 1996.

De M, Azargohar R, Dalai AK, Shewchuk SR. Mercury removal by bio-char based modified activated carbons. Fuel 2013; 103: 570-578.

Diamantopoulou I, Skodras G, Sakellaropoulos GP. Sorption of mercury by activated carbon in the presence of flue gas components. Fuel Processing Technology 2010; 91: 158-163.

Driscoll CT, Han Y-J, Chen CY, Evers DC, Lambert KF, Holsen TM, et al. Mercury contamination in forest and freshwater ecosystems in the Northeastern United States. Bioscience 2007; 57: 17-28.

Engle MA, Gustin MS. Scaling of atmospheric mercury emissions from three naturally enriched areas: Flowery Peak, Nevada; Peavine Peak, Nevada; and Long Valley Caldera, California. Science of the Total Environment 2002; 290: 91-104.

Engle MA, Gustin MS, Lindberg SE, Gertler AW, Ariya PA. The influence of ozone on atmospheric emissions of gaseous elemental mercury and reactive gaseous mercury from substrates. Atmospheric Environment 2005; 39: 7506-7517.

Engle MA, Gustin MS, Zhang H. Quantifying natural source mercury emissions from the Ivanhoe Mining District, north-central Nevada, USA. Atmospheric Environment 2001; 35: 3987-3997.

Ericksen JA, Gustin MS, Xin M, Weisberg PJ, Fernandez GCJ. Air-soil exchange of mercury from background soils in the United States. Science of the Total Environment 2006; 366: 851-863.

Ettler V, Navratil T, Mihaljevic M, Rohovec J, Zuna M, Sebek O, et al. Mercury deposition/accumulation rates in the vicinity of a lead smelter as recorded by a peat deposit. Atmospheric Environment 2008; 42: 5968-5977.

Farella N, Lucotte M, Davidson R, Daigle S. Mercury release from deforested soils triggered by base cation enrichment. Science of the Total Environment 2006; 368: 19-29.

Feng XB, Wang SF, Qiu GA, Hou YM, Tang SL. Total gaseous mercury emissions from soil in Guiyang, Guizhou, China. Journal of Geophysical Research: Atmospheres 2005; 110.

Fitzgerald WF, Lamborg CH, Hammerschmidt CR. Marine biogeochemical cycling of mercury. Chemical Reviews 2007; 107: 641-662.

Fritsche J, Obrist D, Alewell C. Evidence of microbial control of Hg^0 emissions from uncontaminated terrestrial soils. Journal of Plant Nutrition and Soil Science - Zeitschrift für Pflanzenernährung und Bodenkunde 2008; 171: 200-209.

Fukuda N, Takaoka M, Doumoto S, Oshita K, Morisawa S, Mizuno T. Mercury emission and behavior in primary ferrous metal production. Atmospheric Environment 2011; 45: 3685-3691.

Galbreath KC, Zygarlicke CJ. Mercury transformations in coal combustion flue gas. Fuel Processing Technology 2000; 65: 289-310.

Gale TK, Lani BW, Offen GR. Mechanisms governing the fate of mercury in coal-fired power systems. Fuel Processing Technology 2008; 89: 139-151.

Gillis AA, Miller DR. Some local environmental effects on mercury emission and absorption at a soil surface. Science of the Total Environment 2000; 260: 191-200.

Grant SL, Kim M, Lin P, Crist KC, Ghosh S, Kotamarthi VR. A simulation study of atmospheric mercury and its deposition in the Great Lakes. Atmospheric Environment 2014; 94: 164-172.

Gu B, Bian Y, Miller CL, Dong W, Jiang X, Liang L. Mercury reduction and complexation by natural organic matter in anoxic environments. Proceedings of the National Academy of Sciences of the United States of America 2011; 108: 1479-1483.

Gustin MS. Are mercury emissions from geologic sources significant? A status report. Science of the Total Environment 2003; 304: 153-167.

Gustin MS, Coolbaugh MF, Engle MA, Fitzgerald BC, Keislar RE, Lindberg SE, et al. Atmospheric mercury emissions from mine wastes and surrounding geologically enriched terrains. Environmental Geology 2003; 43: 339-351.

Gustin MS, Engle M, Ericksen J, Lyman S, Stamenkovic J, Xin M. Mercury exchange between the atmosphere and low mercury containing substrates. Applied Geochemistry 2006; 21: 1913-1923.

Gustin MS, Stamenkovic J. Effect of watering and soil moisture on mercury emissions from soils. Biogeochemistry 2005; 76: 215-232.

Gustin MS, Taylor GE, Maxey RA. Effect of temperature and air movement on the flux of elemental mercury from substrate to the atmosphere. Journal of Geophysical Research: Atmospheres 1997; 102: 3891-3898.

Hall GEM, Pelchat P, Percival JB. The design and application of sequential extractions for mercury, Part 1. Optimization of HNO3 extraction for all non-sulphide forms of Hg. Geochemistry: Exploration, Environment, Analysis 2005; 5: 107-113.

Hammerschmidt CR, Bowman KL. Vertical methylmercury distribution in the subtropical North Pacific Ocean. Marine Chemistry 2012; 132: 77-82.

Hooda PS. Trace Elemnts in Soils. West Sussex: John Wiley & Sons Ltd, 2010.

Iverfeldt Å. Structural, thermodynamic and kinetic studies of mercury compounds; applications within the environmentlal mercury cycle. (PhD). University of Göteborg, 1984.

Jiang T, Wei S-Q, Flanagan DC, Li M-J, Li X-M, Wang Q, et al. Effect of Abiotic Factors on the Mercury Reduction Process by Humic Acids in Aqueous Systems. Pedosphere 2014; 24: 125-136.

Kim CS, Bloom NS, Rytuba JJ, Brown GE. Mercury speciation by X-ray absorption fine structure spectroscopy and sequential chemical extractions: A comparison of speciation methods. Environmental Science & Technology 2003; 37: 5102-5108.

Kretzschmar R, Mansfeldt T, Mandaliev PN, Barmettler K, Marcus MA, Voegelin A. Speciation of Zn in Blast Furnace Sludge from Former Sedimentation Ponds Using Synchrotron X-ray Diffraction, Fluorescence, and Absorption Spectroscopy. Environmental Science & Technology 2012; 46: 12381-12390.

Langova S, Matysek D. Zinc recovery from steel-making wastes by acid pressure leaching and hematite precipitation. Hydrometallurgy 2010; 101: 171-173.

Laurier FJG, Mason RP, Gill GA, Whalin L. Mercury distributions in the North Pacific Ocean - 20 years of observations. Marine Chemistry 2004; 90: 3-19.

Leipe T, Moros M, Kotilainen A, Vallius H, Kabel K, Endler M, et al. Mercury in Baltic Sea sediments-Natural background and anthropogenic impact. Chemie der Erde - Geochemistry 2013; 73: 249-259.

Lindberg SE, Jackson DR, Huckabee JW, Janzen SA, Levin MJ, Lund JR. Atmospheric emission and plant uptake of mercury from agricultural soils near the Almadén mercury mine. Journal of Environmental Quality 1979; 8: 572-578.

Lindberg SE, Zhang H, Gustin M, Vette A, Marsik F, Owens J, et al. Increases in mercury emissions from desert soils in response to rainfall and irrigation. Journal of Geophysical Research: Atmospheres 1999; 104: 21879-21888.

Lopez-Delgado A, Perez C, Lopez FA. The influence of carbon content of blast furnace sludges and coke on the adsorption of lead ions from aqueous solution. Carbon 1996; 34: 423-431.

Ma JJ, Yao H, Luo GQ, Xu MH, Han J, He XM. Distribution of Hg, As, Pb, and Cr in a Coke Oven Plant. Energy & Fuels 2010; 24: 5289-5290.

Makkonen HT, Heino J, Laitila L, Hiltunen A, Poylio E, Harkki J. Optimisation of steel plant recycling in Finland: dusts, scales and sludge. Resources, Conservation and Recycling 2002; 35: 77-84.

Malina J, Radenovic A. Kinetic Aspects of Methylene Blue Adsorption on Blast Furnace Sludge. Chemical and Biochemical Engineering Quarterly 2014; 28: 491-498.

Mansfeldt T, Dohrmann R. Chemical and mineralogical characterization of blast-furnace sludge from an abandoned landfill. Environmental Science & Technology 2004; 38: 5977-5984.

Mason RP, Choi AL, Fitzgerald WF, Hammerschmidt CR, Lamborg CH, Soerensen AL, et al. Mercury biogeochemical cycling in the ocean and policy implications. Environmental Research 2012; 119: 101-117.

Mason RP, Fitzgerald WF, Morel FMM. The Biogeochemical Cycling of Elemental Mercury - Anthropogenic Influences. Geochimica et Cosmochimica Acta 1994; 58: 3191-3198.

Mason RP, Rolfhus KR, Fitzgerald WF. Mercury in the North Atlantic. Marine Chemistry 1998; 61: 37-53.

Mason RP, Sheu GR. Role of the ocean in the global mercury cycle. Global Biogeochemical Cycles 2002; 16.

Morey GB, Lively RS. Background levels of mercury and arsenic in Paleoproterozic rocks of the Mesabi iron range, northern Minnesota. Minnesota Geological Survey Information Circular 1999; 43.

Nacht DM, Gustin MS. Mercury emissions from background and altered geologic units throughout Nevada. Water, Air, & Soil Pollution 2004; 151: 179-193.

Nogami H, Yagi J-i, Kitamura S-y, Austin PR. Analysis on material and energy balances of ironmaking systems on blast furnace operations with metallic charging, top gas recycling and natural gas injection. Isij International 2006; 46: 1759-1766.

Obrist D. Atmospheric mercury pollution due to losses of terrestrial carbon pools? Biogeochemistry 2007; 85: 119-123.

Obrist D, Fain X, Berger C. Gaseous elemental mercury emissions and CO_2 respiration rates in terrestrial soils under controlled aerobic and anaerobic laboratory conditions. Science of the Total Environment 2010; 408: 1691-1700.

Poissant L, Pilote M, Casimir A. Mercury flux measurements in a naturally enriched area: Correlation with environmental conditions during the Nevada Study and Tests of the Release of Mercury From Soils (STORMS). Journal of Geophysical Research: Atmospheres 1999; 104: 21845-21857.

Ravichandran M. Interactions between mercury and dissolved organic matter - a review. Chemosphere 2004; 55: 319-331.

Remus R, Monsonet MAA, Roudier S, Sancho LD. Best Available Techniques (BAT) Reference Document for Iron and Steel Production, Luxembourg, 2013.

Rinklebe J, During A, Overesch M, Wennrich R, Staerk H-J, Mothes S, et al. Optimization of a simple field method to determine mercury volatilization from soils-Examples of 13 sites in floodplain ecosystems at the Elbe River (Germany). Ecological Engineering 2009; 35: 319-328.

Rinklebe J, Wennrich R, Du Laing G, Staerk HJ, Mothes S. Mercury emissions from flooded soils and sediments in Germany are an underestimated problem: challenges for reliable risk assessments and management strategies. Proceedings of the 16th International Conference on Heavy Metals in the Environment 2013; 1.

Rocha JC, Sargentini E, Zara LF, Rosa AH, dos Santos A, Burba P. Reduction of mercury(II) by tropical river humic substances (Rio Negro) - Part II. Influence of structural features (molecular size, aromaticity, phenolic groups, organically bound sulfur). Talanta 2003; 61: 699-707.

Roederer C, Gourtsoyannis L. Technical steel research - Coordinated study 'steel-environment'. European Commission Directorate-General XII Science, Research and Development, Luxembourg, 1996.

Schlüter K. Review: evaporation of mercury from soils. An integration and synthesis of current knowledge. Environmental Geology 2000; 39: 249-271.

Schroeder WH, Munthe J. Atmospheric mercury - An overview. Atmospheric Environment 1998; 32: 809-822.

Selin NE. Global Biogeochemical Cycling of Mercury: A Review. Annual Review of Environment and Resources 2009; 34: 43-63.

Selin NE, Jacob DJ, Yantosca RM, Strode S, Jaegle L, Sunderland EM. Global 3-D land-ocean-atmosphere model for mercury: Present-day versus preindustrial cycles and anthropogenic enrichment factors for deposition. Global Biogeochemical Cycles 2008; 22.

Shao DK, Hutchinson EJ, Cao HB, Pan WP, Chou CL. Behavior of chlorine during coal pyrolysis. Energy & Fuels 1994; 8: 399-401.

Sigler JM, Lee X. Gaseous mercury in background forest soil in the northeastern United States. Journal of Geophysical Research: Biogeosciences 2006; 111.

Skyllberg U, Bloom PR, Qian J, Lin CM, Bleam WF. Complexation of mercury(II) in soil organic matter: EXAFS evidence for linear two-coordination with reduced sulfur groups. Environmental Science & Technology 2006; 40: 4174-4180.

Slemr F, Brunke EG, Ebinghaus R, Kuss J. Worldwide trend of atmospheric mercury since 1995. Atmospheric Chemistry and Physics 2011; 11: 4779-4787.

Song XX, Van Heyst B. Volatilization of mercury from soils in response to simulated precipitation. Atmospheric Environment 2005; 39: 7494-7505.

Strode SA, Jaegle L, Selin NE, Jacob DJ, Park RJ, Yantosca RM, et al. Air-sea exchange in the global mercury cycle. Global Biogeochemical Cycles 2007; 21.

Swain EB, Engstrom DR, Brigham ME, Henning TA, Brezonik PL. Increasing Rates of Atmospheric Mercury Deposition in Midcontinental North-America. Science 1992; 257: 784-787.

Trung ZH, Kukurugya F, Takacova Z, Orac D, Laubertova M, Miskufova A, et al. Acidic leaching both of zinc and iron from basic oxygen furnace sludge. Journal of Hazardous Materials 2011; 192: 1100-1107.

UNEP. Global Mercury Assessment, UNEP Chemicals Branch, Geneva, Switzerland 2002.

UNEP. Global Mercury Assessment 2013, Sources, Emissions, Releases and Environmental Transport, UNEP Chemicals Branch, Geneva, Switzerland, 2013.

Valente RJ, Shea C, Humes KL, Tanner RL. Atmospheric mercury in the Great Smoky Mountains compared to regional and global levels. Atmospheric Environment 2007; 41: 1861-1873.

Van Metre PC. Increased atmospheric deposition of mercury in reference lakes near major urban areas. Environmental Pollution 2012; 162: 209-215.

Veres J, Jakabsky S, Lovas M. Zinc recovery from iron and steel making wastes by conventional and microwave assisted leaching. Acta Montanistica Slovaca 2011; 16: 185-191.

Veres J, Jakabsky S, Sepelak V. Chemical, Physical, Morphological and Structural Characterization of Blast Furnace Sludge. Diffusion Fundamentals 2010; 12: 88-91.

Veres J, Lovas M, Jakabsky S, Sepelak V, Hredzak S. Characterization of blast furnace sludge and removal of zinc by microwave assisted extraction. Hydrometallurgy 2012; 129: 67-73.

Wang J, Hayes J, Wu C-Y, Townsend T, Schert J, Vinson T, et al. Characterization of Vapor Phase Mercury Released from Concrete Processing with Baghouse Filter Dust Added Cement. Environmental Science & Technology 2014; 48: 2481-2487.

Wang Q, Shen WG, Ma ZW. Estimation of mercury emission from coal combustion in China. Environmental Science & Technology 2000; 34: 2711-2713.

Wedepohl KH. The composition of the continental crust. Geochimica et Cosmochimica Acta 1995; 59: 1217-1232.

Wei Z, Wu G, Su R, Li C, Liang P. Mobility and contamination assessment of mercury in coal fly ash, atmospheric deposition, and soil collected fron Tianjin, China. Environmental Toxicology and Chemistry 2011; 30: 1997-2003.

Weiss-Penzias P, Jaffe DA, McClintick A, Prestbo EM, Landis MS. Gaseous elemental mercury in the marine boundary layer: Evidence for rapid removal in anthropogenic pollution. Environmental Science & Technology 2003; 37: 3755-3763.

WHO. Mercury in drinking-water. Background document for develoment of WHO Guidelines for drinking-water quality. Geneva: World Health Organisation (WHO/SDE/WSH/05.08/10), 2005.

Wilcox J, Rupp E, Ying SC, Lim D-H, Negreira AS, Kirchofer A, et al. Mercury adsorption and oxidation in coal combustion and gasification processes. International Journal of Coal Geology 2012; 90: 4-20.

World Steel Association. Crude steel production, 1980-2013, published online November 2014, retrieved on September 12, 2015 from http://www.worldsteel.org/dms/internetDocumentList/statistics-archive/production-archive/steel-archive/steel-annually/steel-annually-1980-2013/document/steel%20annually%201980-2013.pdf 2014a.

World Steel Association. Fact Sheet - Steel industry by-products, published online October 2014, retrieved on September 12, 2015 from http://www.worldsteel.org/publications/fact-sheets/content/01/text_files/file/document/Fact_By-products_2014.pdf, 2014b.

World Steel Association. Sustainable steel - Policy and indicators 2014, published online October 2014, retrieved on September 12, 2015 from http://www.worldsteel.org/dms/internetDocumentList/bookshop/2014/Sustainable-indicators-2014/document/Sustainable%20indicators%202014.pdf. 2014c.

World Steel Association. World Steel in Figures 2014, published online May 2014, retrieved on September 12, 2015 from http://www.worldsteel.org/dms/internetDocumentList/bookshop/World-Steel-in-Figures-2014/document/World%20Steel%20in%20Figures%202014%20Final.pdf, 2014d.

Xia K, Skyllberg UL, Bleam WF, Bloom PR, Nater EA, Helmke PA. X-ray absorption spectroscopic evidence for the complexation of Hg(II) by reduced sulfur in soil humic substances. Environmental Science & Technology 1999; 33: 257-261.

Xu L, Chen J, Yang L, Yin L, Yu J, Qiu T, et al. Characteristics of total and methyl mercury in wet deposition in a coastal city, Xiamen, China: Concentrations, fluxes and influencing factors on Hg distribution in precipitation. Atmospheric Environment 2014; 99: 10-16.

Yao AJ, Qing CL, Mu SS, Reardon EJ. Effects of humus on the environmental activity of mineral-bound Hg: Influence on Hg volatility. Applied Geochemistry 2006; 21: 446-454.

Yuan CG, Li QP, Feng YN, Chang AL. Fractions and leaching characteristics of mercury in coal. Environmental Monitoring and Assessment 2010; 167: 581-586.

Zehner RE, Gustin MS. Estimation of mercury vapor flux from natural substrate in Nevada. Environmental Science & Technology 2002; 36: 4039-4045.

Zeydabadi BA, Mowla D, Shariat MH, Kalajahi JF. Zinc recovery from blast furnace flue dust. Hydrometallurgy 1997; 47: 113-125.

Zhang H, Lindberg S, Gustin M, Xu XH. Toward a better understanding of mercury emissions from soils. In: Cai Y, Braids OC, editors. Biogeochemistry of Environmentally Important Trace Elements. 835, 2003, pp. 246-261.

Zhang H, Lindberg SE. Processes influencing the emission of mercury from soils: A conceptual model. Journal of Geophysical Research-Atmospheres 1999a; 104: 21889-21896.

Zhang H, Lindberg SE. Processes influencing the emission of mercury from soils: A conceptual model. Journal of Geophysical Research: Atmospheres 1999b; 104: 21889-21896.

Zhang H, Lindberg SE, Marsik FJ, Keeler GJ. Mercury air/surface exchange kinetics of background soils of the Tahquamenon River watershed in the Michigan Upper Peninsula. Water, Air, & Soil Pollution 2001; 126: 151-169.

Zhang Y, Jaegle L, Thompson L. Natural biogeochemical cycle of mercury in a global three-dimensional ocean tracer model. Global Biogeochemical Cycles 2014; 28: 553-570.

Zheng W, Hintelmann H. Mercury isotope fractionation during photoreduction in natural water is controlled by its Hg/DOC ratio. Geochimica et Cosmochimica Acta 2009; 73: 6704-6715.

Chapter 7 Summary

Mercury (Hg) is considered as one of the most important environmental pollutants as the element and many of its compounds are highly toxic, persistent, and readily released into the environment due to their high mobility and volatility. Among others, Hg occurs naturally in the charge materials of pig iron production, mainly coke and iron ores. Similar to elements such as zinc (Zn), lead (Pb), sodium (Na), and potassium (K), Hg evaporates in the blast furnace during the melting production process due to its low boiling point. Hence, it is present in the effluent gas both in its gaseous form and associated with particles of the charge material. Subsequently, Hg is enriched in the sludge generated by the wet cleaning process of the effluent gas, referred to as blast furnace sludge (BFS). Despite its ecotoxicological potential arising from trace metal contamination (mainly Zn and Pb), BFS has long been dumped in sedimentation ponds. Sixty-five samples from seven former BFS dumpsites in Europe were investigated regarding mercury (Hg) for the first time. The total Hg content in BFS ranged between 0.006 and 20.8 mg kg^{-1} with a median of 1.63 mg kg^{-1}. The NH_4NO_3-solubility of Hg in the samples was rather low and did not exceed 0.43 % of total Hg.

To investigate the potential pollution status of BFS, a set of 14 samples from the former BFS dumpsites in Europe with total Hg contents ranging from 3.91 to 20.8 mg kg^{-1} were sequentially extracted. Total recovery ranged between 72.3 and 114 % indicating that the Hg-specific procedure for soils and sediments was reliable when adopted to this industrial waste. Mercury mainly resided in the fraction of "elemental" Hg (48.5–98.8 %) rather being present as slightly soluble Hg species associated with sludge particles. Further, minor amounts were found as mercuric sulfide (0.725–37.3 %) and Hg in crystalline metal ores and silicates (2.21–15.1 %). The ecotoxically relevant fractions were not of major significance (F1, <limit of quality; F2, 0.509–9.61 %, n=5).

As these samples were dumped for years up to decades and hence mobile Hg might already have been leached out or volatilized, a fresh sample of BFS mixed with basic oxygen furnace sludge (BOFS; total Hg: 0.178 mg kg^{-1}) was studied for Hg volatilization. Basic oxygen furnace sludge is a residue of gas purification from steel making, which is often processed simultaneously in the cleaning devices of BFS. Sealed column experiments were conducted for four weeks at three temperatures (15, 25, and 35 °C).

Volatilization ranged between 0.366 and 0.151 ng at 15 °C, between 12.9 and 2.82 ng at 25 °C, and between 3.16 and 1.52 ng at 35 °C. Surprisingly, Hg fluxes were lower at 35 than 25 °C. For all temperature variants, an elevated Hg flux was observed within the first 100 h followed by a slight decrease of volatilization afterwards. However, background level of ambient air was not obtained at the end of the experiments indicating that BFS mixed with BOFS still possessed a potential of Hg volatilization.

Blast furnace sludge can be regarded as potential hazardous waste since among other elements Hg is significantly enriched in this waste. Mercury mainly resides in fractions being immobile under natural conditions, hence the long-term risk is rather low, particularly taking into account the low amount of Hg in ecotoxically relevant fractions. Despite low volatilization of Hg from fresh BFS/BOFS for all studied temperature ranges, emissions of Hg to the atmosphere are of global, environmental concern due to the long atmospheric lifetime and the bioaccumulation after deposition.

Chapter 8 Zusammenfassung

Quecksilber (Hg) und viele seiner Verbindungen werden auf Grund ihrer hohen Toxizität, Mobilität und Volatilität als Umweltschadstoff von übergeordneter Bedeutung eingestuft. Neben anderen Spurenelementen ist auch Hg geogen in den Ausgangsstoffen der Roheisenproduktion, im Wesentlichen Koks und Eisenerze, enthalten. Auf Grund seines geringen Schmelz- bzw. Siedepunktes verflüchtigt sich Hg, ähnlich wie Zink (Zn), Blei (Pb), Natrium (Na) und Kalium (K), während des Schmelzvorganges im Hochofen und gelangt so in die Abluft. Hier ist Hg sowohl in der Gasphase als auch als sorbierte Spezies an Partikel der Ausgangsstoffe vorhanden. Durch die Nassreinigung der Abluft des Hochofens reichert sich Hg in den anfallenden Schlämmen an. Diese werden als Gichtgasschlämme (GGS) bezeichnet.

Trotz der bereits bekannten Kontamination (v.a. mit Zn und Pb) wurden GGS während des 20. Jahrhunderts in Oberflächenhalden deponiert. Einige (n = 7) dieser ehemaligen Deponien in Europa wurden beprobt (n = 65) und erstmalig hinsichtlich einer Hg-Kontamination untersucht.

Der Hg-Gehalt der untersuchten Schlämme schwankte zwischen 0,006 und 20,8 mg kg^{-1}, der Median lag bei 1,63 mg kg^{-1}. Der NH_4NO_3-lösliche Anteil an Hg wurde mit maximal 0,43 % des Gesamtgehalts als eher gering eingestuft. Um das Gefährdungspotenzial der GGS abzuschätzen wurden 14 Proben der ehemaligen Deponien mit Gesamtgehalten von 3,91 bis 20,8 mg kg^{-1} sequentiell extrahiert. Eine Wiederfindungsrate zwischen 72,3 bis 114 % deutet auf eine verlässliche und sichere Anwendung der Hg-spezifischen Methode für Böden und Sedimente auf die untersuchten Industrieschlämme hin. Quecksilber wurde überwiegend (48,5–98,8 %) in der Fraktion des „elementaren" Hg nachgewiesen. Hierbei handelt es sich vermutlich eher um schwach lösliche Spezies, welche mit Schlammpartikeln assoziiert waren. Desweitern wurden geringe Anteile zum einem als Hg-Sulfide (0.725–37.3 %) und zum anderem als Hg in kristallinen Eisenerzen und Silikaten (2,21–15,1 %) extra-

hiert. Die direkt umweltrelevanten Fraktionen waren von untergeordneter Bedeutung (F1 < Nachweisgrenze; F2: 0,509–9,61 %, n=5).

Allerdings befanden sich alle Proben bereits seit Jahren bzw. Jahrzehnten auf Oberflächendeponien wonach potentiell vorhandenes, mobiles Hg bereits ausgewaschen oder entgast sein könnte. Um eine mögliche Hg-Verflüchtigung einzuschätzen, wurde eine frische Probe von GGS vermischt mit Konverterschlämmen (KS) untersucht (Gesamt-Hg: 0.178 mg kg^{-1}) – KS sind ein Abfallprodukt der Abgasreinigung in der Stahlerzeugung, welche häufig zeitgleich und in situ mit der Gichtgasreinigung durchgeführt wird. Für die Untersuchung wurden geschlossene Säulenversuche bei drei Temperaturstufen (15, 25 und 35 °C) für jeweils vier Wochen durchgeführt.

Die Hg-Entgasung betrug zwischen 0,151 und 0,366 ng bei 15 °C, zwischen 2,82 und 12,9 ng bei 25 °C, und zwischen 1,52 und 3,16 ng bei 35 °C. Unerwarteter Weise, lag die Hg-Flussrate bei 35 °C unter der Rate von 25 °C. Allen Temperaturstufen gemein war eine anfänglich erhöhte Hg-Entgasung innerhalb der ersten 100 h gefolgt von einer leichten Abnahme. Hintergrundgehalte der Raumluft wurden jedoch bei allen drei Varianten nicht erreicht. Hier raus lässt sich ableiten, dass auch noch nach vier Wochen ein Entgasungspotenzial vorhanden war.

Gichtgasschlämme sind als umweltgefährdend zu klassifizieren, da sie neben Hg ebenfalls auch mit anderen Elementen angereichert sind. Unter natürlichen Bedingungen liegt Hg überwiegend in immobiler Form vor, daher ist eine langfristige Gefährdung eher als gering zu bewerten. Belegt wird dies durch die geringen Hg-Gehalte in den unmittelbar umweltgefährdenden Fraktionen. Trotz einer eher als gering zu betrachtenden Hg-Entgasung von frischen GGS/KS in allen untersuchten Temperaturstufen ist diese Hg-Quelle durch die lange Verweildauer in der Atmosphäre und der bioakkumulierenden Wirkung nach seiner Deposition von einem starken umweltrelevantem Interesse.

Erklärung

Ich versichere, dass ich die von mir vorgelegte Dissertation selbständig angefertigt, die benutzten Quellen und Hilfsmittel vollständig angegeben und die Stellen der Arbeit − einschließlich Tabellen, Karten und Abbildungen −, die anderen Werken im Wortlaut oder dem Sinn nach entnommen sind, in jedem Einzelfall als Entlehnung kenntlich gemacht habe; dass diese Dissertation noch keiner anderen Fakultät oder Universität zur Prüfung vorgelegen hat; dass sie −abgesehen von unten angegebenen Teilpublikationen −noch nicht veröffentlicht worden ist, sowie, dass ich eine solche Veröffentlichung vor Abschluss des Promotionsverfahrens nicht vornehmen werde. Die Bestimmungen der Promotionsordnung sind mir bekannt. Die von mir vorgelegte Dissertation ist von Prof. Dr. Tim Mansfeldt betreut worden.

Köln, Oktober 2016   Corinna Földi

Eigenbeteiligung an den Veröffentlichungen

1. **Földi, C**, Dohrmann, R, Mansfeldt, T. 2014. Mercury in dumped blast furnace sludge. *Chemosphere* 99, 248–253.
   Erhebung der Daten im Labor: 40 %
   Auswertung und Interpretation: 85 %
   Verfassen der Publikation: 90 %

2. **Földi, C**, Andrée, C-A, Mansfeldt, T. 2015. Sequential extraction of inorganic mercury in dumped blast furnace sludge. *Environmental Science and Pollution Research* 22, 15755-15762.
   Erhebung der Daten im Labor: 80 %
   Auswertung und Interpretation: 95 %
   Verfassen der Publikation: 95 %

3. **Földi, C**, Dohrmann, R, Mansfeldt, T. 2015. Volatilization of elemental mercury from fresh blast furnace sludge mixed with basic oxygen furnace sludge under different temperatures. *Environmental Science: Process & Impact* 17, 1915-1922.
   Erhebung der Daten im Labor: 95 %
   Auswertung und Interpretation: 95 %
   Verfassen der Publikation: 95 %

Köln, Oktober 2016   Corinna Földi

Curriculum vitae

14.11.1984	geboren in München, deutsche Staatsbürgerin
1991 – 1995	Grundschule (Spitalschule Leonberg / Katholische Grundschule Kirchstraße, Leichlingen)
1995 – 2005	Städtisches Gymnasium Leichlingen, Abschluss: allgemeine Hochschulreife
2005 – 2006	Auslandsaufenthalt Neuseeland
1.10.2006 – 31.03.2012	Studium der Geographie (Universität zu Köln), Nebenfächer Geologie (Universität zu Köln) und Bodenkunde (Rheinische Friedrich-Wilhelm-Universität Bonn), Abschluss: Diplom-Geographin
01.04.2012 – 31.03.2015	Wissenschaftliche Mitarbeiterin in der Arbeitsgruppe Bodenkunde und Bodengeographie, Geographisches Institut, Universität zu Köln
Seit 01.06.2015	Wissenschaftliche Mitarbeiterin in der Arbeitsgruppe Bodenkunde und Bodengeographie, Geographisches Institut, Universität zu Köln

Köln, Oktober 2016   Corinna Földi